

UNCLASSIFIED

AD. 296 558

*Reproduced
by the*

**ARMED SERVICES TECHNICAL INFORMATION AGENCY
ARLINGTON HALL STATION
ARLINGTON 12, VIRGINIA**



UNCLASSIFIED

NOTICE: When government or other drawings, specifications or other data are used for any purpose other than in connection with a definitely related government procurement operation, the U. S. Government thereby incurs no responsibility, nor any obligation whatsoever; and the fact that the Government may have formulated, furnished, or in any way supplied the said drawings, specifications, or other data is not to be regarded by implication or otherwise as in any manner licensing the holder or any other person or corporation, or conveying any rights or permission to manufacture, use or sell any patented invention that may in any way be related thereto.

63-2-4

Duncan

8640-6006-CU000

(1)

MONTHLY PROGRESS REPORT NO. 2

SPECIFICATION DESIGN STUDY

FOR

FLIGHT TESTING INERTIAL GUIDANCE SYSTEMS

GEM

(GUIDANCE EVALUATION MISSILE)

ASTIA
FEB 25 1963

23 January 1962

RECEIVED
FEB 25 1963

296 558

STL/Rep 8640-6006-CU000

AD NO.

ASTIA FILE COPY


29 6558

SPACE TECHNOLOGY LABORATORIES, INC.
No. 1 Space Park
Redondo Beach, California

MONTHLY PROGRESS REPORT NO. 2
SPECIFICATION DESIGN STUDY
FOR
FLIGHT TESTING INERTIAL GUIDANCE SYSTEMS
G E M
(GUIDANCE EVALUATION MISSILE)

23 JANUARY 1962


L. N. Jenks

Approved: 
for A. N. Drucker

Approved: 
T. W. Layton

SPACE TECHNOLOGY LABORATORIES, INC.
No. 1 Space Park, Redondo Beach, California

IDENTIFICATION OF THIS PROGRESS REPORT IS AS FOLLOWS:

CONTRACT NUMBER: AF 29(600)-3300

AIR FORCE PROGRAM STRUCTURE NUMBER: 730D

ARDC PROJECT NUMBER: 5177

ARDC TASK NUMBER: 517703

C O N T E N T S

	PAGE
FOREWORD	1
ABSTRACT	1
CONTRIBUTING ORGANIZATIONS	2
I. INTRODUCTION	3
II. PROGRESS DURING REPORTING PERIOD	5
A. ESTABLISHMENT OF TEST PHILOSOPHY, TEST OBJECTIVES AND TEST CONDITIONS	5
B. TRAJECTORY REQUIREMENTS	5
C. ANALYSIS REQUIREMENTS EFFORT	29
D. TEST ITEM REQUIREMENTS	45
III. ACTUAL PROGRESS VERSUS PLANNED PROGRESS	52
IV. POSSIBLE SOURCES OF DELAY TO STUDY PROGRAM	53
<u>APPENDICES:</u>	
1. ENGINEERING TASK LAYOUT - PROJECT GEM	54
2. GROUND TRACKING SYSTEM CRITERIA	55
3. SURVEY OF WSMR/HAFB EXISTING FACILITIES	64
4. TRAJECTORY ANALYSIS	71
5. AERODYNAMICS	85
6. THERMODYNAMICS	96
7. ATTITUDE CONTROL PROPULSION LAYOUT	104
8. FPS-16 RADAR ACCURACY STUDY	108
9. TEST ITEM REQUIREMENTS	113
10. STELLAR/INERTIAL TEST FIXTURE DESIGN REQUIREMENT	119
11. GYRO ORIENTATION STUDIES	123
12. REFERENCES	129

FOREWORD

The study progress described in this report was accomplished during the period 15 December 1961 through 22 January 1962 in partial fulfillment of the requirements of the Specification Design Study under Contract AF 29(600)-3300.

ABSTRACT

This report describes the second month's progress ^{is reported} of a ~~Specification Design Study~~ for flight testing inertial guidance systems. Areas of effort accomplished during the reporting period include continued development of the error simulation program, final establishment of criteria for ground tracking system, and survey of existing tracking facilities. Trajectory analysis, thermodynamic and aerodynamic studies, preliminary layout of the final stage vehicle including recovery and telemetry, preliminary layout of control and guidance systems and development of test item criteria were accomplished.

CONTRIBUTING ORGANIZATIONS

The GEM study program at the Space Technology Laboratories, Inc., is being accomplished by a task force organization, the members of which come from the several laboratories and departments. Listed below by name are those engineers who have contributed effort to the progress described in this report.

INERTIAL GUIDANCE AND CONTROL LABORATORY

Inertial Guidance Department

A. N. Drucker - Chairman, GEM Steering Committee
L. N. Jenks - GEM Task Force Director

R. A. Bain - External Tracking Systems
K. H. Baird - Telemetry
W. J. McLaughlin - Command Guidance Studies & Inertial Guidance Testing
J. P. Miller - Inertial Guidance Testing
M. F. Popelka - Survey and Optical Alignment
R. A. Moore)
J. R. Westlake) - Error Analysis and Simulation Program

Controls Department

E. P. Blackburn - Control System Analysis
R. J. Goad - Control System Analysis
H. Kaichi - Control System Analysis
R. B. Sherwood - Control System Analysis

GUIDANCE LABORATORY

Radio Guidance and Tracking Department

R. Anders - External Tracking and Command Guidance
W. R. Sorkin - External Tracking and Command Guidance

SYSTEMS RESEARCH LABORATORY

Systems Design Department

L. Becker - Booster Configuration - FSV Design
P. C. King - Booster Configuration - FSV Design
C. A. Knight - Booster Configuration - FSV Design
J. Orr - Antenna Design

Systems Analysis Department

B. A. Wine - Trajectory Analysis

AEROSCIENCES LABORATORY

Aerodynamics Department

D. H. Baer - Aerodynamics
G. Lippmann - Thermodynamics
D. H. Mitchell - "
H. R. Wilkinson - Aerodynamics

COMMUNICATIONS LABORATORY

Communications Equipment Department

G. S. Kasai - Antenna Design

I. INTRODUCTION

On 15 November 1962, Space Technology Laboratories, Inc. was placed on Contract AF 29(600)-3300 with AFMDC to accomplish a preliminary engineering design for the GEM (Guidance Evaluation Missile). This design effort is to be completed within three and a half months of the above date with the final report being submitted within six months.

The objective of this engineering effort is to provide the specification design and methodology to implement non-destructive testing of inertial guidance systems and components through use of a pre-programmed flight test vehicle. Included therein is the ancillary instrumentation to provide the precise meaningful data required to accomplish inertial system evaluation. The detailed objectives of this design effort are contained in the Statement of Work AF 29(600)-3300.

The STL design study effort is organized in three main task areas, these being further divided into sub tasks. Appendix 1 is a diagram of this task layout as proposed for accomplishment. Generally, once the GEM test philosophy, test objectives, and test conditions have been established, the study is divided into three areas; analysis requirements, trajectory requirements, and test item requirements. Inspection of Appendix 1 will indicate the further subdivisions and interface of the tasks. Each block of the task layout is the responsibility of some individual or organization within STL. Further, the GEM task layout is based on a rough three-month time scale, reading from top to bottom chronologically. It is to be noted that such a layout is essential for planning, guidance, control, and coordination within the Task Force and should not be interpreted otherwise. Obviously, such a layout must be flexible so as to be subject to possible modification as problem areas are disclosed and design criteria becomes progressively defined.

Discussion of the study progress during the reporting period which follows may more easily be followed by occasional reference to the task layout (Appendix 1). By so doing, the reader will readily obtain a clear picture as to detailed task interface and study progress. Task accomplishment to date is shown on Appendix 1 as cross-hatched and shaded areas.

This report discusses the engineering effort that has occurred subsequent to that effort covered by the first month's report. (Reference 6).

Paragraph II (Progress During Reporting Period) covers the conclusions and the significant study features. The various appendices provide the study detail, as known at this time, some of which may be a repeat of portions of Paragraph II.

II. PROGRESS DURING REPORTING PERIOD

A. Establishment of Test Philosophy, Test Objectives and Test Conditions

This was defined and documented during preceding reporting period.
(Ref. (a); Par. II A, Appendix 2, and Appendix 3).

B. Trajectory Requirements

1. Completion of the analysis requirement study, as partially reported in Reference (7) at the end of last reporting period, has indicated the extreme desirability of effecting a two-fold GEM trajectory capability. Such a duality entails (1) a retro-thrusting 2nd stage in tandem with an upward-thrusting 1st stage complex and (2) a delayed upward-thrusting 2nd stage in tandem with an upward-thrusting 1st stage complex. For convenience and clarity, these two trajectory sequences shall be designated Program A and Program B* respectively. Together, these two programs will comprise the Phase I GEM system. The two trajectory programs are plotted in Figures 1 and 7 of Appendix 4 and tentative event schedules are illustrated in Figures 1 and 2 at the end of this section. A more detailed discussion of the two trajectories will be given in paragraphs a and b below.
 - a. Program A (Phase IA) - The necessity for this trajectory sequence has been discussed in detail in Reference (7). Figure 3 illustrates the manner in which the various accelerometer error coefficients, with magnitudes as indicated, propagate, the nature of such growth being ideally suited to the separation of the non-linear error functions such as the quadratic and cubic acceleration terms as well as the servo lag term. Figure 4 illustrates, for the same trajectory, the behavior of the gyro error terms. Under these conditions, the gyro compliance and bias, due to lateral acceleration, are accentuated for purposes of identification and verification. It is to be noted, however, that the constant drift, misalignment and mass unbalance terms tend to highly correlate (and hence become somewhat unidentifiable) when exercised under Program A.

*The terms Phase IA and Phase IB are synonymous with Program A and Program B, respectively.

- b. Program B (Phase IB) - The merits of this trajectory sequence were also discussed in Reference (7). Figure 5 illustrates the propagation of the accelerometer errors when exercised on the delayed trajectory. The advantage of this sequence over Phase IA, as far as accelerometers are concerned, is the increased separation of the bias and cubic terms from the other terms. Figure 6 illustrates the growth of gyro errors when subjected to Program B and points up the separation of the constant drift, compliance, and mass unbalance terms.
2. The expansion of the trajectory sequences into Programs A and B does not alter the selection of the booster configuration adopted during last reporting period (shown in Drawing PD 28-009 for Phase IA). The requirements of error analysis, as discussed in Reference (7), when considered in the light of Program B, accentuates the desirability of the improved Algol/Pershing B-2 combination. This is principally due to the low average thrust and low impulse of the delayed and retro stages of the Pershing configuration if used for both programs. Since Reference (7) details these considerations, further discussion will not be attempted herein.

Program A has been in existence for some time and the trajectory sequence has been established as follows: (Additional trajectory information is contained in Appendix 4).

PITCH PROGRAM

1ST STAGE

VERTICAL RISE	-	2 SECONDS
.2° SEC	-	8 SECONDS
.075° SEC	-	40 SECONDS
CONSTANT ATTITUDE	-	10 SECONDS

COAST PERIOD

CONSTANT ATTITUDE

RETRO STAGE

-.17°/SEC	-	46 SECONDS (ENTIRE STAGE)
-----------	---	---------------------------

COAST AND RE-ENTRY PERIOD

CONSTANT ATTITUDE

Phase IB is now being completed, the status of which is described in Appendix 4.

3. Final Stage Vehicle Design Layout

- a. As discussed above, the GEM analysis requirements now specify two distinct trajectories - Program A and Program B. After establishing such a vehicle requirement, it was decided that the most feasible course of action was to insure that the FSV be designed to accommodate both programs with one set of hardware. Drawing PD 28-010 shows the FSV preliminary layout and the assemblies for the two programs. The most critical problem involved in the design of an FSV capable of mounting the Pershing B-2 either fore or aft, is the location of the pitch and yaw attitude control nozzles. Due to a shift in the Pershing B2/FSV center of gravity with each engine location, the control jets cannot be located, relative to the FSV, in the same position for both programs. The roll nozzles, however, will remain in the same location relative to the FSV for both programs. As is discussed under the control system, the combination hot and cold gas control propulsion will facilitate this nozzle shifting. Two distinct interstage structures will be required due to differences in structural stiffness requirements of the two configurations. At this time, it appears that these two areas represent the only special item requirements when considering inter-program standardization of hardware. Drawing PD 28-010 illustrates this point by showing that the fairings, some of the interstages, and most of the FSV will remain unchanged for both program missions.
- b. Aerodynamics - Computations have been completed for aerodynamic coefficients and center of pressure as function of Mach number. Based on these figures and Reference (13) data, the FSV flap deflection was increased from 15° to 20° . This was dictated because the flap hinge was ineffective at $+15^{\circ}$, particularly in the critical transonic region. The aerodynamic data is being used to determine stability for control design, as drag inputs to the trajectory programs, and to calculate structural loading of FSV. For re-entry guidance system study, acceleration vs. altitude was

plotted for various $\frac{W}{C_{DA}}$ ratios. (See Figure 7.) Appendix 5 describes the aerodynamic effort.

- c. Thermodynamics - Thermal analyzer programs were run for various stations on the FSV for the portions of the trajectory below 300,000 feet. The results are summarized in the following table:

	<u>Maximum Temperature</u>
Ascent stagnation point	1813°F (Outside) 132°F (Inside)
Re-entry stagnation point	1866°F (Outside) 302°F (Inside)
Ascent payload skin	388°F
Re-entry payload shell	570°F

The trajectory used for these calculations is that anticipated for the abort case and is considered the most stringent as far as dynamics is concerned.

Appendix 6 details the results of the thermodynamics studies to date. Considering the practice of utilizing AVCOAT on structures where the skin temperature exceeds 500°F, it appears that AVCOAT will be required in a relatively light coat.

- d. Bending Mode Calculation effort has been initiated to compute bending mode shapes, frequencies, and other modal properties for the Program A vehicle. Five time points along the trajectory have been selected for calculations, namely:

- (1) Launch
- (2) T + 26 Sec (Max wind shear)
- (3) Algol Burnout
- (4) Pershing Ignition
- (5) Pershing Burnout

Due to a lack of improved Algol bending data at present, calculations are being based on the standard Algol data to obtain bending information for initiation of dispersion, control design and guidance studies. If improved Algol data differs significantly from the standard, the bending mode computations will have to be repeated.

e. Recovery System - A preliminary parachute system analysis indicates that a three chute cluster is desirable for minimum weight, maximum reliability, and maximum stability. This represents a change from earlier considerations which favored a reefed-expanded single chute method. Investigation disclosed that a single drogue chute should first be deployed at about 15,000 feet altitude (see Figure 8) in case tumbling of the FSV occurred. The single drogue will stabilize far more reliably than a large bulky reefed chute. The deployment command would be generated by a barometric pressure switch. A timer would then activate the release system, ensuing the drogue chute to pull out the final three chute cluster about 12,000 ft. altitude. The lower deployment altitude will facilitate chute operation and minimize drift from prevailing winds. The weight of the complete parachute package will be approximately 75 pounds. The drogue chute will be approximately 16 feet in diameter and each of the three final chutes, 38 feet in diameter, all being off-the-shelf-items.

f. Structure Design - Design of the FSV flap system has been partially completed (see Drawing PD 28-007A). It can be noted that the system offers simplicity and reliability while maintaining the original design criteria of being automatically deployed by the separation command. When opening, each flap moves slightly under the aerodynamic shield allowing maximum protection at the critical "leading-edge". The material under consideration for the shield is high-temperature refrasil phenolic fiberglass molded in segments.

Although the flaps are designed mainly to withstand the aerodynamic re-entry heating, they can be made frangible to absorb "impact" loads that may result from toppling of the FSV after initial ground contact.

g. Weight and Balance Effort - Work continues on inertia calculations and it is anticipated that within the next three days the following will be issued:*

- (1) Inertia vs. time curve
- (2) Weight vs. time curve
- (3) C.G. vs. time curve

*(Note: These calculations were received on 29 January 1962 and will be included in final report.)

Information received during the past two weeks from Martin, Orlando and Chance-Vought has materially assisted in the above undertaking. Data received from Martin were official, but Chance-Vought data remains to be confirmed as of this date.

Final information is still lacking concerning final stage equipment, i.e., weights, sizes and power requirements.

4. Flight Control and Command Guidance System Evaluation

- a. Control - The study effort in the control area has been concentrated on the evaluation of control techniques and hardware. System analysis has not been emphasized due to the lack of necessary preliminary aerodynamic calculations (as discussed above). However, such will be forthcoming shortly and the control analysis will proceed. It has been decided to use the Sissenwine wind criteria, modified for southwest United States, as the data provided by AFMDC does not contain 3σ values. The control system configuration as now envisaged, is described below:

(1) Payload Control System

- (a) Function - The payload contains the gyro reference package consisting of three MIG gyros to generate control command signals during both powered and coast phase of flight. An electronic programmer generates the pitch programs in addition to the required discrete signals for all stages. A guidance command unit accepts command signals transmitted from the ground and applies them as torquing signals to the gyros. The payload attitude control system controls the attitude of the Pershing-Payload combination during coast prior to Pershing ignition, and the same system controls attitude of the payload about all three axes from Pershing separation until re-entry, and about the roll axis from re-entry until parachute deployment.
- (b) Configuration - Payload control torque is supplied by twelve reaction engines. Eight of these engines, utilizing nitrogen gas, provide control before re-entry and are

located at the nose of the payload for Program A missions. Roll control during payload re-entry is provided by four hot gas monopropellant engines, tentatively located at the rear of the payload near the re-entry flaps. Appendix 7 describes tentative layout of the cold gas and the hot gas systems.

- (c) Thrust Level - The pitch and yaw control reaction engines must provide 14 lbs. of thrust each. This sizing is based upon a dynamic pressure at first stage burnout not to exceed 5 lbs/ft². In addition, the staging transients at Algal separation and at Pershing separation are assumed to be less than 2°/sec rate impulse imparted by the separation springs. The re-entry roll control engines provide 24 lbs of thrust, with a mounting distance between the engines of 2.75 ft. This level of roll control torque is required to counteract the roll moment imparted to the vehicle during re-entry. Prior to re-entry, the low thrust level roll engines, providing 2.2 lbs. of thrust each, are adequate for roll control.
 - (d) Total Impulse - The 3σ roll disturbance torque from re-entry to parachute deployment will result in an estimated total torque impulse of 4730 ft-lb-sec resulting in a minimum required hot gas roll control impulse of 3430 lb-sec for this phase of flight. Total estimated cold gas control impulse for the Program A mission is 400 lb/sec. The Program B mission with the longer coast times will require a cold gas impulse of 2000 lb/sec but the required roll control impulse for re-entry will remain the same.
- (2) Powered Flight Control Systems
- (a) Improved Algal - Control of the vehicle during burning of the first stage is effected by jet vanes in the Algal exhaust stream in combination with aerodynamic fins. Control characteristics for this stage have been summarized in Reference (14).

(b) Pershing B-2 - The Pershing stage is controlled by jet vanes in the Pershing motor exhaust stream. Pershing control system characteristics are described in Reference (15).

- b. Command Guidance System - The effort in the command guidance area has been concentrated upon a study of FPS-16 accuracy with the view as to its applicability as the input to the command system.

Further component design cannot proceed until such time as a control system dispersion has been accomplished. Continued discussions with WSMR Range Safety must be accomplished to insure complete incorporation of the safety requirements and will take place late in January 1962.

(1) FPS-16 Tracking Accuracy

FPS-16 velocity tracking accuracies were determined in a Cartesian coordinate system for two FPS-16 site locations, viz. Tula Range Camp and "C" station. The purpose of this study was to determine the adequacy of the FPS-16's in tracking GEM for backup radio guidance purposes and details of the study are in Appendix 8.

Two trajectory points were chosen from the Phase I GEM trajectory, one near first stage burnout during maximum ascent velocity, the other at low (about 10-20 degrees) elevation angles as seen by the site in question. Velocity errors at these points should exceed those at intermediate points.

For the Tula Range Camp site, velocity errors in the Cartesian set were about 4 ft/sec. in each direction for the high velocity tracking point and about 2 ft/sec. in each direction for the low elevation angle trajectory point.

It is expected that velocity accuracies determined with respect to the other FPS-16 sites at White Sands would approximate the values obtained for the Tula Range Camp and C Station sites.

Flame attenuation effects were not explicitly considered and these effects may rule out the use of the C Station site, but the Tula Range Camp site will certainly be good enough for backup guidance purposes.

5. Vehicle System Operation

Study effort has been devoted to the GEM system operation during both powered flight and free flight. Abort capability system operational schedule and antenna criteria have been defined and are discussed below.

- a. Abort Capability - Recovery of the GEM test item is highly desirable for both normal and abnormal vehicle behaviour. At the same time, the scope of the program is such that abort systems of the complexity and size of those used for manned space programs, for example, are not warranted. Consequently, it is felt that all aborts should be ground commanded and that the vehicle should contain no specific abort instrumentation nor abort propulsion.

The abort commands will depend on the particular test vehicle fault. A command guidance system is tentatively planned as an override in case of minor vehicle deviations, but certain vehicle failures, such as engine ignition failure or control system failure will lead directly to abort procedures. The following abort sequences are considered possible.

(1) First Stage Fire, Second Stage Misfire, Under Control

Separate re-entry vehicle from second stage and go through normal recovery sequence. Such an abort condition will involve re-entry at higher than normal velocities and accelerations, but the re-entry heat cap and insulation will be designed to withstand the environment.

(2) First Stage Fire, Second Stage Fire, Second Stage Out of Control

Terminate thrust, turn off all control, separate the re-entry vehicle and attempt the normal recovery sequence. Since the control system failure may be in components in the re-entry vehicle, it is deemed wiser not to attempt re-entry vehicle control. The tumbling re-entry vehicle will stabilize,

though probably not in roll. The parachute system will be designed to deploy successfully under these circumstances.

(3) First Stage Fire, Out of Control

Thrust terminate the first stage (via destruct charge), prevent second stage ignition, attempt separation and recovery sequence. This attempt may not be successful depending on the nature and time of the failure.

System layout must incorporate provisions to accomplish the above sequences and further discussion with WSMR is required to insure that such abort procedures are compatible with range safety requirements.

- b. System Operational Schedule - Based upon the trajectory analysis, the abort requirements, and FSV design, the following tentative event schedule has been established for Program A and for abort. Program B's schedule will be similar, the major differences will be in time and altitude.

GEM -- "A" CONFIGURATION

Event Schedule -- Normal Operation

<u>Event</u>	<u>Event Initiated By</u>	<u>Approx. Time Sec.</u>	<u>Approx. Alt. Ft.</u>
Launch	Ground Signal	0	4000 GL
Start Programmer	Ground Signal	0	4000 GL
Control with Algol System	Ground Signal	0	4000 GL
Program pitch rate (1)	Programmer	2	--
Program pitch rate (2)	Programmer	10	--
Program pitch rate (3)	Programmer	50	--
Algol Separation (At near Burnout)	Axial Accel. (Near zero reading) (Arm with Programmer)	60	230,000
Nose Fairing Jettison	Same signal as Algol Separation	60	230,000
Assume Control with FSV System	Same signal as Algol Separation	60	230,000

GEM -- "A" CONFIGURATION (Cont'd)

Event Schedule -- Normal Operation

<u>Event</u>	<u>Event Initiated By</u>	<u>Approx. Time Sec.</u>	<u>Approx. Alt. Ft.</u>
Displace Algol	2 second timer Set by Separation Signal	62	245,000
Pershing Ignition	Programmer	70	305,000
Assume Control with Pershing System	Programmer	70	305,000
Program Pitch Rate (4)	Programmer	70	305,000
Program Pitch Rate (5)	Programmer	112	
Pershing Separation Open FSV Flaps Assume Control with FSV System	Axial Accel.	117	395,000
Displace Pershing	2 Second Timer Set By Separation Signal	119	390,000
Turn off Pitch & Yaw Control on FSV	Axial Accel. (Arm with Programmer)	182	150,000
Deploy Drogue Chute & Drop Heat Cap	Barometric Switch (Arm with Programmer)		15,000
Actuate Reefing Line Cutters and deploy main parachute cluster	Timer set by above Barometric Switch		12,000

Ground Commands -- Abort

Abort Condition A -- 2nd stage misfires

No ground commands needed

Abort Condition B -- 2nd stage out of control

1. Thrust terminate 2nd stage
2. Turn off all control
3. Separate FSV

Abort Condition C -- 1st stage out of control

1. Thrust terminate 1st stage -- destruct charge
2. Turn off all control
3. Cancel Pershing, displacement rockets, ignition signal and
all separation signals
4. Separate Algol
5. Separate FSV
6. Deploy parachute at 15,000' (may occur automatically depending on
abort condition)

6. Antenna Requirements

Four antenna systems for the GEM vehicle are under study. The following general characteristics have been determined from the limited data available to date.

a. Radar Tracking Beacon

- (1) Frequency: 5500 mc, C-band
- (2) Tape: Flush mounted traveling wave or phased slots
- (3) Coverage: IA1 0° to 90°
IA2 -30° to $+130^{\circ}$
- (4) Polarization: Linear (vertical or horizontal)

b. Command Destruct System

- (1) Frequency: 465 mc, Lp-band
- (2) Type: Scimitar or loop elements phased for turnstile array
- (3) Coverage: Omnidirectional
- (4) Polarization: RHCP aft
- (5) Gain: 0 db

c. Telemetry

- (1) Frequency: 2200 mc, S_C-band
- (2) Type: Phased slots diplexed for both PCM/FM and FM/FM telemetry
- (3) Coverage: IA1 0° to 90°
IA2 15° to 105°
(assumed receiver location at King 1)
- (4) Polarization: Linear

d. Interferometer Tracking

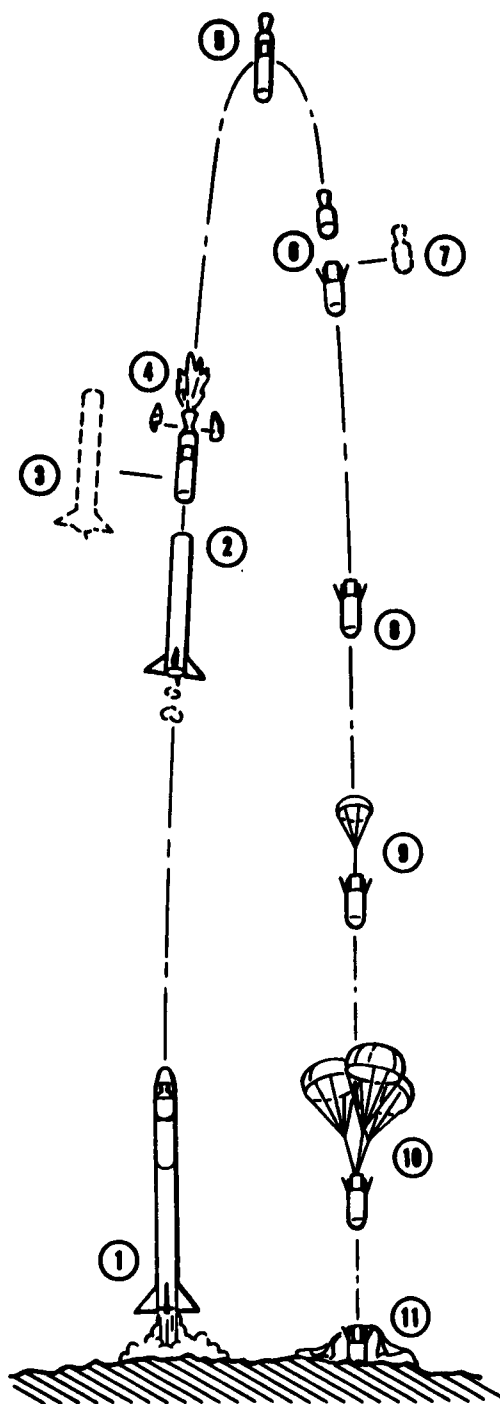
- (1) Frequency: X-band
- (2) Type: Single horn
- (3) Coverage: Approximately 130° in ϕ and 90° in θ
- (4) Polarization: Linear

The above antennas represent a first approximation to the requirements of the GEM vehicle. A large change in these general antenna characteristics is not anticipated. However, further studies are under way

to determine more specific data on which antenna design may be based. Among these studies are:

- a. A computer program to determine IA1, IA2, and slant range as a function of time from C-Station, King 1 and Phillips Hill to determine exact coverage.
- b. A power budget study of each system's r.f. link to determine gain requirements and signal margins.
- c. Interferometer vs. trajectory geometry and phase stability requirements for the airborne tracking antenna.

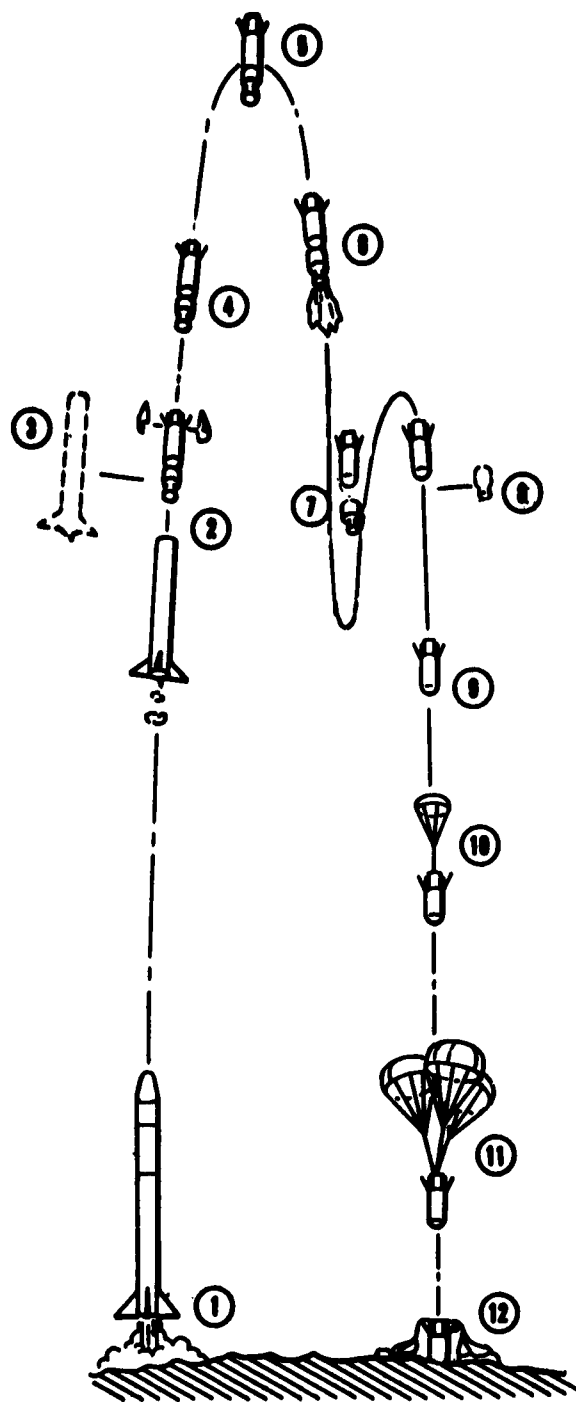
Early power budget calculations for both telemetry and command destruct systems have been made and signal margins of 8 - 14 db for the telemetry and 50 - 60 db for the command system are anticipated with the assumed antennas.



PROGRAM 1A EVENT SCHEDULE

EVENT	TIME (sec)	ALTITUDE (ft)
1. Launch	0.0	4,000
2. First Stage Burnout, Separation, Jettison Fairing	60.0	225,000
3. First Stage Displacement	62.0	240,000
4. Ignite second stage	70.0	300,000
5. Apogee	102.0	420,000
6. Second Stage Burnout, Separation, (flaps extend)	117.0	396,000
7. Displace Second Stage	119.0	390,000
8. Re-entry	148.0	300,000
9. Deploy Drogue Chute	279.0	15,000
10. Deploy main chute cluster	289.0	13,600
11. Impact and recover	900.0	4,000

FIGURE 1



PROGRAM 1B EVENT SCHEDULE

EVENT	TIME(sec)	ALTITUDE (ft)
1. Launch	0.0	4,000
2. First Stage Burnout, Separation Jettison Fairing	60.0	225,000
3. Displacement First Stage	62.0	240,000
4. Coast		
5. Apogee	312.0	1,152,000
6. Ignite second stage	502.0	620,000
7. Second Stage Burnout, Separation	550.0	530,000
8. Displace Second Stage	552.0	533,000
9. Re-entry	723.0	300,000
10. Deploy Drogue Chute	849.0	15,000
11. Deploy main chute cluster	859.0	13,600
12. Impact and recover	1259.0	4,000

FIGURE 2

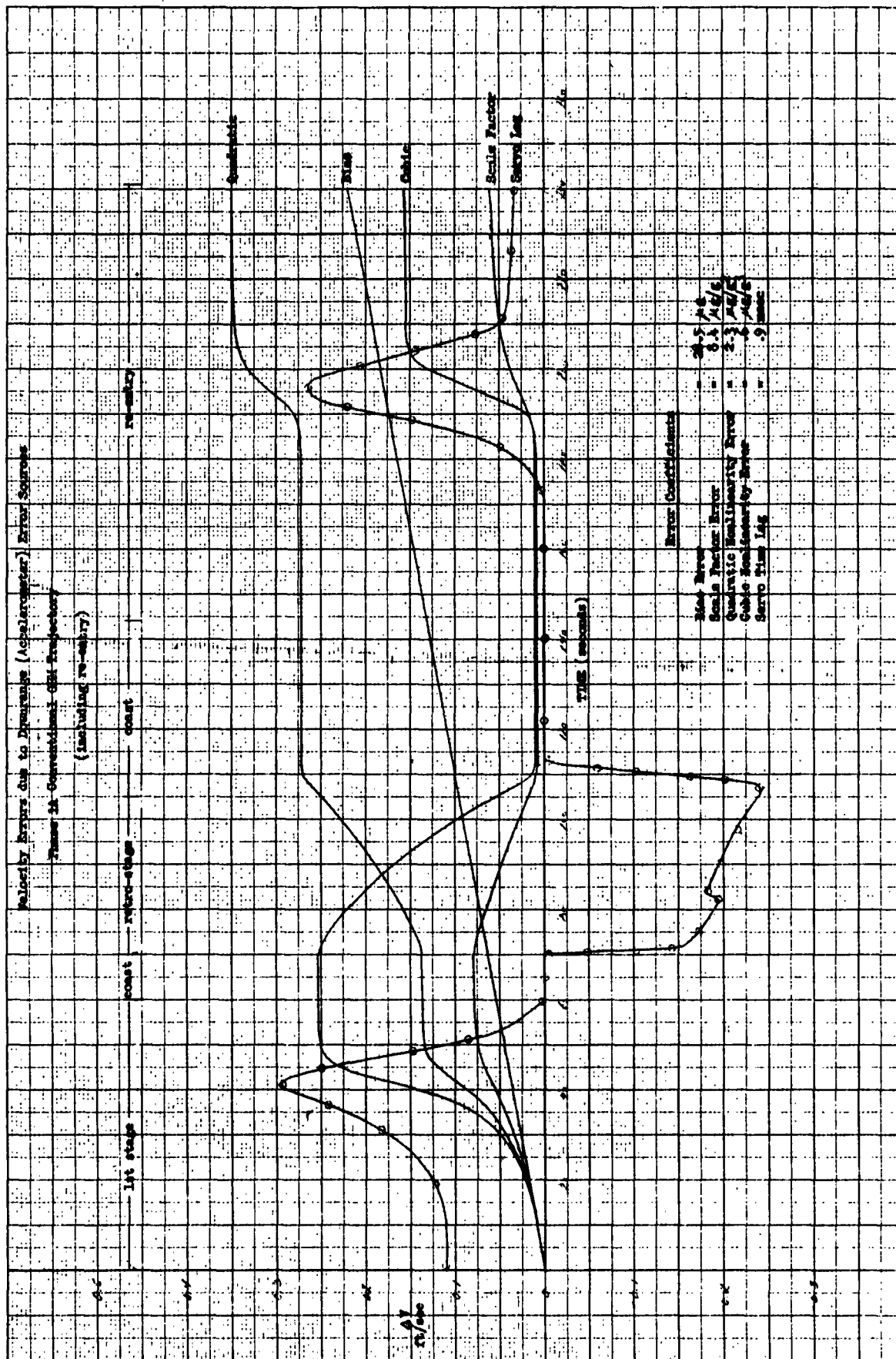


FIGURE 3

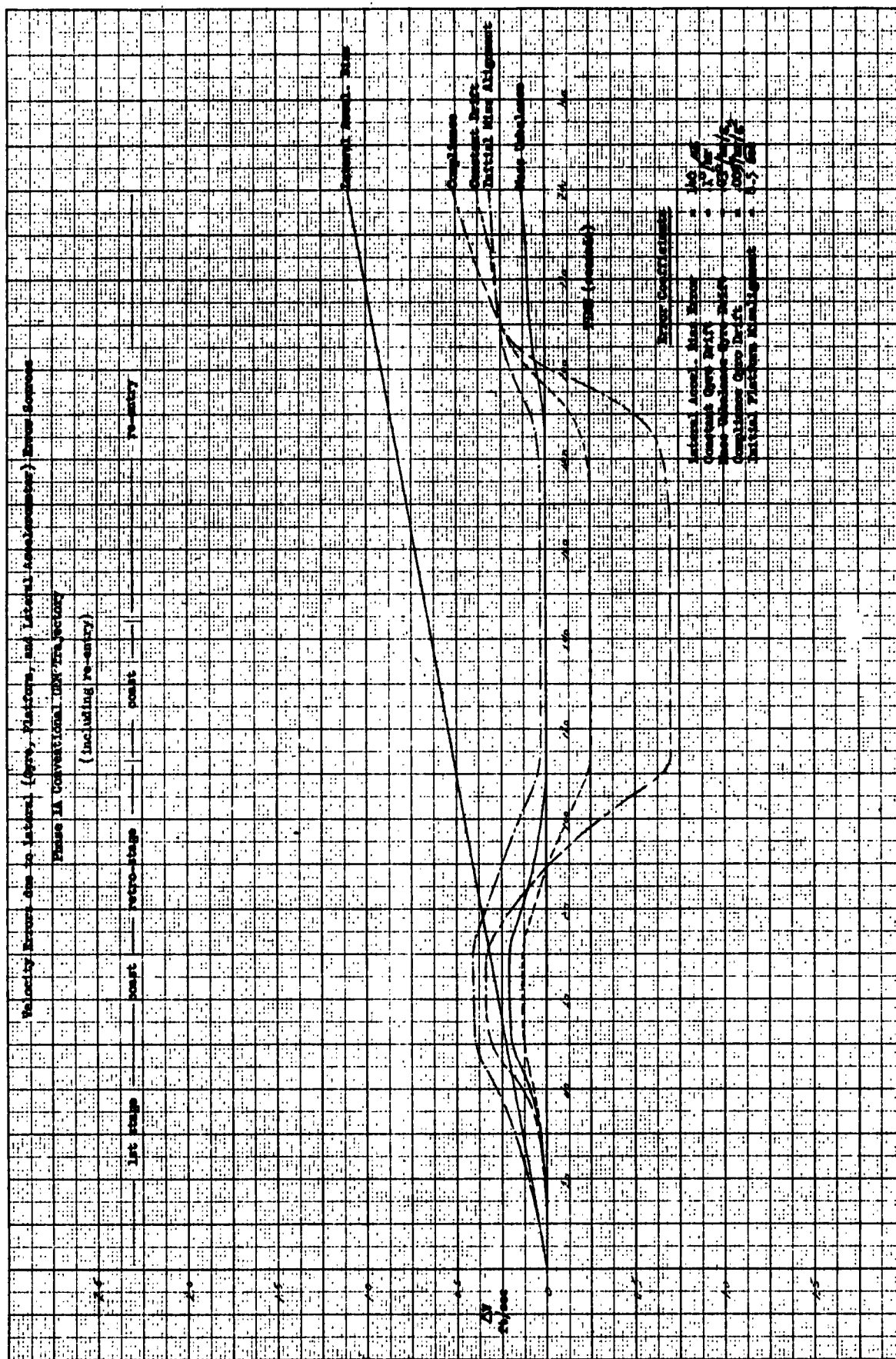


FIGURE 4

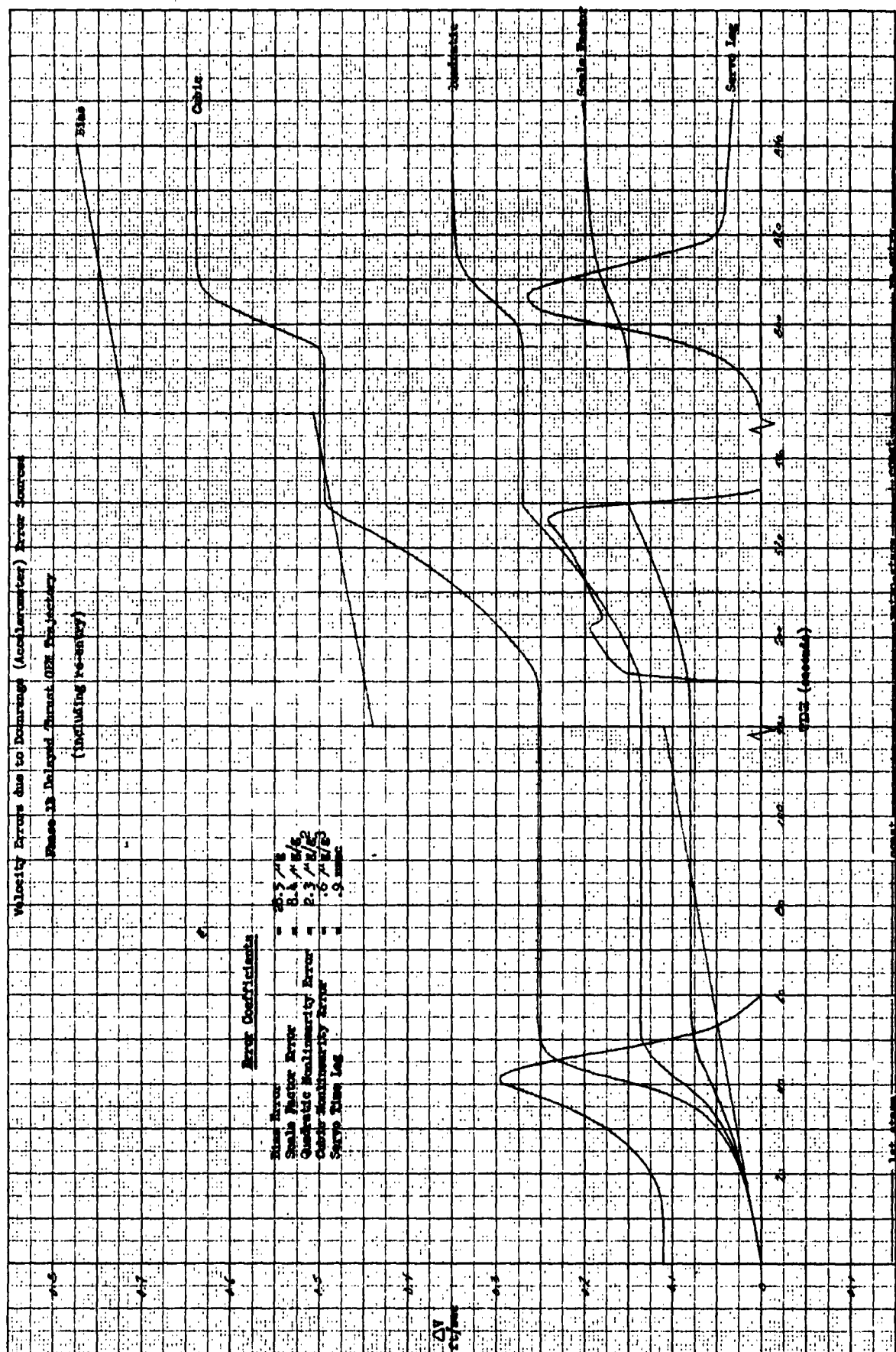


FIGURE 5

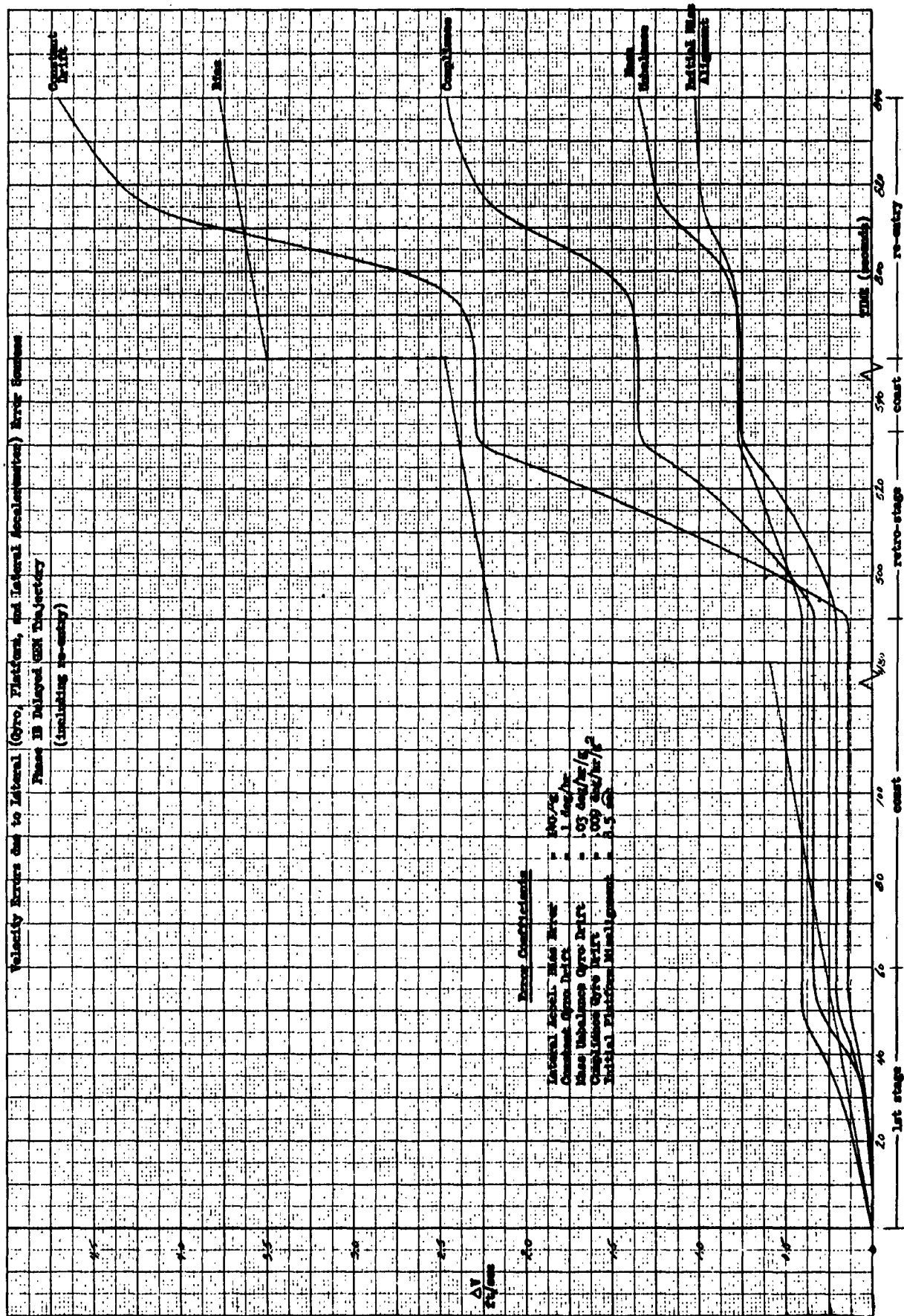


FIGURE 6

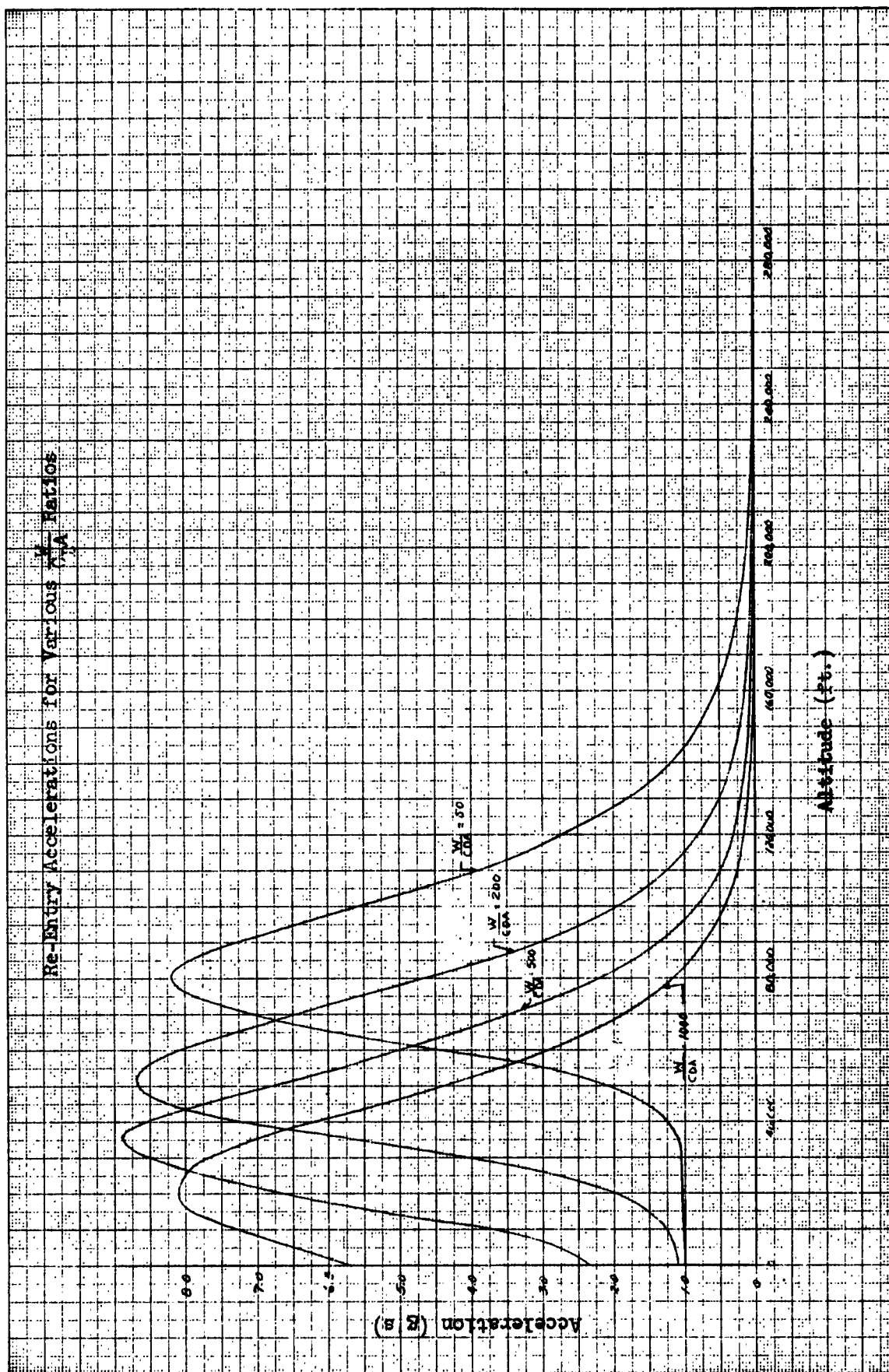
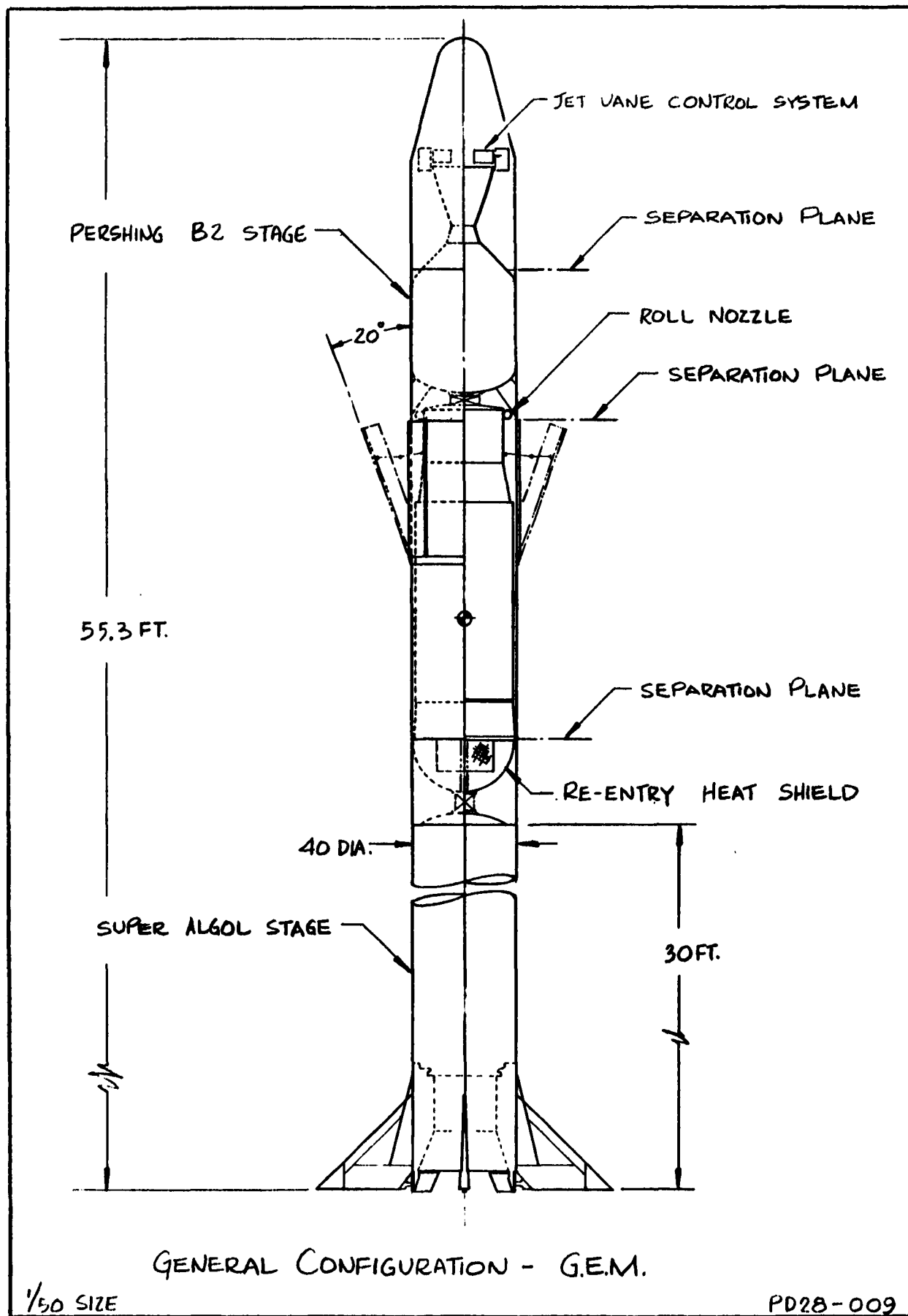


FIGURE 7



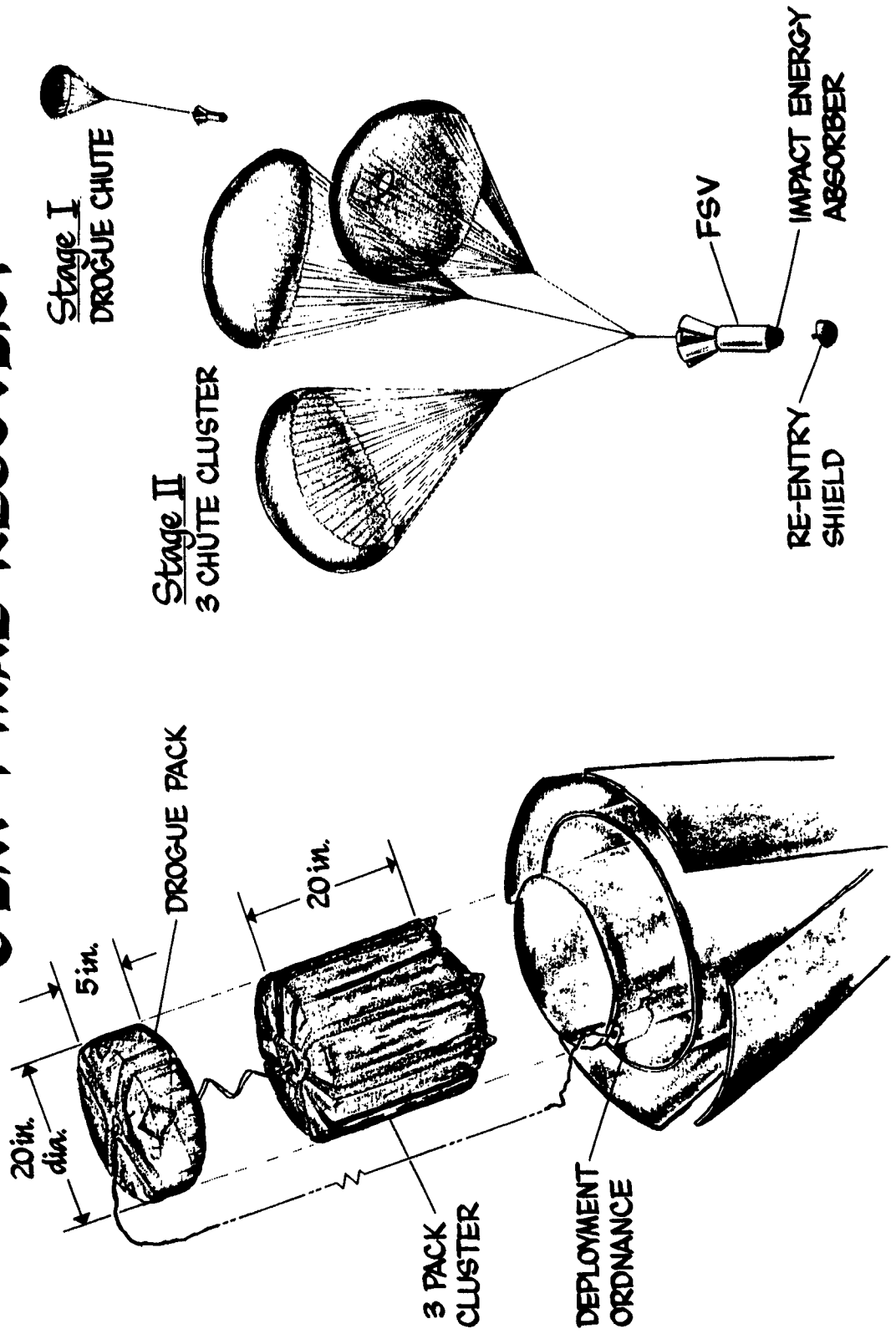
GENERAL CONFIGURATION - G.E.M.

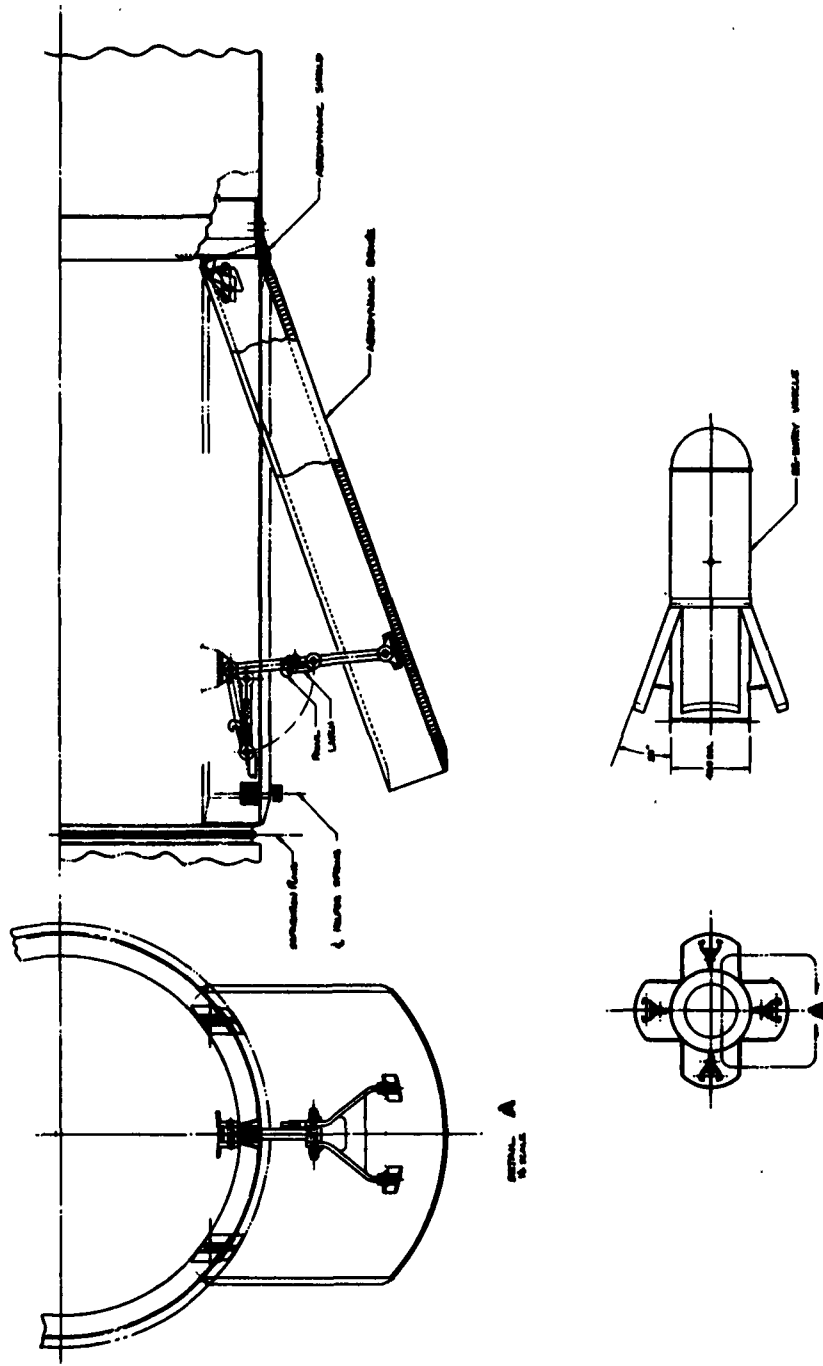
1/50 SIZE

PD28-009

1-8-62

GEM FINAL RECOVERY





C. Analysis Requirements Effort

1. Establishment of error coefficient recovery requirement was accomplished in Appendix 3, Reference 6. Based upon such a requirement, study of the tracking system, error analysis programs and internal data monitoring (telemetry) was extended, the results of which are discussed below.

2. External Data Requirements

- a. Further study was applied towards the establishment of a GEM Ground Tracking System Criteria. (Appendix 4 of Reference (6) was reviewed and corrected, the resulting comments being attached in Appendix 2.)

The available documents on the accuracy and system specifications on accurate tracking systems were studied. The systems include Azusa, G.E. Mod III, Mistram, and the STL advanced guidance system study. The advanced guidance system study as reported in Reference (5) and (9) is particularly applicable to the study of very accurate tracking systems.

Two factors which seriously limit the accuracy of most tracking systems are the survey accuracy and the baseline length. An analytical discussion of these factors is given in Appendix 2 and a summary is given below.

- (1) Survey

Considering the time element and presently available equipment, the best survey of White Sands would be achieved by the Coast and Geodetic Service with a probable accuracy of 2 parts per million in both length and angle. If all portions of the tracking system and the launch point are tied together with this accuracy, the resulting errors in azimuth A, and elevation E, will vary between 2.5 and 5 ppm over most of the GEM trajectory. The errors in azimuth rate and elevation rate will vary from 5 to 10 ppm of the angular rate.

(1) Survey (Continued)

These errors are most serious during the period of highest velocity which would occur at the end of the first stage of the GEM trajectory. A typical point during the early portion of the trajectory may have the following parametric values:

$$E = 45^\circ \quad \dot{E} = .03 \text{ radians/sec}$$

$$R = 150,000 \text{ ft.} \quad \dot{R} = 4000 \text{ ft/sec}$$

Under these conditions the errors in A , E , \dot{A} and \dot{E} , with the 2 ppm survey, may be expected to be 2.5 microradians in angle and .15 microradians/second in angular rates. This will give rise to the errors $\Delta \dot{\theta} R$ and $\Delta \dot{\theta} \dot{R}$ of .01 ft/sec and .025 ft/sec respectively in each of two lateral directions perpendicular to the range direction. On a delayed thrust - GEM trajectory, the $\Delta \dot{\theta} R$ term could attain a value of .025 ft/sec to .05 ft/sec at maximum range.

The above figures are order of magnitude numbers assuming independent survey errors and an average rms value. It can be anticipated, then, that the best possible survey will probably result in errors up to .025 ft/sec over the portion of the GEM trajectory where the velocities are high. Over a large portion of the standard GEM flight however, the velocities are low so that these errors would be insignificant.

(2) Baseline Length Requirements

Three error sources that are functions of baseline length were considered, viz., survey, propagation, range differences and range rate differences.

The survey errors considered here were uncertainties in placement of the phase center of a receiving system with respect to an accurately surveyed benchmark. A reasonable figure for the accuracy of stable placement of the phase center of a receiving antenna appears to be .01 foot (1/8 inch). If the effect of this placement error is not to propagate into the overall survey accuracy, the error should be kept to less than one part per million of the baseline length. This indicates the baseline length should be at least 10,000 feet based on the .01 foot placement error.

The propagation error considered is due to atmospheric noise caused by the motion, with respect to the line of sight, of a non-homogeneous atmosphere. The value attributed to this effect was assumed to be about $1/3$ of the magnitude measured at Maui. Based on this assumption, and a 10,000 foot baseline, atmospheric noise will cause an angular error of about 1 microradian over most of the GEM trajectory. Assuming a $\frac{1}{2}$ cps cutoff filter is applied to the velocity data, the angular rate error for the same conditions will amount to about .1 microradians/sec.

For the standard GEM trajectory this could give rise to velocity errors of .05 ft/sec and on the delayed thrust GEM trajectory, .1 ft/sec. For long baselines, the atmospheric noise is inversely proportional to the product of baseline length and the square root of the averaging time. If the filtering is to be kept to a minimum to preserve response, then the baseline will have to be about 50,000 feet to reduce the atmospheric noise to .02 ft/sec over the delayed thrust GEM trajectory.

The third baseline dependent factor considered was the effect of limitations in the accuracy of measuring range differences and range rate differences. Although not as well documented as the preceding baseline length effects, studies of existing and proposed systems suggest that for long baseline interferometer systems, the limiting accuracy in the measurement of range difference and range difference rate with limited filtering, appears to be about .01 ft. for range differences and .001 ft/sec for range difference rates.

These errors propagate into an angular error which can be approximated by dividing the difference error by the baseline. Thus, for a 10,000 ft. baseline the angular errors due to the above difference measurement errors would be about 1 microradian and .1 microradian per second. This error is

the same order of magnitude as that due to the assumed effects of propagation at White Sands and, therefore, the same conclusions hold as to baseline requirements.

From the above considerations, it appears that a 10,000 ft. baseline would be marginal to meet the GEM accuracy requirements and baseline lengths of 50,000 ft. or over would be desirable.

(3) Ballistic Cameras

One of the difficulties encountered with the use of very long baselines is calibration of the baseline measurements. For GEM, one or more strobe lights will be carried in order to obtain an accurate calibration point. A very accurate ballistic camera net will be required for this purpose and will consist of three or more 600 mm focal length ballistic cameras, located by the most accurate survey possible in a geometry selected to optimize the accuracy for the GEM trajectory.

If the B.C. plate can be read to 3 microns, which is optimistic, the resulting angular error will be about 5 parts per million. If this accuracy is to be attained, the highest possible data reduction quality will have to be obtained in the reading of the B.C. plates.

For ballistic camera data to be an integral part of the GEM tracking scheme, it is most important that rapid reduction of B.C. data be provided by the use of semi-automatic plate reading equipment. Following a flight, a maximum time delay of three days is allowable for the delivery of reduced B.C. data in order to effect the timely processing of external data and complete the guidance system analysis prior to the next GEM flight.

(4) Conclusions

The following items represent some tentative conclusions as to the characteristics of the tracking system needed to achieve the GEM accuracy requirements:

- (a) The tracking system should be composed of at least three stations operating coherently with a single transmitter

- and transponder so as to form an interferometer system with long, perpendicular baselines separating the stations.
- (b) Range rates and range rate differences should be obtained from an X-band carrier frequency.
 - (c) The system could measure both position and velocity or, as an alternate, rate only. In order to use a rate only system, the probability of obtaining accurate ballistic camera data must be high and the probability of more than a momentary loss of signal must be very low.
 - (d) A ballistic camera net composed of 3 or more 600 mm focal length cameras will be needed.
 - (e) An extremely accurate survey will be required to tie together the tracking system stations, the ballistic camera sites and the launch point.
 - (f) Four of the factors that must be considered in selecting tracking sites are:
 - 1. Accuracy optimization by insuring a minimum geometric dilution of precision over the GEM trajectories.
 - 2. Avoidance of the flame by programming the look angle with respect to the roll axis to be greater than 15 degrees.
 - 3. Compatability with a single airborne antenna which has acceptable signal strength and phase variation characteristics.
 - 4. Compatability with survey requirements.
 - (g) High gain, X-band antennas will be required at each station in order to attain accurate tracking at the lowest possible elevation angle. Even with this requirement fulfilled, the accurate tracking system will not be able to cover the first 2 - 4 miles of the near vertical trajectory (approximately the first 15 seconds). As can be seen from the error curves of Appendix 3 of the first monthly progress report, this does not appear to be a serious limitation but the necessity of an early launch phase system will be further investigated.

- (h) In order to achieve the necessary accuracy in the external tracking system, special calibration schemes must be implemented to determine the tracking system error model. In this regard, an elaborate data reduction program will be required to accept this calibration information for correction of the external data and should be included in the specification of the final data plan.
- b. Effort was completed on the survey of the WSMR/HAFB existing facilities:
- (1) The White Sands Missile Range tracking capabilities were surveyed as to their applicability for use on the GEM program. The results of this survey are included in Appendix 3. The major emphasis of this study was placed on the AME (angle measuring equipment), DME (distance measuring equipment), and proposed Doppler.
- (2) An error budget for the AME/DME/Doppler (Integrated Tracking System - ITS) configuration was prepared. Only a limited estimation of equipment errors are included since a thorough analysis of these errors is not available at this time. Errors caused by tropospheric and ionospheric propagation uncertainties, flame effects survey errors, and calibration errors are discussed. The ITS accuracy is largely limited by the relatively short baselines and/or low frequencies employed by the AME/DME/Doppler system. Tracking accuracies of .05 ft/sec. or better in the range rate and lateral rate directions are required for the GEM program. At altitudes of moderate to large ionospheric disturbances, the probable accuracy that can be accomplished with the AME/DME/Doppler system is a 1σ error on the order of $\frac{1}{2}$ ft/sec. in both range rate and the lateral rate directions.
- c. Based upon the survey of the WSMR complex and the tracking accuracy requirements imposed by the GEM system, it is concluded that none of the systems presently available at WSMR (with the exception of the Ballistic Camera System) can be used as the primary tracking system.

Most of the problems external to the equipment, which cause excessive errors, are baseline and/or frequency dependent. The Ballistic Cameras in conjunction with airborne strobe lights, will be used to provide calibration points during coast periods. It is also considered advisable to employ the ITS as a backup tracking system since it is currently within the WSMR range planning program. However, it is to be emphasized that the ITS cannot fulfill the requirement of a primary data source.

d. Initial study of the Preliminary Layout of a Proposed Ground Tracking System covered several areas:

(1) Flame Attenuation

Electromagnetic effects of the rocket exhaust have been considered in connection with telemetry and tracking. While the effect of greatest importance, with respect to telemetry, is attenuation, variable phase shifts caused by the ionized exhaust is of greater importance with respect to tracking, since variable phase shifts induce a velocity error.

Flame effects of the GEM missile were studied in order to determine the criteria for r.f. frequency, look angles and antenna patterns necessary to minimize velocity errors. Preliminary conclusions reached were:

Frequency	-	X Band
Min. Look Angle	-	15° from Roll Axis
Antenna Pattern	-	Main Lobe - 45° minimum between half power points in a plane at right angles to roll axis - 90° points in a plane including roll axis. Null from exhaust end of roll axis to 15°.

These results may be modified as better information is integrated into continuing studies.

(2) Determination of the Airborne Antenna Requirements was initiated by defining some preliminary considerations. As the study of the tracking system requirements and layout is in the early stages, it is extremely difficult to specify any tracking system

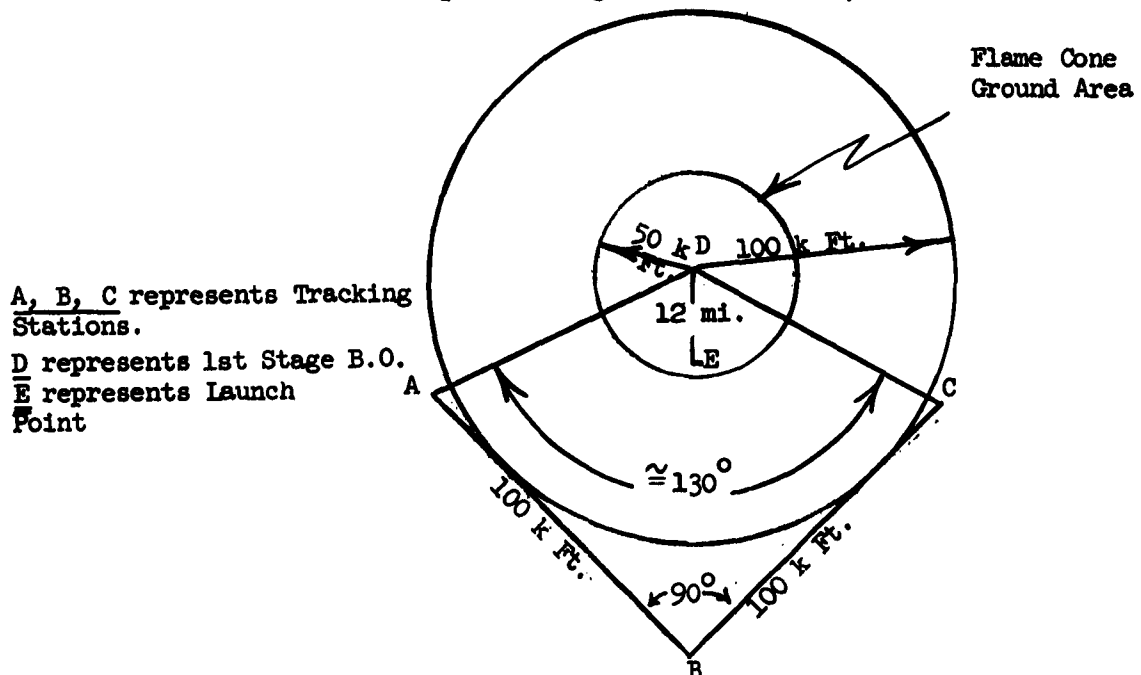
airborne transponder requirements. However, to insure some antenna study progress, initial estimates of the antenna parameters were established. The following antennas and frequencies are being considered:

1. Telemetry (FM/FM and PCM/FM)-2200 MC (dictated by antenna size)
2. Command Receiver - 409 MC - (assigned by WSMR)
3. C Band Beacon - 5500 MC - (assigned by WSMR)

In order to initiate the study of a transponder antenna, the following tracking system is considered to be an acceptable model of the final system. The primary constraints considered were flame attenuation, baseline length, Phase I A trajectory and the desirability of a single antenna. The following parametric values were assumed:

- (a) Baseline length of 100,000 feet
- (b) Three tracking stations in an L form
- (c) Flame cone to be avoided 15° off missile center line
- (d) The maximum ground radius of the flame occurs near 1st stage burnout and results in a circular ground area to be avoided having a diameter of 100,000 feet, centered under the 1st stage burnout point or 5 miles down range.
- (e) The radius of 100,000 feet provides a margin of safety and reduces the required antenna beam width.

With these considerations, one possible tracking system geometry, with launch point and ground flame area, is shown below:



The following antenna requirements must be met to accomplish accurate GEM tracking using the above configuration:

- (a) Frequency - X band about 9 KMC
- (b) Beam width about the roll axis - greater than 130°
- (c) Shape of antenna beam about pitch axis - null about 12° from roll axis with minimum transmission inside 12° , about 90° beam width extending from 15° to 105° .
- (d) Phase shifts must be kept to a minimum across the main beam. Phase shifts changes should not exceed $18^{\circ}/\text{sec}$. since the look angle to the sites sweep through the area of the mainbeam during the flight.

The exact location of the tracking system is not fixed and the above example is only for the purpose of determining the antenna problem anticipated in this general situation. The antenna properties listed above represent typical requirements for a final system.

In addition to the above antenna, it is advisable to plan the use of a backup tracking system, viz., the ITS presently available at White Sands with an additional antenna at 210-300 mc. Since the ITS station will generally be north of the trajectory a single broad beam antenna should suffice.

It will also be necessary to carry strobe lights for the ballistic cameras and, in order to obtain the best geometry, it would be desirable to surround the ground projection point of the vertical trajectory with ballistic cameras. The cameras will be removed as far as possible from the trajectory plane which may require two lights in parallel on opposite sides of the missile.

3. Establishment of the Internal Data Requirement

- a. The monitoring of internal GEM data can be divided into two general areas - pre-flight operation and air-borne operation. The former will be monitored via AGE recorders and will be discussed elsewhere. The air-borne operation will be monitored via an air-borne telemetry system, the detailed requirements of which will be discussed below.

- b. The GEM air-borne data requirement may be further subdivided into two classes - vehicle data and test-item data:
- (1) Vehicle Data - These data will be a requirement for the early phase of the GEM flight program to aid in vehicle development, A/B trouble isolation and GEM performance analysis. The data requirements quite probably will vary from flight to flight and will be of a low frequency, qualitative nature.
 - (2) Test Item Data - These data are required to accomplish qualitative and quantitative analysis of test item performance.
- c. To estimate the required telemeter capacity, it is necessary to establish a generalized measurement list for each of the above two classes. A list of the measurements, with a description of each, is given below:
- (1) Test Item
 - (a) Functional - These signals describe test item operation and are comprised of torquing functions, gyro and accelerometer pickoff signals, caging currents, intermediate servo loop voltages and power supplies. For the most part it can be said that these signals represent qualitative monitors only, as opposed to precision data references, so the accuracy requirements are not unusually high.
 - (b) Guidance Sensor Outputs - This type of function will yield important data since it represents the prime input to the error analysis program. As far as the various guidance systems are concerned, these data will be the most variable as to type. String frequencies, pulse frequencies, sawtooth ramp frequency and position, and code wheels are but a few of the types already under test. Generally, this signal is quantized at about .1 ft/sec/pulse (scale factor). The level may possibly be too coarse for the error analysis requirements which could require at least .01 ft/sec/bit. Computation of

accelerometer bias, for example may require special provisions to obtain this information, particularly during low accelerometer output periods.

- (c) Computer Words - Word length, bit rates and sync pattern will be varied over a large range, depending upon the style and format of the airborne computer used in the system undergoing test. The telemetry system must have the capacity to monitor the full range of computer outputs.
- (d) Vibration Measurements - To provide complete information concerning the acceleration environment, vibration measurements must be made at the inertial sensor inputs. Such measurements will normally be made along three orthogonal axes and the transducers used must be accurate in the low frequency region (5 to 10 CPS).

(2) Test Item Measurement List

The following generalized measurement list reflects the requirements of guidance system monitoring as discussed above:

<u>Measurement Type</u>	<u>Quantity</u>	<u>Range</u>	<u>Freq. Response (CPS)</u>
1. Power Voltages	10	0 - \pm VDC	1
2. Temperatures	6 to 10	50-150° F	1/2
3. Vibration	3 to 6	\pm 20 G's	{ 660 1200 & lower 2000
4. Inertial Accelerometer Output	3 to 6	(Square wave to be sampled at 6400 SPS & 3200 SPS (Requirement will vary)	
5. Servo Voltages	6	\pm 20 VDC	20
6. Pick off Signals	6 to 10	7 VCMs (Suppressed carrier modulated 4.8 KC)	20
7. Caging Functions	2	20 VDC	20
8. Torquing Signals	4	Determine Pulse Time	20 CPS
9. Computer Words	50	24 Bit words	400 KC

(3) Vehicle Measurements

The exact character of these measurements cannot be firmly established at this time since they depend upon the test objectives of the initial GEM vehicle flight tests. These objectives will be determined by the vehicle, engine, structure and control system designers. A general vehicle measurement list has been developed, as shown below, to serve as a guide in the establishment of the technical design criteria.

(4) Vehicle Measurement List

FM/FM Telemetry			
Measurement	Quantity	Intelligence Freq. C.P.S.	Range
Vibration	6	1200	\pm 20 G's
Temperature	10	.05	50 - 150°F
Strains	8	220	
Events - Mtr. Ignition, Separation, Etc.	4-6	Switching (Discrete)	
Mtr. Chamber Pressures	2	160	0-10VDC
Power Supply	1	1.0	0-20VDC
Vehicle Accelerations	1	20	\pm 10VDC
Vehicle Attitude	3	25	0-5VDC
Control System Parameters, Vane Positions	16	1-2	0-10VDC
Confirmation of Signal Receptions	1	1-2	0-5 VDC

- d. Based upon the above internal data requirement, study effort was initiated to establish a Telemetry Design Criteria. The telemeter requirements can be satisfied by utilizing two distinct systems, namely, PCM/FM (Pulse Code Modulation) and FM/FM (Frequency Modulation). This decision is based on extensive experience in field testing,

GEM error analysis requirements, and anticipated requirements of future guidance systems. Such an arrangement would generally use the PCM/FM system to monitor the guidance test item and FM/FM system to monitor vehicle functions.

(1) FM/FM

The establishment of a design criteria for a suitable FM/FM telemetry link for the GEM concept should be straight forward. The three basic requirements of any system of instrumentation are:

- (a) The recorded data must be a faithful reproduction of the variable quantities being measured.
- (b) The record must be unaffected by and independent of all other variables to which the system may be subjected, whatever their nature or origin.
- (c) The measuring device must impose negligible load upon the variable quantity of the measurement.

At present, the instrumentation market offers a wide selection of small, rugged, solid state, system components that easily fulfill the above requirements. In addition, at least two instrumentation systems companies have qualified complete VHF systems (215-260 MC) that would, with certain minor modifications, be compatible with the GEM system.

Therefore, it remains the task of the instrumentation system designer to choose a proper combination of components or a complete system to meet the requirements of a specific application.

In the case of the GEM FM/FM T/M subsystem, special consideration must be given to the RF transmission system. The GEM antenna designer requires an RF carrier within the 2.2 to 2.3 KMC band, due to size limitations of the airborne antenna with respect to the missile overall size. This limitation will impose a trade-off between antenna size and transmitter size and complexity. This is brought about by the fact

that the 2.2 to 2.3 KMC band has only recently been allocated for F/M transmission and development of transmitters at these frequencies is still at an early stage.

Investigation into the problem has yielded tentative specifications and costs from two sources which for all practical purposes, are identical. In general, the transmitters are designed around individual customer specifications in regard to RF power out, shape, cooling, and environmental conditions. The basic system consists of a standard VHF T/M transmitter (215 to 260 MC) used as an exciter. The output of the exciter is multiplied by a series of VHF cavities and amplifiers up to the 2.2 KMC band. The stability and FM characteristics of the transmitter are determined by the VHF exciter. It will be necessary to pressurize the package due to voltage levels and operating altitude.

Tentative specifications are:

Frequency stability	0.005%
Modulation frequency	20 cps to 100 KC
Power output	5 watts
Efficiency	5%
Power required	28 VDC 3.7 amps.
Weight	11 pounds pressurized including power supply
Size	7" x 7" x 5"
Temperature	-55°C to + 90°C
Vibration	10g 0-500 cps 15g 500-2000 cps
Delivery	90 days (depends on qualifying required)

A unique telemetry transmitter has been developed for the 2.2 KMC band. The unit is basically an all solid state, phase modulated, design, employing high efficiency frequency multiplier stages converting power at 94 MC (crystal oscillator) into power in the 2.2 KMC telemetry band.

This transmitter offers several significant advantages over other available hardware, e.g., weight, less than 30 oz., small size, and low power consumption. On the other hand, this system to date has only been bench qualified electrically. Considerable development effort will be required to package and test qualify to meet the GEM environmental conditions.

In summary, the FM/FM design criteria will be based on the following requirements:

RF carrier frequency	2.2 - 2.3 KMC
RF Power out	3 - 5 watts
Subcarrier channels	10 channel, Z channel commutated (channel frequency assignment to be determined when measurement list is firmed)
In-flight calibration	Not required
Weight	21 pounds (including power supplies, transmitter, and commutator)

(2) PCM/FM

Pulse Code Modulation Telemetry is the most suitable choice for a guidance monitoring instrumentation subsystem for the recoverable GEM vehicle. Such technique is essentially mandatory when one considers the vast quantity of digital data that characterizes current and future guidance components. Further, it is the simplest type of transmission and provides a relatively noise free signal due to its basic on-off characteristics, and is especially worthwhile since the output signal may be readily applied to a magnetic tape record.

However, as contrasted to the more common frequency systems of telemetry, PCM systems and components at the present time are usually tailored to a specific instrumentation application. This confronts the instrumentation system designer with the problem of not having available a wide variety of standard and/or shelf item systems and components as is the case with frequency systems.

A preliminary investigation and survey of existing systems and the overall market has indicated that it will be possible to build a PCM subsystem for GEM using modified existing components or systems.

It is proposed to use an RF carrier frequency within the 2.2 to 2.3 KMC band. As with the FM/FM subsystem previously described, a similar transmitter must be used in the PCM subsystem keyed on or off by the coder converter.

It is anticipated that prime telemetry effort will be spent establishing the design criteria for a PCM/FM subsystem.

4. Determination of Analysis Technique for Optimizing Information Recovery

a. Simulation Program

The simulation program will be operational by January 29, 1962 with the exception of the addition of telemetry noise. Some modifications have been made since the documentation in Reference (6). The loop in the flow diagram that simulates the radar error and noise will be designed to handle other systems in addition to Mistran, e.g., a cruciform base line system and FPS-16 systems. The filter program, as utilized in the simulation, requires data inputs at equal time intervals. In order to circumvent an interpolation routine prior to entering the filter program, constant integration steps are being used in the N-stage trajectory computation program. The use of small integration steps, in order to increase the number of data points to correspond to the real situation, could lead to problems in round-off error propagation. This phenomenon is being investigated and, if the analysis reveals a limit, incompatible with the simulation requirements, an interpolation routine will probably be utilized.

The correlation coefficient program has been exercised on the trajectory described in Appendix 4. This preliminary result points up the desirability of the positive and negative thrust phases but, at the same time, accentuates the need for an accurate accelerometer scale factor and bias determination on a pre-flight calibration. The graphs at the end of this section represent a running time history of the cross correlation between four terms in the accelerometer error model, i.e., $\rho_{ij}(t_k)$ represents the correlation between ψ_i and ψ_j on the interval $0 \leq t \leq t_k$.

It should be emphasized that this only represents a preliminary result and further correlation studies will be performed. Due to the importance of this study and other aspects of the simulation program, interim reports will be issued to keep the study progress documented and up to date.

- b. An analytical discussion of platform orientation for gyro coefficient determination is included in Appendix 11. The study covers one particular platform and points up the cross coupling problems that will occur in the data analysis for this platform configuration.

D. Test Item Requirements

The weight and size constraints that a test item must meet, in order to be accommodated on the GEM test vehicle, are discussed in Appendix 9. Environmental conditions such as temperature limits, shock impulses, vibration and acoustic pressure are also reviewed. Based upon the requirements of present inertial and stellar-inertial systems, umbilical and access requirements are delineated.

In addition, a general listing of components and sub-systems that will be required for alignment, erection, stabilization and calibration is given in Appendix 10.

K&E 10 X 10 TO THE CM. 359T-14
 KEUFFEL & ESSER CO. MADE IN U.S.A.
 ALBANY, N.Y.

12

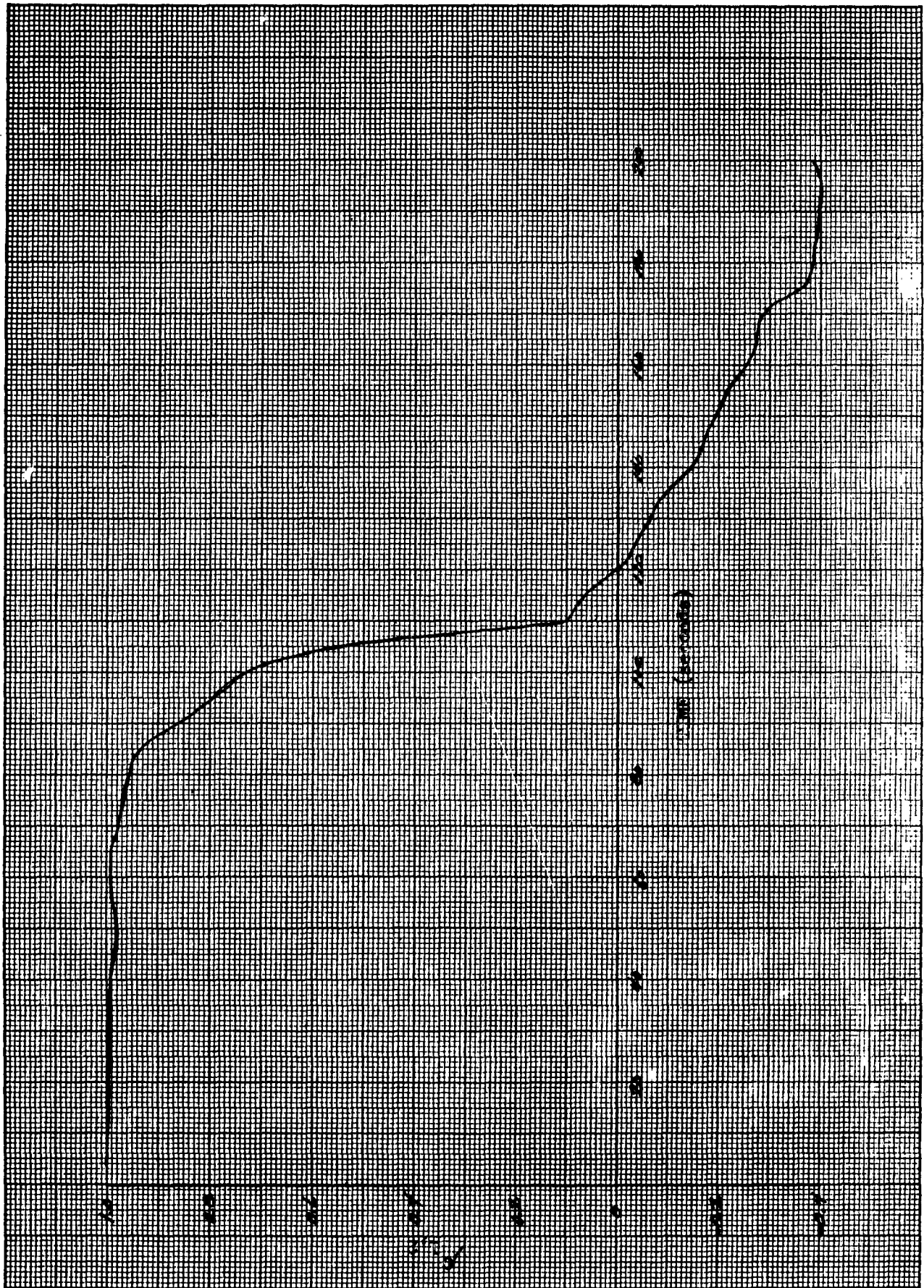


Fig. 1 Correlation Coefficient $\rho_{1,2}$

K&E 10 X 10 TO THE CM. 359T-14
 KEUFFEL & ESSER CO. MADE IN U.S.A.
 ALBANY, N.Y.

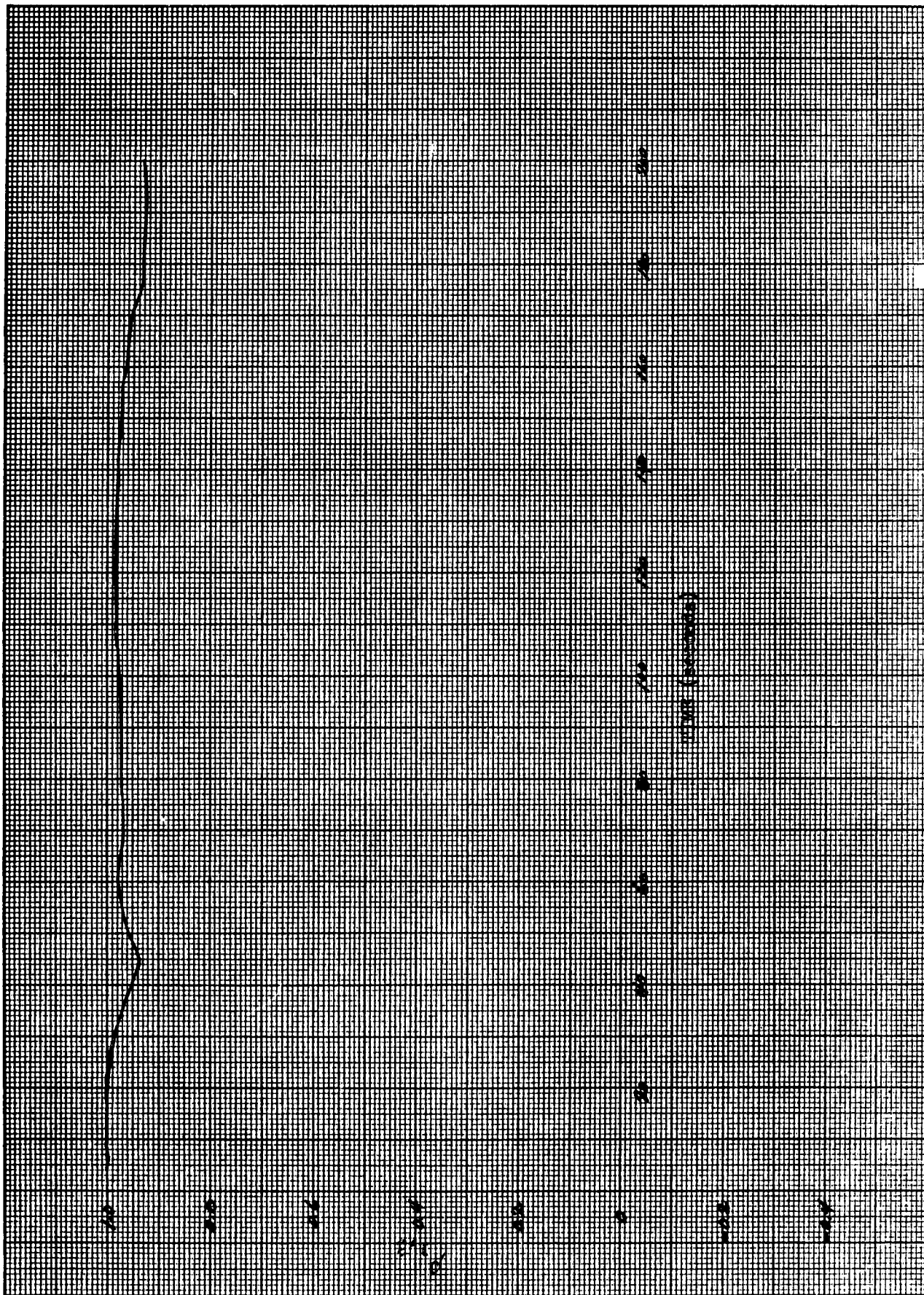


Fig. 2 Correlation Coefficient $\rho_{1.3}$

K·E 10 X 10 TO THE CM. 359T-14
KEUFFEL & ESSER CO. MADE IN U.S.A.
ALBANY, N.Y.

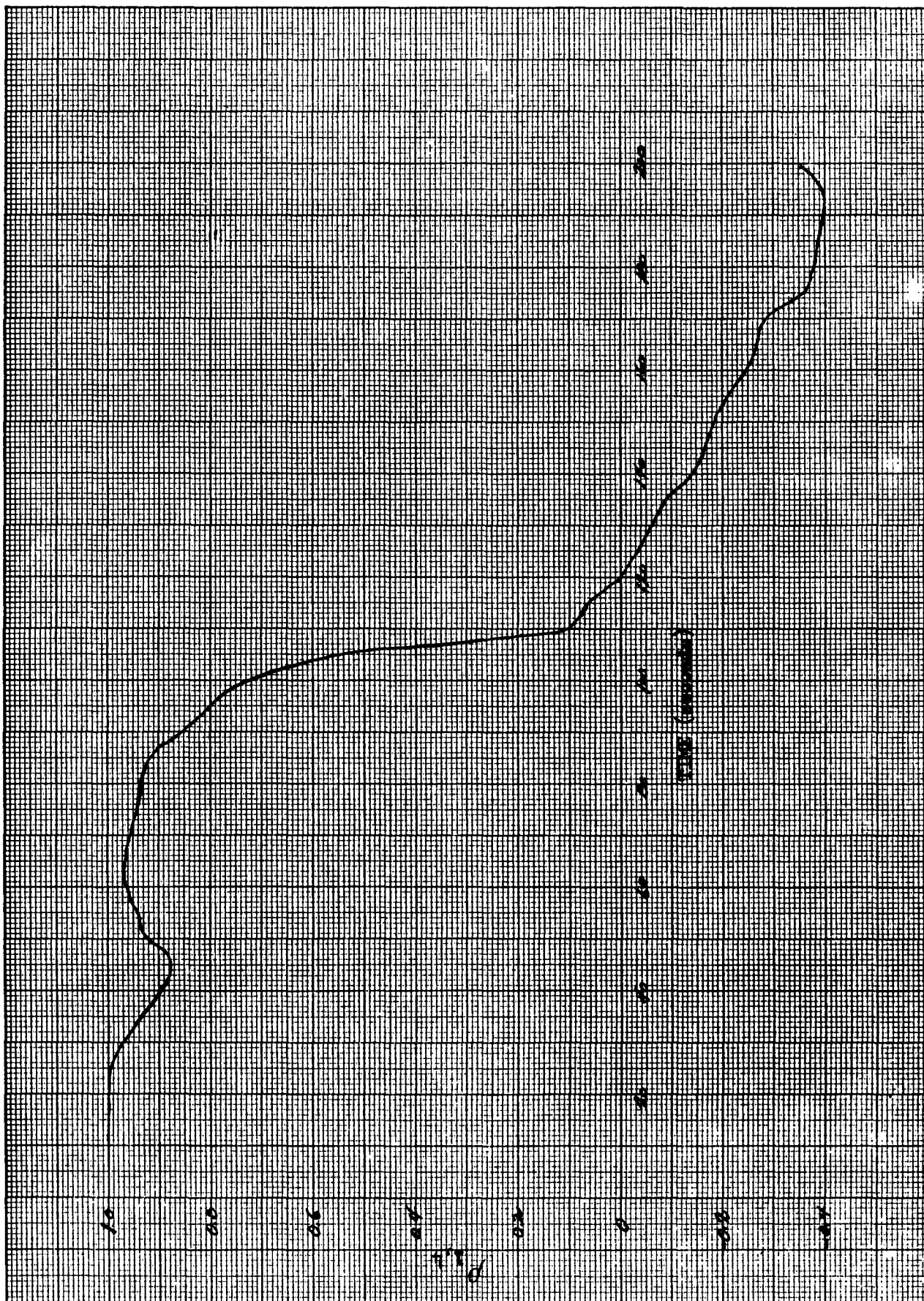


Fig. 3 Correlation Coefficient $\rho_{1,4}$

K&E 10 X 10 TO THE CM. 359T-14
 KEUFFEL & ESSER CO. MADE IN U.S.A.
 ALBANY, N.Y.

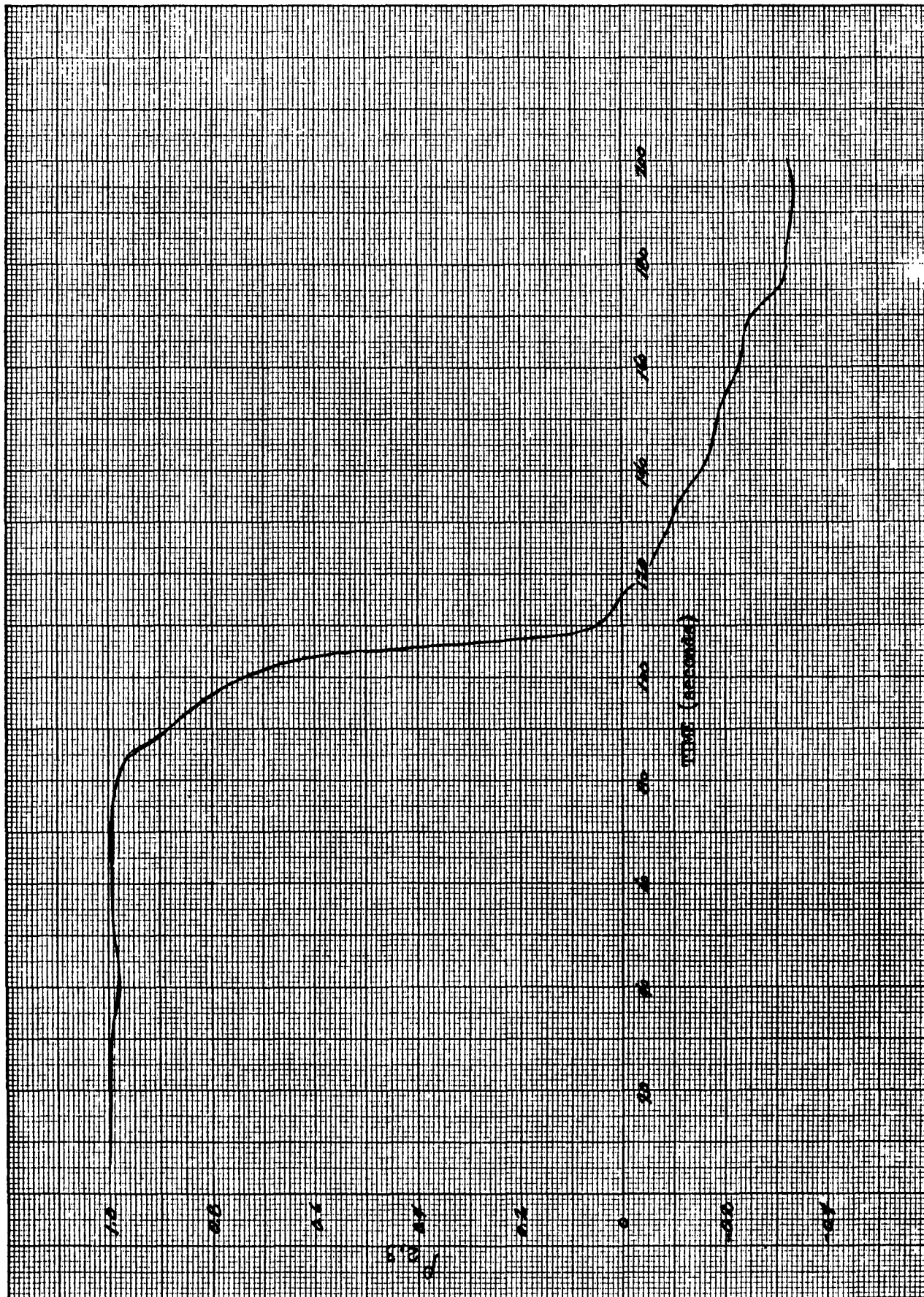


Fig. 4 Correlation Coefficient $\rho_{2.3}$

K&E 10 X 10 TO THE CM. 359T-14
 KEUFFEL & ESSER CO. MADE IN U.S.A.
 ALBANY, N.Y.

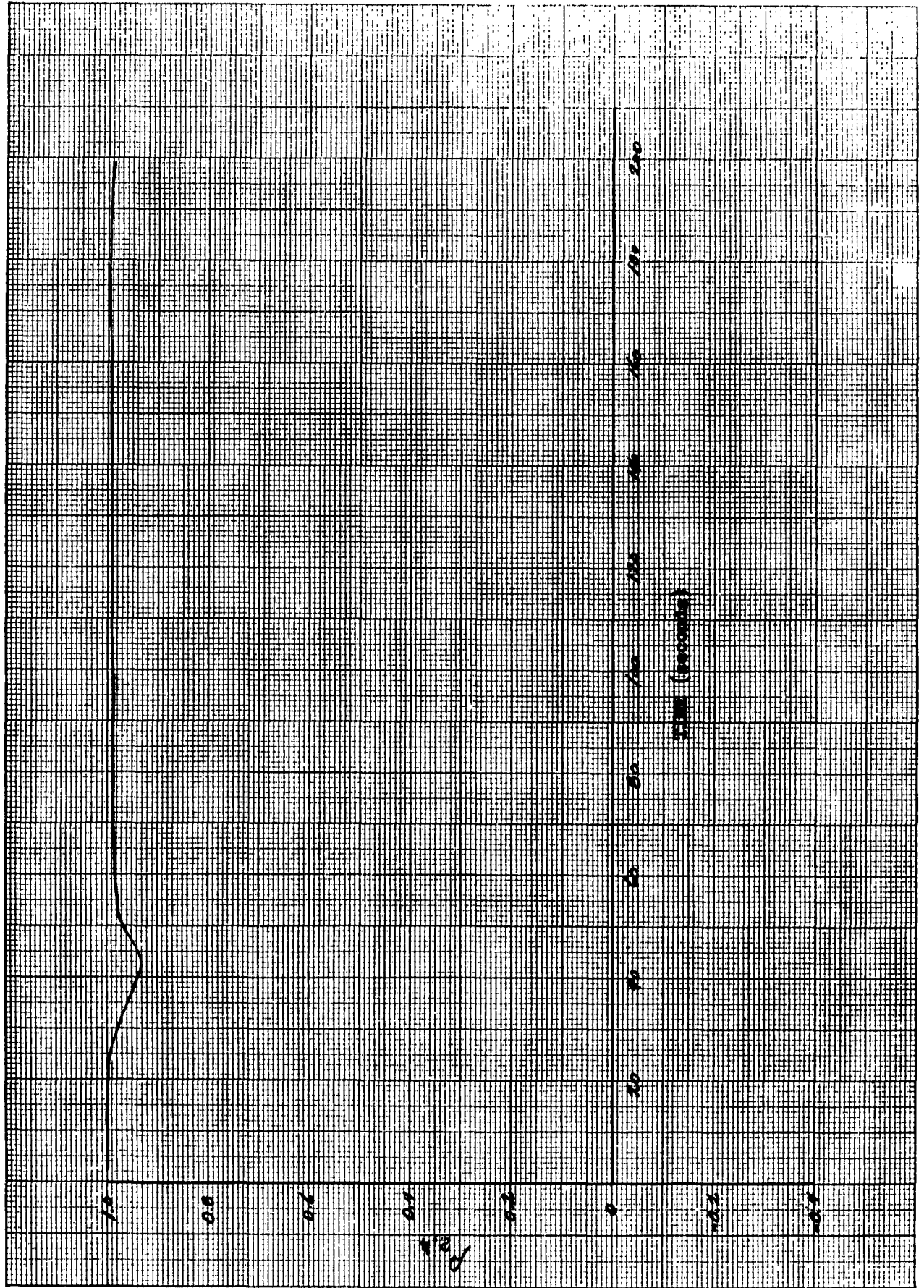


Fig. 5 Correlation Coefficient $\rho_{2,1}$

K Σ 10 X 10 TO THE CM. 359T-14
KEUFFEL & ESSER CO. MADE IN U.S.A.
ALBANY, N.Y.

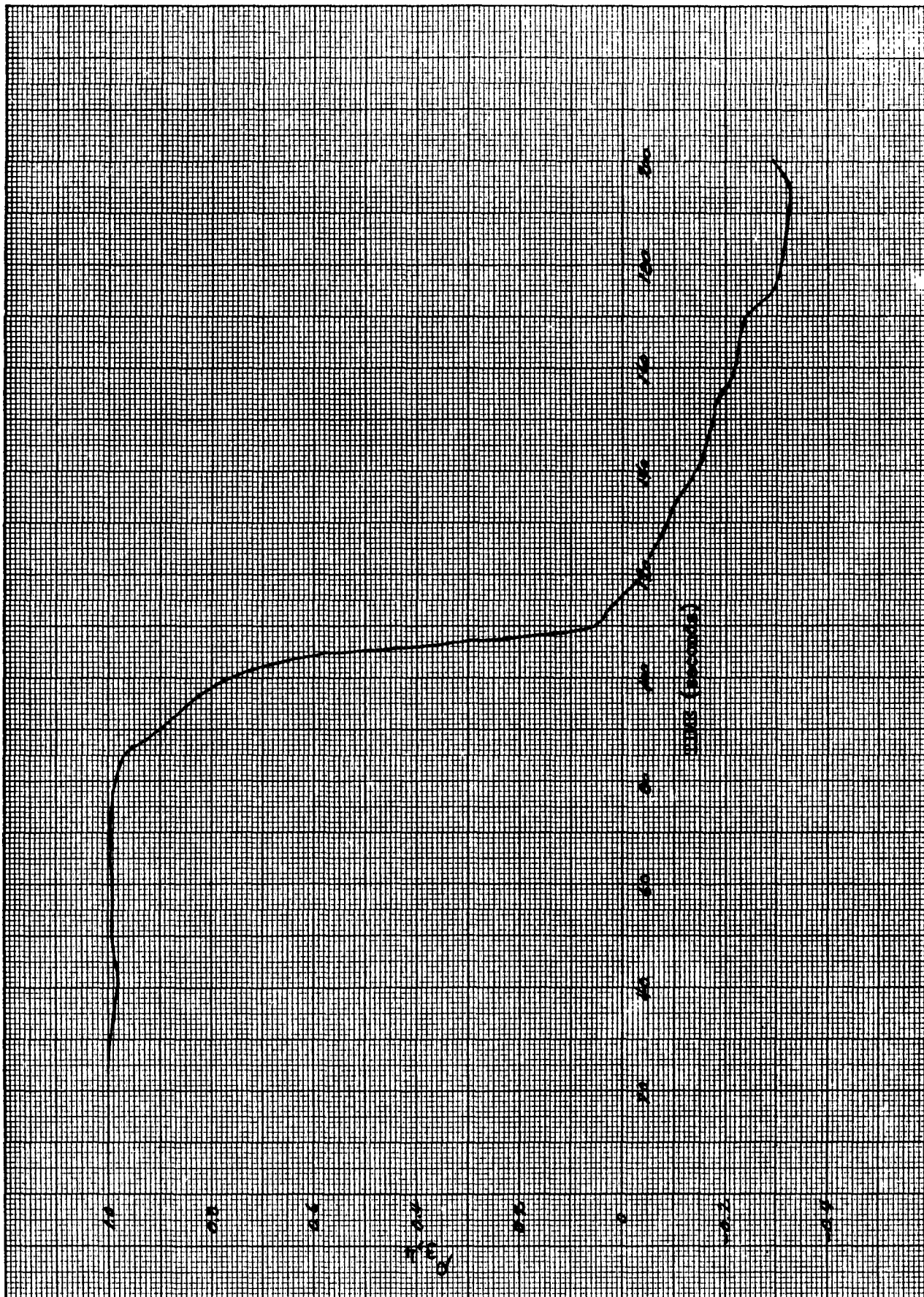


Fig. 6 Correlation Coefficient $p_{3,4}$

III. ACTUAL PROGRESS VERSUS PLANNED PROGRESS

The second month's effort has yielded anticipated progress in almost all areas as reference to Appendix 1 will indicate. The firm establishment of the trajectory program details has provided sufficient criteria to proceed with tracking system planning, aerodynamic/thermodynamic studies, and control system design.

Some few areas of effort have not reached the level of progress anticipated by the task layout for the end of the second month. The simulation program has been plagued by lack of computer priority; however, this is a management problem which has been alleviated and the program will be operational by late January. The transponder antenna study has been hampered by non-availability of tracking criteria and a tracking system layout. Such a situation cannot be completely alleviated in such a study effort as obviously all engineering can not proceed concurrently. A similar situation exists in the computation of FSV weights and centers of gravity since they are dependent upon the selection of the various components within the FSV. The final dispersion studies are paced by the weights, and center of gravity determination.

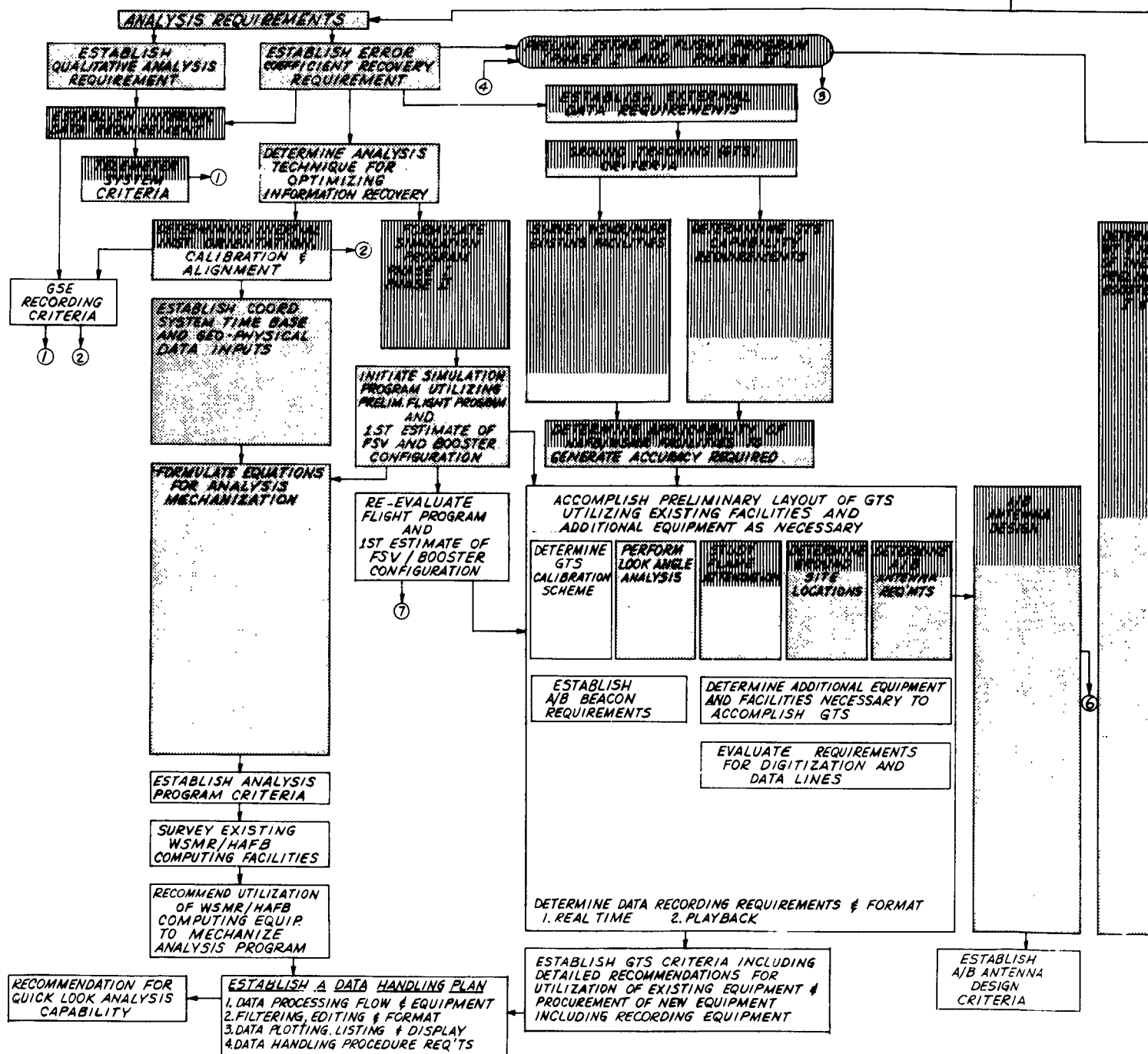
Although the above slow areas are critical to the final study completion, the situation will be overcome by concerted final month's effort to tie together all study segments. Such concentration of effort was anticipated by the task organization and is no cause for alarm.

IV. POSSIBLE SOURCES OF DELAY TO THE STUDY PROGRAM

Those possible sources of delay discussed in the first month's report have been dispensed with and no longer pose a problem.

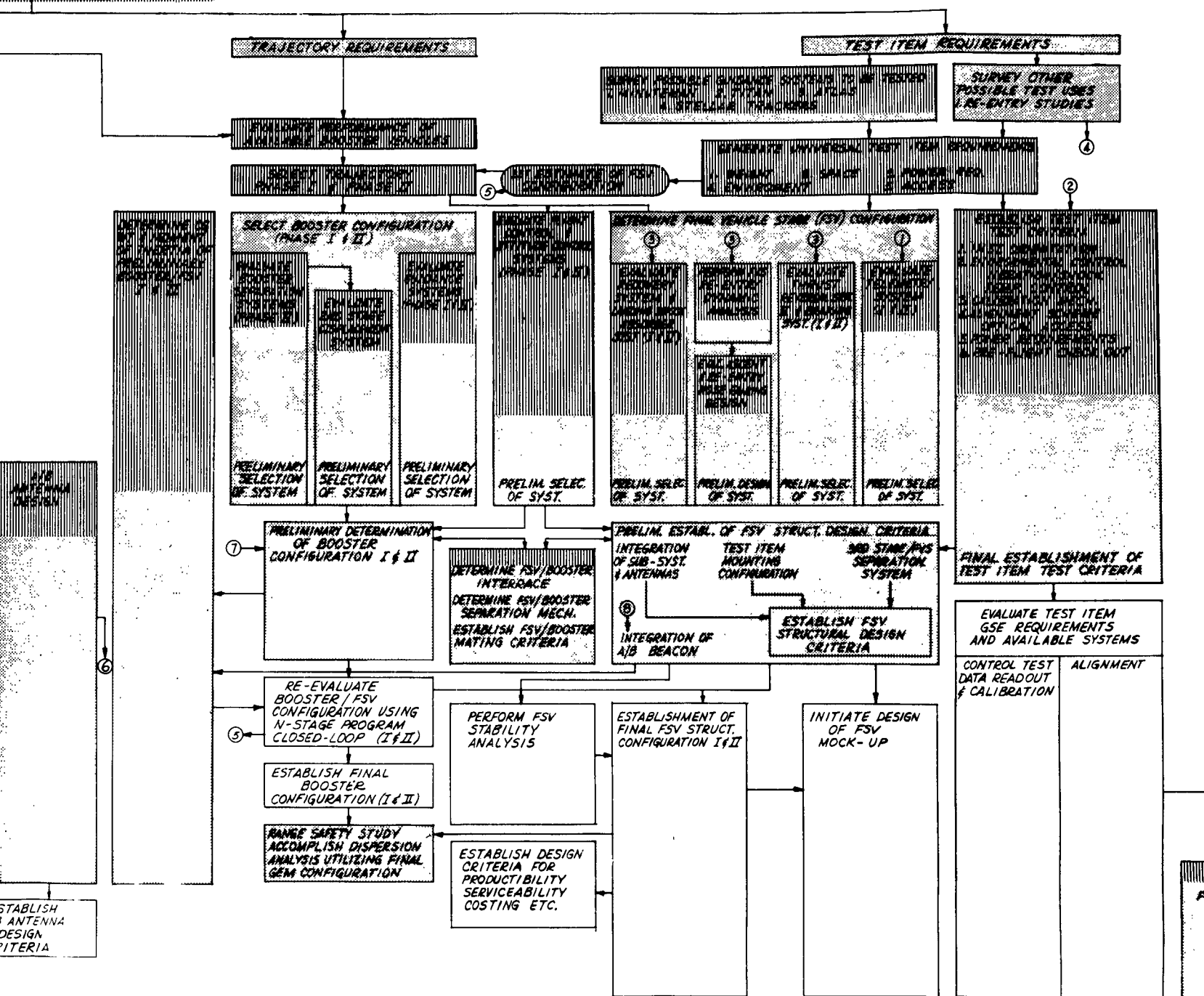
It appears at this time that no foreseeable study delay sources exist other than within the task organization. If these do become critical, they will be resolved.

Appendix 1
ENGINEERING TASK LAYOUT -
PROJECT GEM



TASK LAYOUT

MISSION OBJECTIVES
CONSTRAINTS



Appendix 2
GROUND TRACKING
SYSTEM CRITERIA

APPENDIX 2

GROUND TRACKING SYSTEM CRITERIA

A. CORRECTION AND CLARIFICATION OF THE TRACKING SYSTEM ACCURACY STUDY

Appendix 4 of Reference 6 has an error in the equation at the bottom of the first page (page 29 of the Progress Report). The equation is not complete and should read:

$$\Delta V_{\max}^2 = (\Delta \dot{R} + R\dot{\theta}\Delta\theta)^2 + (\Delta R\dot{\theta} + R\Delta\dot{\theta} + \dot{R}\Delta\theta)^2$$

This adds the term $R\dot{\theta}\Delta\theta$, an error in the range rate direction, but does not add a new error source since $\Delta\theta$ has been considered in the last half of the equation. If the $R\dot{\theta}\Delta\theta$ error were large however, it would result in a reduction of the maximum allowable $\Delta\theta$. On Page 31, $(\dot{R})_{\max}$ was realistically assumed to be $V_{\max}/2$ or 5,000 ft/sec. and, on page 33, $\Delta\theta_{\max}$ was limited to 2×10^{-6} radians. Under these conditions, $(R\dot{\theta}\Delta\theta)$ would have a maximum value of 1×10^{-2} ft/sec. Assuming $\Delta\dot{R}$ and $\Delta\dot{\theta}$ are independent errors and using RMS addition, the error in the \dot{R} direction would increase from 0.02 ft/sec to 0.022 ft/sec. The addition of this term does not have a significant effect on the preliminary considerations for GEM trajectories. It should be noted that the analysis developed in Appendix 3 of the Monthly Progress Report No. 1 did include this term.

Throughout the discussion of the errors in measured parameters, an average value of ΔV^2 or $\Delta \dot{V}^2$ is implied, i.e., $\Delta\theta$, $\Delta\dot{\theta}$, $\Delta\dot{R}$ and $\Delta\ddot{R}$ are assumed to be error sources with zero mean and standard deviation given by the Δ 's.

Statistical independence of the error sources is assumed and rms addition of the individual variances may be used to obtain the total variance, since covariances between error sources are zero under this assumption.

Certain favorable geometric considerations of the GEM trajectory were not incorporated in the preliminary study leading to a pessimistic estimate of the error arising from certain terms. The net effect of these errors would be reduced, by perhaps a factor of 2, when one considers that the velocity is minimal when range is maximal and angular rates are maximal in the early portion of the flight. Furthermore, the values used in the analysis are larger than would be encountered on the GEM trajectory described in Appendix 7. Consequently, under the impact of these errors, the system would provide a velocity with an accuracy of from 0.005 to 0.02 ft/sec in all directions of interest for inertial guidance evaluation.

It should be understood that this preliminary study was directed at only those error sources which are directly specified in the basic measurement equations. The error sources considered were:

- (1) Equipment phase shifts vs. ranging frequency.
- (2) Velocity of light uncertainties.
- (3) Frequency uncertainty.
- (4) Frequency measurement accuracy and equipment frequency shifts.
- (5) Short term stabilities.
- (6) Minimum baseline requirements vs. phase stability of angle measuring equipment.
- (7) Difference frequency measurement requirements.
- (8) Survey accuracy.

Error sources which are expected in an accurate tracking system but which were not discussed directly include:

- (1) Quantization and roundoff errors.
- (2) Multipath.
- (3) Dynamic response errors.
- (4) Timing errors.
- (5) Propagation errors.
- (6) Calibration errors.
- (7) Noise.

B. BASELINE REQUIREMENTS

There are certain considerations which dictate the baseline length requirements of an interferometer system in order to obtain a given accuracy. The following paragraphs will discuss the most important factors and from this discussion, conclude the requirements for the baseline lengths needed for GEM accuracies.

1. Survey

The best survey, between benchmarks, will have an accuracy of about 2 parts per million in both distance and angular direction. The uncertainty in the position of the receiving antenna, i.e., the phase center of the antenna, with respect to the benchmarks must be considered and, in order to keep this measurement from deteriorating the survey accuracy, the uncertainty in the location of the phase center divided by the baseline length should not exceed one part per million. If 0.01 feet is a reasonable value for the accuracy in location and stabilization of the phase center of the antenna with respect to a benchmark, a minimum baseline of 10,000 feet is required.

2. Propagation

Fluctuation of the index of refraction along the ray paths to a missile, due to the motion of a nonhomogeneous atmosphere with respect to the line of sight, will result in low frequency noise in the measurement of the angle of arrival of the signal. This effect has been measured at Maui, Hawaii and Colorado. A similar noise has been evidenced in tracking systems at AMR. The noise in angular measurement is baseline dependent and will result in angular and angular rate errors (see References 8 and 16).

If the baseline is 10,000 feet, the effective baseline is reduced to 3,500 feet when the elevation angle of the line of sight is 20° . For an effective baseline of 3,500 ft., the average value of the Maui data gives an rms angular error of about 5 microradians (Reference 2). The atmosphere at Colorado may more nearly reflect that of White Sands, consequently, an average error of 2 microradians would be more likely with similar effective baseline conditions. The elevation angle will be greater than 45° for most of the GEM flight and, with a 10,000 ft. baseline, the average error may be anticipated as 1 microradian, an acceptable condition for meeting GEM requirements, except at very low elevation angles.

The effect of this atmospheric noise on angular rate errors is dependent on both the baseline length and the smoothing time or averaging time as discussed in the references. If the minimum cutoff frequency allowable in the GEM data reduction is 1/2 cps, the averaging time applicable to the Maui data is about 1 second.

For 1 second smoothing with an effective baseline length of 7,000 feet, the Maui data would indicate an rms angular rate error of about .25 microradians/second. At White Sands, this may be expected to be reduced to about 0.1 microradians/second.

The magnitude of the noise is approximately proportional to the inverse of the product of baseline length and the square root of the smoothing time.

The angular rate errors will result in velocity errors normal to the line of sight and with magnitude $R\dot{\theta}_{rms}$. At a range of 10^6 feet and with a baseline of 10,000 ft, the error will have an rms magnitude of 0.1 ft/sec but, for the basic GEM trajectory, the range will not exceed 5×10^5 feet in which case the error would be 0.05 ft/sec. If it is desirable to reduce this error to 0.025 ft/sec, at maximum range, a 20,000 ft. baseline is necessary.

3. Range Differences and Range Rate Differences Accuracy

An error in the measurement of range differences and range rate differences is related to an angular measurement and an angular rate measurement respectively by:

$$\theta = \frac{\Delta D}{(\sin \theta)b} \quad \dot{\theta} = \frac{\Delta \dot{D}}{(\sin \theta)b}$$

where b is the baseline length.

GE Mod III data, Mistram specifications and STL studies performed in the Advanced Guidance System contract suggest that the limiting accuracy in ΔD is about .01 ft. and that the limiting accuracy in $\Delta \dot{D}$ is about .001 ft/sec. These values give rise to angular error and angular rate errors that are the same magnitude as the propagation errors discussed above. Therefore, the conclusions concerning baseline length, discussed in the propagation section, also apply here.

4. Conclusions

From the above discussion, it is apparent that the minimum baseline acceptable is 10,000 ft. and that the above error sources will result in lateral velocity errors of .1 ft/sec at a range of 1,000,000 ft. and .05 ft/sec at the maximum range of the standard GEM trajectory. A baseline of 20,000 ft. would reduce these errors to about .02 ft/sec on the standard GEM trajectory and to about .05 ft/sec on the delayed thrust trajectory.

C. INTERFEROMETRIC SYSTEM SURVEY ERRORS

There are three types of errors which should be considered:

- . Azimuth misalignment of baselines
- . Error in length of baseline
- . Horizontal plane (elevation) misalignment of baselines

1. Effect of Survey Errors on Measurement of Angles

Consider a system which measures $\ell = \cos \alpha$, $m = \cos \beta$ and R (azusa coordinates).

a. If the azimuth of the baselines are misaligned by dA_ℓ and DA_m for the ℓ and m legs respectively, then the errors in ℓ and m caused by this misalignment are given by:

$$d_\ell = m dA_\ell; \quad d_m = -\ell dA_m$$

If the measurements are calibrated at m_0 and ℓ_0 , then the survey error after calibration is:

$$d_\ell = (m - m_0) dA_\ell; \quad d_m = -(\ell - \ell_0) dA_m \quad (1)$$

b. If the theoretical baseline length is k and there is an error of dk in the measurement of k , then the resulting errors in ℓ and m are given by:

$$d\ell = \ell \frac{dk}{k} \quad d_m = m \frac{dk}{k_m}$$

After zero set the errors are:

$$d\ell = (\ell - \ell_0) \frac{dk}{k}; \quad d_m = (m - m_0) \frac{dk}{k_m} \quad (2)$$

c. For an error of dE_ℓ in the angle between the ℓ leg and the local horizontal and a similar error dE_m for the m leg, the resulting errors in ℓ and m are:

$$d\ell = \sin E \, dE_\ell; \quad d_m = \sin E \, dE_m$$

letting $\sin E = n$ and the calibrated value of $\sin E_0 = n_0$, then the post calibration error in ℓ and m are:

$$d\ell = (n - n_0) \, dE_\ell; \quad d_m = (n - n_0) \, dE_m \quad (3)$$

To transform errors in ℓ and m to errors in angle A and E , consider the case when ℓ contains the trajectory plane, then $m \approx 0$ and $\ell = \cos E$

$$dA = \frac{dm}{\cos E}; \quad dE = -\csc E \, d\ell \quad (4)$$

The errors in A and E caused by survey errors are given in the following tables:

TABLE 2 - Without Zero Set

	<u>Azimuth Errors</u>	<u>Length Errors</u>	<u>Elevation Errors</u>
dA	dA_m	≈ 0	$\tan E \, dE_m$
dE	≈ 0	$\csc E \frac{dk}{k}$	dE_ℓ

TABLE 2 - With Zero Set

	<u>Azimuth Errors</u>	<u>Length Errors</u>	<u>Elevation Errors</u>
dA	$(1 - \frac{\cos E_0}{\cos E}) dA_m$	$(-\cos \beta_0) / \cos E \frac{dk}{k_m}$	$(\frac{\sin E - \sin E_0}{\cos E}) dE_m$
dE	$(-\cos \beta_0) / \sin E \, dA_\ell$	$(\frac{\cos E - \cos E_0}{\sin E}) \frac{dk}{k}$	$(1 - \frac{\sin E_0}{\sin E}) dE_\ell$

2. Effect of Survey Errors on the Measurement of Angular Rates

From the preceeding paragraph the velocity errors can be obtained as follows:

a. Without Zero Set

From equations (1), (2) and (3)

$$d\dot{\ell} = \dot{m} dA_{\ell} \quad d\dot{m} = -\dot{\ell} dA_m \quad (1')$$

$$d\dot{\ell} = \dot{\ell} \frac{dk_{\ell}}{k_{\ell}} \quad d\dot{m} = \dot{m} \frac{dk_m}{k_m} \quad (2')$$

$$d\dot{\ell} = \cos E \dot{E} dE_{\ell} \quad d\dot{m} = \cos E \dot{E} dE_m \quad (3')$$

From equations (4)

$$d\dot{A} = \frac{d\dot{m}}{\cos E} + \frac{\sin E (\dot{E})}{\cos^2 E} dm$$

$$d\dot{E} = -\frac{d\dot{\ell}}{\sin E} + \frac{\cos E (\dot{E})}{\sin^2 E} d\ell$$

(1) Azimuth Rate Errors

$$\begin{aligned} d\dot{A} = & \left[\frac{-\dot{\ell}}{\cos E} - \frac{\sin E (\dot{E})}{\cos^2 E} \ell \right] dA_m \\ & + \left[\frac{\dot{m}}{\cos E} + \frac{\sin E (\dot{E})}{\cos^2 E} m \right] \frac{dK_m}{K_m} \\ & + \left[\dot{E} + \frac{\sin E (\dot{E})}{\cos^2 E} \sin E \right] dE_m \end{aligned} \quad (5)$$

$$\text{letting: } \ell = \cos E \quad m \approx 0$$

$$\dot{\ell} = \sin E (\dot{E}) \quad \dot{m} = \cos E (\dot{A})$$

Then

$$\begin{aligned} d\dot{A} = & \left[\tan E(\dot{E}) - \tan E(\dot{E}) \right] dA_m \\ & + \left[\dot{A} + 0 \right] \frac{dk_m}{k_m} \\ & + \left[\dot{E} + \tan^2 E(\dot{E}) \right] dE_m \end{aligned}$$

or:

$$d\dot{A} \cong \dot{A} \frac{dk_m}{k_m} + \frac{\dot{E}}{\cos^2 E} dE_m \quad (6)$$

(2) Elevation Rate Errors

Similar to preceeding paragraph:

$$\begin{aligned} d\dot{E} = & \left[-\frac{\dot{m}}{\sin E} + \frac{\cos E(\dot{E})}{\sin^2 E} m \right] dA_l \\ & + \left[-\frac{\dot{l}}{\sin E} + \frac{\cos E(\dot{E})}{\sin^2 E} l \right] \frac{dk_l}{k_l} \\ & + \left[-\text{ctn } E(\dot{E}) + \frac{\cos E}{\sin E} \dot{E} \right] dE_l \end{aligned} \quad (7)$$

and then:

$$\begin{aligned} d\dot{E} = & \left[\text{ctn } E(\dot{A}) + 0 \right] dA_l \\ & + \left[(\dot{E}) + \text{ctn}^2 E(\dot{E}) \right] \frac{dk_l}{k_l} \\ & + \left[-\text{ctn } E(\dot{E}) + \text{ctn } E(\dot{E}) \right] dE_l \end{aligned}$$

or:

$$= \text{ctn } E(\dot{A}) dA_l + \frac{\dot{E}}{\sin^2 E} \frac{dk_l}{k_l} \quad (8)$$

b. With Zero Set

$$\begin{aligned} d\dot{A} \cong \dot{A} \frac{dk_m}{k_m} + \frac{\dot{E}}{\cos^2 E} dE_m \\ + \left[\frac{\sin E \dot{E}}{\cos^2 E} \right] \left[\ell_o dA_m - m_o \frac{dk_m}{k_m} - \sin E_o dE_m \right] \end{aligned} \quad (9)$$

$$\begin{aligned} d\dot{E} = \text{ctn } E(\dot{A}) dA_\ell + \frac{\dot{E}}{\sin^2 E} \frac{dk_\ell}{k_\ell} \\ - \left[\frac{\cos E(\dot{E})}{\sin^2 E} \right] \left[m_o dA_\ell + \ell_o \frac{dk_\ell}{k_\ell} + \sin E_o dE_\ell \right] \end{aligned} \quad (10)$$

or:

$$\begin{aligned} d\dot{A} = \left[\dot{A} - \frac{m_o \sin E(\dot{E})}{\cos^2 E} \right] \frac{dk_m}{k_m} \\ + \left[\frac{\sin E(\dot{E}) \ell_o}{\cos^2 E} \right] dA_m \end{aligned} \quad (11)$$

$$\begin{aligned} + \left[\frac{\dot{E}}{\cos^2 E} \left\{ 1 - \sin E \sin E_o \right\} \right] dE_m \\ d\dot{E} = \left[\text{ctn } E(\dot{A}) - \frac{\cos E(\dot{E}) m_o}{\sin^2 E} \right] dA_\ell + \left\{ \frac{\dot{E}}{\sin^2 E} + \frac{\ell_o \cos E(\dot{E})}{\sin^2 E} \right\} \frac{dk_\ell}{k_\ell} \\ + \left[\frac{\sin E_o \cos E(\dot{E})}{\sin E} \right] dE_\ell \end{aligned} \quad (12)$$

If the zero set is done near burnout by the use of ballistic camera data, then there will be no position error near that point due to the survey of the electronic systems but only that due to calibration. The velocity error due to the electronic system survey errors is given by the first terms of 5 and 7, i.e.:

$$\dot{dA} = \tan E(\dot{E}) \dot{dA}_m + \dot{A} \frac{dk_m}{k_m} + \dot{E} \dot{dE}_m \quad (13)$$

$$\dot{dE} = \cot E(\dot{A}) \dot{dA}_\ell + \dot{E} \frac{dk_\ell}{k_\ell} - \csc E(\dot{E}) \dot{dE}_\ell \quad (14)$$

c. Conclusion

It can be seen from equations 6, 8, 13 and 14 that regardless of calibration there is an error in the measurement of angular rates that is proportional to the angular rate and is minimized when the elevation angle E is 45° and can be approximated by

$$\dot{dE} \approx 2\dot{E} ds$$

where ds is the survey error. Further, all errors are assumed to be uncorrelated and the following equalities hold:

$$ds = dE_\ell = dE_m = dA_\ell = dA_m = \frac{dk_\ell}{k_\ell} = \frac{dk_m}{k_m}$$

If the elevation angle is kept to within 70° to 20° , the angular rate error, with calibration, is approximately bounded by:

$$2\dot{E} ds \leq \dot{dE} = \dot{dA} \leq 4\dot{E} ds$$

Equations similar to 11 and 12 should be examined in detail once the trajectory as well as the location, configuration and orientation of the tracking system have been determined.

To aid in the grasp of the importance of these terms, an error in the measurement of $\dot{\theta}$ ($\theta = A$ or E) will result in a velocity error at the missile equal to $R\Delta\dot{\theta}$. If R is 200,000 ft. and the effect of $R\Delta\dot{\theta}$ is to be kept less than .02 ft/sec then $\Delta\dot{\theta}$ must be less than 10^{-7} . If the velocity normal to R is 2,000 ft/sec then $\dot{\theta}$ would be .01 radian/sec. Further, if the survey error amounts to 2.5×10^{-6} and E is near 20 degrees, the $\Delta\dot{\theta}$ due to survey alone is 10^{-7} .

Appendix 3
SUMMARY OF WORK/HAZARD
EXISTING FACILITIES

APPENDIX 3

SURVEY OF WSMR/HAFB EXISTING FACILITIES

A. INTRODUCTION

A survey of the available tracking systems at White Sands with some remarks as to the applicability of these systems to GEM was included in last month's progress report (Reference 6). The following paragraphs will discuss the anticipated accuracy of the White Sands systems to the extent that available information will permit.

Before proceeding with this task, it would be well to restate the required tracking system accuracy as derived in Reference 7. The Class II requirements listed in Table 8 of this reference gives a requirement of .05 ft/sec in the range and lateral directions. The approximate accuracy needed, in tracking system coordinates, to meet the above requirements are .02 to .05 ft/sec in range rate, 1 to 5 ft in range, 5 to 10 microradians in angle, and .05 to .1 microradians/second in angular rate.

Some of the errors treated in this appendix, such as propagation errors and survey errors, have been treated in detail in Appendix 2 and are discussed again here only for the sake of completeness.

B. ERRORS IN WHITE SANDS TRACKING SYSTEMS

It is difficult to talk in specific terms about the errors in the White Sands ITS (Integrated Tracking System) because it is not a single coherent system but a combination of at least three types of systems, AME's, DME's, and a Doppler system, and, in addition, more than one of each type may be included in the over-all ITS. Therefore, in order to estimate the tracking system capability, a system will be selected which appears to represent the best non-redundant system that can be achieved

at White Sands. If then, two of these basic systems are used to track the missile, it might be expected that the over-all error should be reduced by a factor of $\sqrt{2}$, assuming equal geometric dilution of precision for the two systems.

AME, DME, and Doppler

This system is assumed to be composed of one DME (operating continuously rather than time sharing the beacon with other DME's), one AME (operating on the DME carrier), and three coherent Doppler stations situated so as to form an L with the center station near the DME-AME site. In this system, the AME-DME is used to obtain position and the Doppler receivers used to obtain three velocity components. Table 1 lists an estimated error budget for this system. The reasoning used to obtain these estimates is given below:

(1) Equipment Errors

A detailed analysis of the equipment errors has not been made available, therefore, the below estimates are based on what little is known about the equipment errors and a few general estimates.

AME - The only errors given by White Sands were 3 ppm noise jitter and 2 ppm quantization. If phase shift uncertainties amounted to 1 electrical degree, then an additional error of 4 ppm would result in the angular measurements. Therefore, a conservative estimate of RSS equipment error is taken as 5 ppm.

DME - Quantization error was given as 1 foot. Assuming a one electrical degree phase shift in the 480 kc ranging frequency would cause an error of about 3 feet, an over-all equipment error of 3 feet would probably be optimistic.

Doppler (Range Rate) - White Sands gives an estimated accuracy of .1 ft/sec.

Doppler (Range Rate Difference or Angular Rates) - These errors are unknown except that they depend, among other things, on the basic Doppler oscillator stability, on the distance between the stations, on the stability of the connection between the stations over which the oscillator frequency is transmitted, and on the accuracy of the timing and data recording.

(2) Tropospheric Propagation

The errors due to tropospheric propagation are based on the tests performed at Maui, Hawaii, as reported in Reference 8.

AME - The Maui data shows that for baselines of 460 feet, the average value of rms angular errors due to tropospheric noise was about 21 microradians. At White Sands, the atmosphere may be less critical than at Maui, therefore, an average value of 7 microradians will be assumed. This value will increase as the effective baseline is reduced at low elevation angles, e.g., at an elevation angle of 30° , the effective baseline length would be 230 feet and the expected atmospheric noise would be about 10 microradians.

DME - With a calibration of the ground index of refraction within an hour or so of launch, the error in the range correction should be no greater than 1 to 2 feet.

Doppler (Range Rate) - The Maui data shows that errors in range rate should be no greater than .005 ft/second.

Doppler (Range Rate Differences or Angular Rate) - This error is unknown for the hypothesized system but the cause and magnitude of this type error is discussed in Appendix 2. If the baseline length between coherent Doppler receivers were known, the error could be estimated.

(3) Ionospheric Propagation Errors

Ionospheric propagation errors were based on material contained in References 10 and 11. An altitude of 100 nautical miles and an elevation angle of about 65° were used to obtain the estimate. This is slightly higher than the Phase 1A trajectory apogee and it is about one-half of the Phase 1B trajectory. An average figure between day and night effects was used since the daytime effects will be about twice the given values and the nighttime effects are expected to be about one-half the given values. Ionospheric errors are inversely proportional to the square of the frequency and a frequency of 300 mc was used for the estimate.

(4) Survey Errors

The best survey accuracy presently available at White Sands is about 5 ppm. This error will affect both angle and angular rate errors but will not affect range or range rate measurements.

DME - In addition to the above benchmark survey accuracy, there will be an effective survey error due to the error in stable placement of the receiving phase centers of the system with respect to the benchmarks (see Appendix 2). It is estimated that the placement error could be kept to within .01 foot (1/8 inch). For the 460-foot baseline

length of the AME, this would cause an apparent survey error of about $.01/460 = 22$ ppm which will induce a trajectory dependent angular error, conservatively approximated by a mean value of $\sqrt{2}$ times the survey error or, for this case, about 30 ppm.

Doppler (Range Rate Differences or Angular Rates) - It is shown in Appendix 2 that the angular rate error is proportional to the angular rate and can be approximated by a mean value of $2 \dot{\theta} ds$ where $\dot{\theta}$ is the angular rate and ds is the survey error. Assuming an average value of .01 radians/second for $\dot{\theta}$ over a large portion of the trajectory, the angular rate error induced by a survey error of 5 ppm will be .1 microradians/second.

(5) Calibration

The accuracy of calibration cannot be determined without knowledge of the techniques and equipment used for calibration. Calibration affects position accuracy but not range rate or range rate differences. If, during the flight, ballistic camera data were used to calibrate the AME, or any other angular measurement, the best that can be expected is an accuracy of 5 to 10 ppm. Range calibration should be accurate to 1 to 2 feet using calibration beacons on the ground. These figures will be used to estimate the calibration error although they are not based on the AME and DME equipment but are general order of magnitude numbers for a good system.

(6) Flame Effects

The effects of flame on the phase of a signal is not known or at least, not yet documented but the amplitude effects

have been observed and reported. An estimate of the magnitude of these effects will not be attempted but a tracking criteria for avoiding propagation throughout the plume will be used. The effective area of the plume and the magnitude of the attenuation decreases with increasing frequency. For the solid fuel Scout vehicle, the look angle necessary to avoid flame effect is estimated at 50° at the 300 mc frequency of the AME-DME-Doppler System. This is based on data in Reference 12 which describes the flame effects on telemetry signals during the firing of a Scout vehicle at Langley Field.

C. CONCLUSIONS

The data in Table 3, which is considered to be an optimistic error budget, shows that the errors of the best possible tracking system at White Sands is at least 4 to 5 times larger than the GEM requirements, giving errors of about .25 ft/sec in the range and lateral direction.

This system is not now available at White Sands and could only be achieved with a detailed and complete implementation planning program, especially in the interconnecting of the Doppler sites and in reducing possible error due to timing between the parts of the system.

If a more thorough analysis were possible, which included all error sources such as the term $R\dot{\theta}\Delta\theta$ in the range direction (see Appendix 2), the errors of this system could easily result in velocity errors in the range and lateral directions of .5 ft/sec or an order of magnitude larger than the GEM requirements.

TABLE I

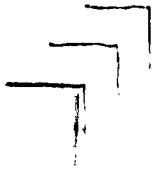
Estimated One σ Error Budget for an AME-DME-Doppler System

Source of Error	ΔR feet	$\Delta \theta$ μ radians	$\Delta \dot{R}$ ft/sec	$\Delta \dot{\theta}$ μ radians/sec
1) Equipment	3	5	.1	*
2) Tropospheric Propagation	1	8	.005	*
3) Ionospheric Propagation**	5	8	.15	.2
4) Survey Errors		30		.1
5) Calibration	2	10		
6) Flame Effect***				
RSS	6.2	34	.18	> .22

*Not sufficient data to estimate

**Based on 100 n.m. altitude

***Not estimated (see discussion)



1

(

TRAJECTORY ANALYSIS

The trajectory analysis for the chosen vehicle configuration (Algol II + Pershing B-2) has been divided into two phases which are:

Phase 1A - A trajectory where the downward thrusting firing of the B-2 stage occurs approximately 10 seconds after Algol II burnout.

Phase 1B - A trajectory where the upward thrusting firing of the B-2 stage is delayed until an altitude of approximately 600,000 feet is reached on the downward leg from apogee.

The Phase 1A trajectory gives the required positive and negative accelerations while keeping the re-entry conditions in a tolerable range. The Phase 1B trajectory gives all positive acceleration to the test item but provides a long duration of test time, again with tolerable re-entry accelerations.

Phase 1A

The Phase 1A trajectory has been determined based on nominal operation of the vehicle with no winds. The weights for the existing components of both stages were obtained from the respective manufacturers while the weights of the new design components were estimated from preliminary layout drawings. A sequential weight breakdown for the vehicle is shown in Table 1. A payload or FSV weight of 1000 pounds is still considered as the nominal for a typical mission.

The engine performance data used in the simulations were the latest available from the respective manufacturers. The actual thrust-time variations for a grain temperature of 75° were used in the simulations along with a percentage reduction for jet vane effects. The simulations were not dynamic in nature and thus the actual control effects were not realized. However, data obtained from the Martin Company indicated that a 1.5 percent loss in impulse would be realized from the four vane system of the first stage while a 0.5 percent loss in impulse was realized from the three vane system of the Pershing B-2 stage. Low values were used due to the assumption of no winds and the low magnitude pitch program required for the mission. The inert slivers in the Pershing B-2 stage were replaced with propellant thus accounting for the additional 75 pounds of expendable weight.

Phase 1A (Continued)

Removal of the slivers extends the B-2 tailoff, increases the available impulse and decreases engine cost; all of which are beneficial to the program.

The trajectories were simulated on the 7090 digital computer using the 3 Dimensional Trajectory Program with an oblate, rotating earth. A vertical launch from an altitude of 4000 feet was assumed. The coordinates of the launch location are given in Table 2. A vertical rise for a period of two seconds was followed by a pitch rate of 0.2 degree per second to a time of 10 seconds. A launch azimuth of 10 degrees from North was assumed to provide the proper impact location of the first stage. From ten seconds to fifty seconds, a pitch rate of 0.075 degrees per second was simulated followed by constant attitude flight (zero pitch rate) to $t = 60$ seconds which is the nominal first stage burnout. A ten second coast phase followed during which the first stage and nose fairing are jettisoned and displaced. The FSV and B-2 stages are controlled at constant attitude by the FSV gas jet system during the coast. At $t = 70$ seconds, the B-2 stage is ignited and flown at a pitch rate of -0.17 degrees per second for 42 seconds of the nominal 47 seconds burning time. The remaining five seconds are flown at constant attitude.

The first stage pitch program was chosen to minimize angle of attack and provide an impact range of approximately 45 nautical miles. Two pitch rates would probably have been sufficient in the first stage but the increased autopilot complexity of including the third value is negligible. The zero pitch rate at the end of both stages helps to minimize the tipoff rates during the respective separation modes. A negative pitch rate in the second stage was required to displace the FSV impact point downrange.

The nominal trajectory parameters as a function of flight time are shown in Figure 1. Included are the FSV re-entry phase, the drogue chute deployment and the main chute deployment and flight to impact. Again, instantaneous dynamics such as instant drogue and main chute deployments were assumed. Chute design was discussed with the Irving Air Chute Company from which chute characteristics were obtained as shown on Table 3. The altitude of chute deployment was assumed as 15,000 feet above sea level which is typical for payload recoveries of this type. Also, low attitude deployment reduces the impact dispersion due

to winds during the parachute phase of flight. The angle of attack and dynamic pressure as a function of first stage burning time are shown in Figure 2. As can be seen, a maximum angle of attack (no winds) of 0.74 degrees is encountered with the aforementioned first stage pitch program. Also, a maximum q (the product of dynamic pressure and angle of attack) of 678 lb-deg/ft² is attained which is considered low for a vehicle of this type.

A more detailed plot of the nominal re-entry phase is shown in Figure 3, while the re-entry conditions for the abort phase are shown in Figure 4. The worst possible abort condition in terms of maximum re-entry characteristics is the failure of the second stage to ignite and retard the first stage velocity. The maximum acceleration of 18.6 g's is probably too high for some of the test item components, however, is sufficiently low for intact recovery, repair and re-use for the majority of FSV and test item components.

Radar look angle and elevation angle as a function of flight time are shown in Figure 5. The radar location indicated on the figure is the location for one of FPS-16 units at "C" station, just south of the assumed launch facility. It is easily seen that the elevation angle requirements are met including some of the parachute phase before the elevation angle approaches the horizontal. The look angle on the other hand goes below the approximate minimum of 15 degrees during the end of first stage burning. The limit is determined by the antenna pattern, the exhaust gas composition and flame shape. In order to alleviate the look angle problem, other downrange radar sites will be investigated.

The map shown in Figure 6 indicates a plot of the instantaneous impact points for both stages of the vehicle. The furthest impact point of the FSV would be approximately that of the burned-out first stage which is the abort condition mentioned previously. The ten degree launch azimuth was required to keep the abort impact location in relatively open terrain.

Phase 1B

The nominal vehicle weight and performance used in the Phase 1A analysis was used for the Phase 1B trajectory simulation. Due to the relocation of the B-2 stage for this phase, directly on top of the Algol II in the normal manner, the assumption of the same weight history is slightly in error.

Phase 1B (Continued)

Future simulations of this phase will include a weight history consistent with the configuration layout, however, the change in performance from that presented here will be slight. The same engine performance was used for this phase as that indicated in Phase 1A.

The first stage trajectory profile is the same as 1A due to the use of the same pitch program. However, after jettisoning the first stage, the B-2 stage + FSV coast through apogee down to an altitude of approximately 620,000 feet. At this time, the ignition of the B-2 stage takes place thrusting upward to retard the overall FSV velocity. The ignition altitude was so chosen to give a maximum re-entry acceleration of approximately 10 g's. During the coast phase prior to B-2 ignition, the vehicle was reoriented slightly to provide an impact range for the FSV of approximately 40 nautical miles. Constant attitude flight was maintained during B-2 burning.

The variation of typical trajectory parameters as a function of flight time are shown in Figure 7. The long flight time of such a trajectory is ideal for obtaining errors that propagate as a function of time. The impact coordinates of the FSV are given in Table 2. Tracking requirements have to be investigated for this vehicle. It is obvious that the look angle problem mentioned for the Phase 1A trajectory exists here if the "C" station radar is considered.

Future Analysis

The dispersion of trajectory parameters due to payload changes, off nominal grain temperature, propellant loading variations, etc., will be considered in future analysis. Such dispersions will be combined with wind and control dispersions to evaluate the probable impact areas for all stages.

TABLE 1
WEIGHT HISTORY - G.E.M.
SUPER ALGOL + SECOND STAGE PERSHING*
*Incl. Jet-Vane Att. Control System

<u>Item</u>	<u>Weight, lbs.</u>
<u>VEHICLE AT LIFT-OFF</u>	<u>29,819</u>
Less Stage 1 Propellant	-21,770
Less Stage 1 Inerts	-115
<u>VEHICLE AT STAGE 1 BURNOUT</u>	<u>7,934</u>
Jettison Stage 1	-3,253
Jettison Nose Fairing	-50
<u>VEHICLE AT STAGE 2 IGNITION</u>	<u>4,631</u>
Less Stage 2 Propellant	-2,860
Less Stage 2 Inerts	-25
<u>VEHICLE AT STAGE 2 BURNOUT</u>	<u>1,746</u>
Jettison Stage 2	-746
<u>VEHICLE AT RE-ENTRY CONDITION</u>	<u>1,000</u>

TABLE 2

LAUNCH AND IMPACT LOCATIONS

LAUNCH SITE

LATITUDE	LONGITUDE
32.416°	-106.3205°

IMPACT LOCATIONS

PHASE	BURNED OUT ALGOL II		FSV	
	<u>LATITUDE</u>	<u>LONGITUDE</u>	<u>LATITUDE</u>	<u>LONGITUDE</u>
1A	33.188°	-106.328°	32.613°	-106.286°
1B	33.188°	-106.328°	33.050°	-106.258°

TABLE 3

DROGUE AND MAIN CHUTE CHARACTERISTICS

	<u>TYPE</u>	<u>DIAMETER</u>	<u>C_D</u>	<u>ALTITUDE OF DEPLOYMENT</u>
DROGUE	Fist Ribbon	17 Feet	0.5	15,000 Ft (MSL)
MAIN	Flat Circular	3 Chutes (a) 37 Feet	0.5	10 seconds after Drogue

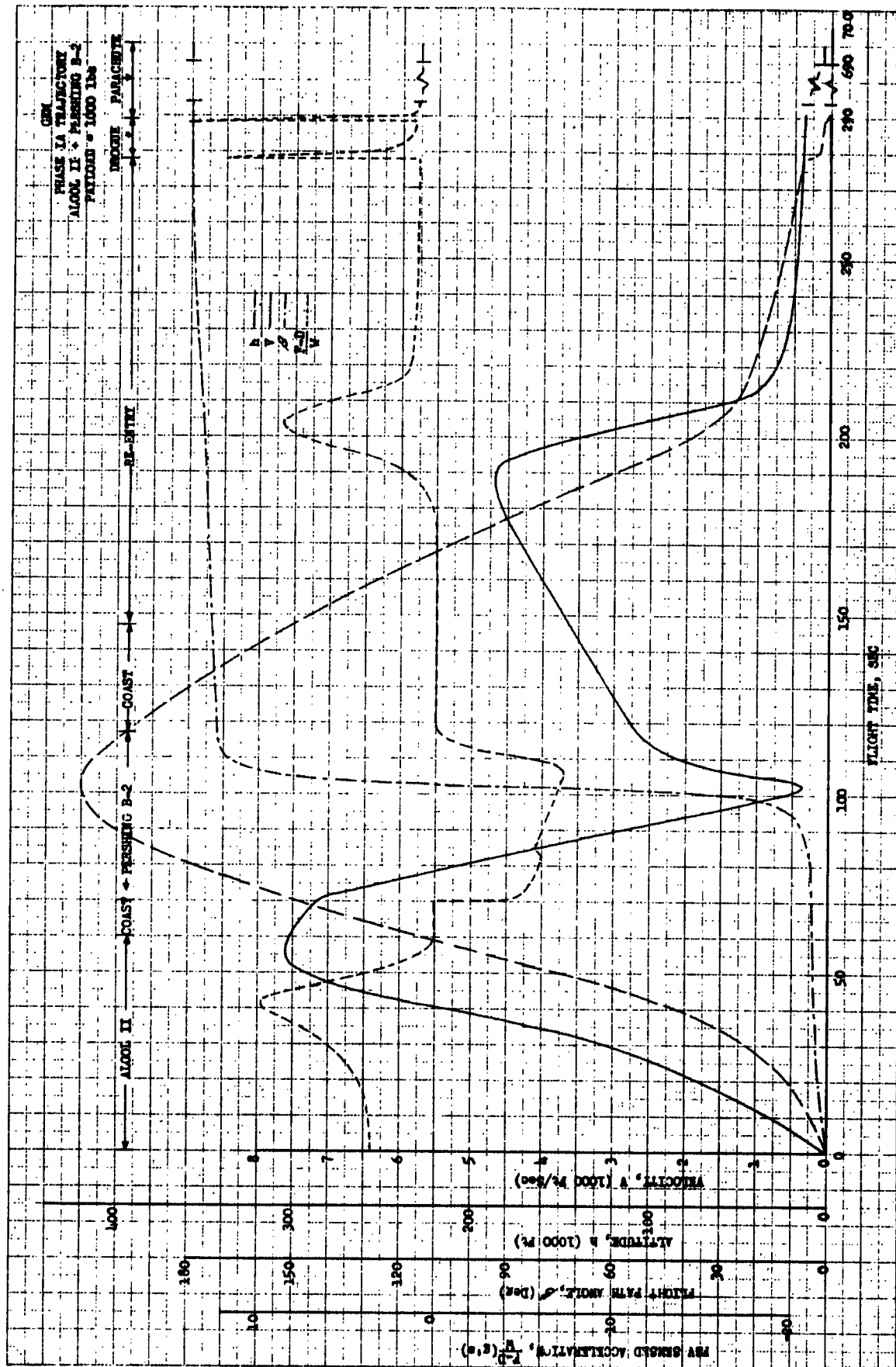


FIGURE 1

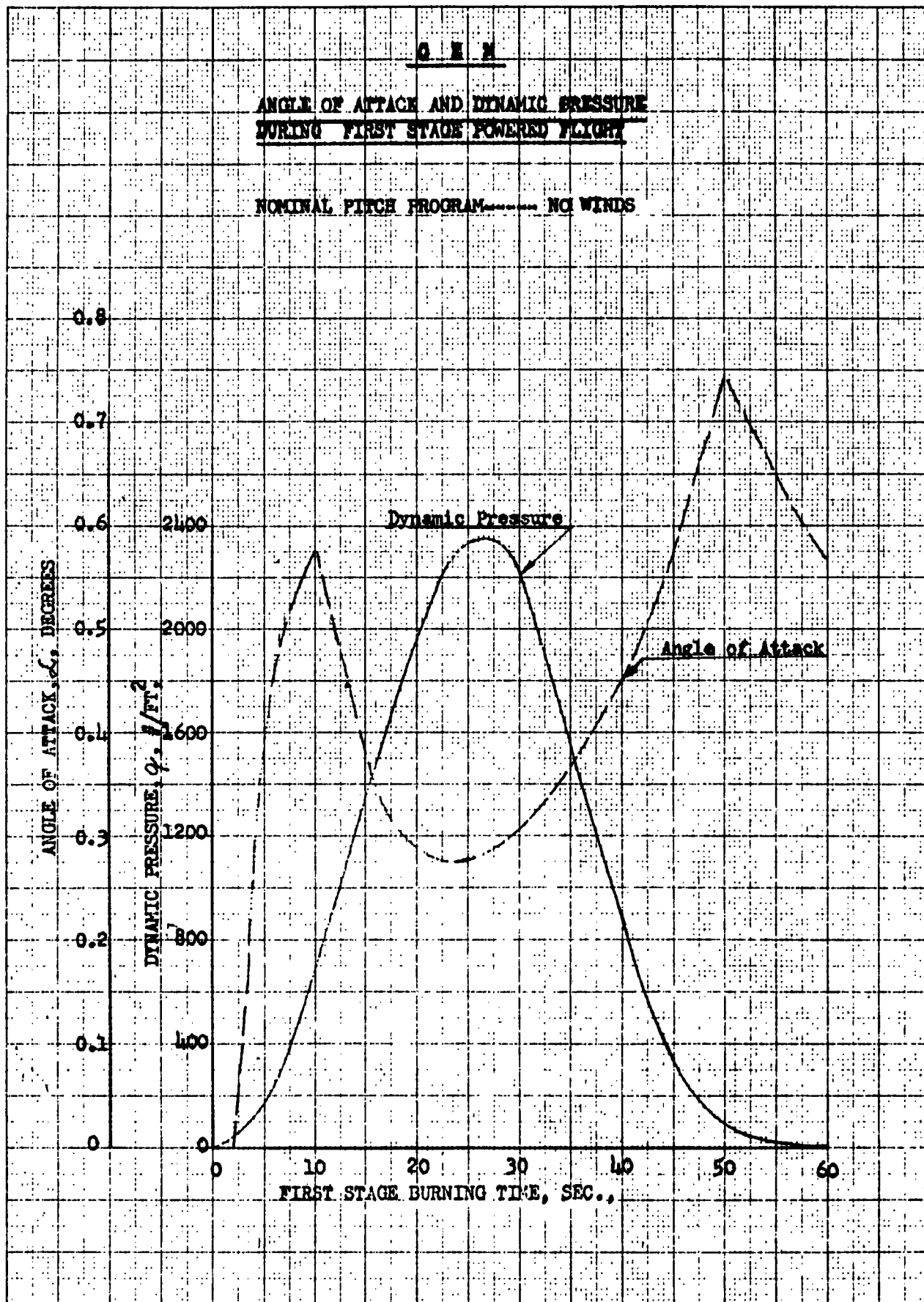


FIGURE 2

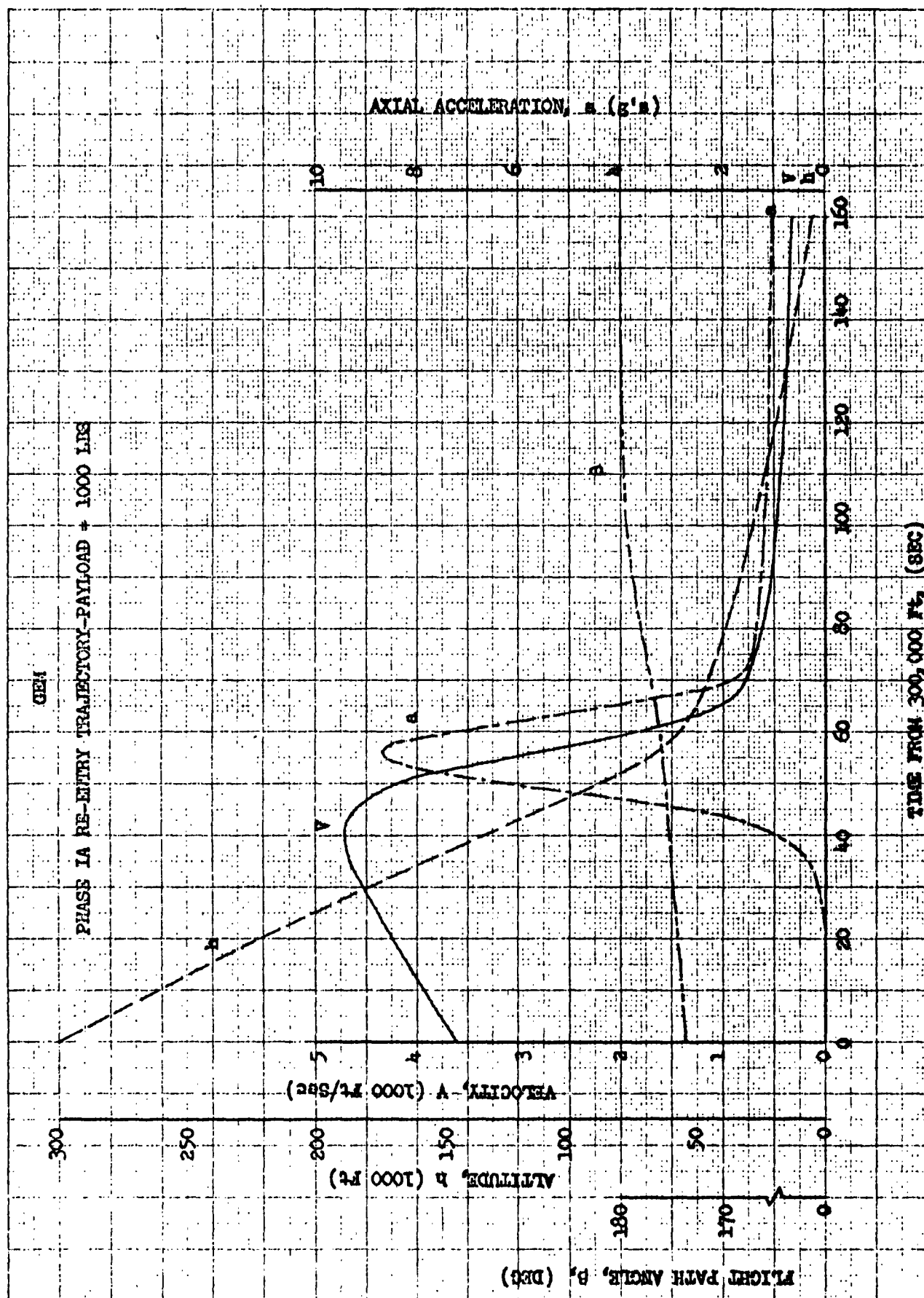


FIGURE 3

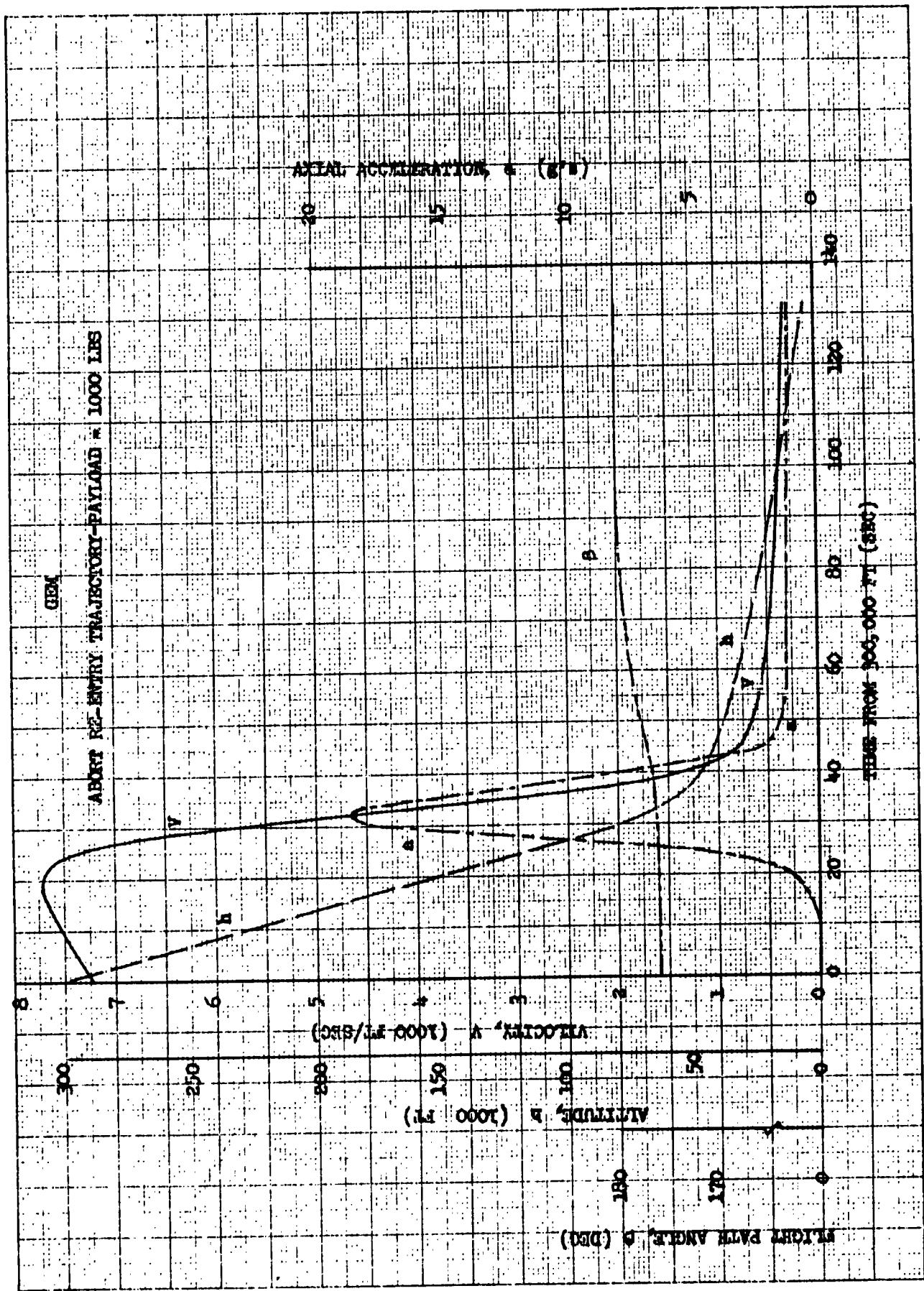


FIGURE 4

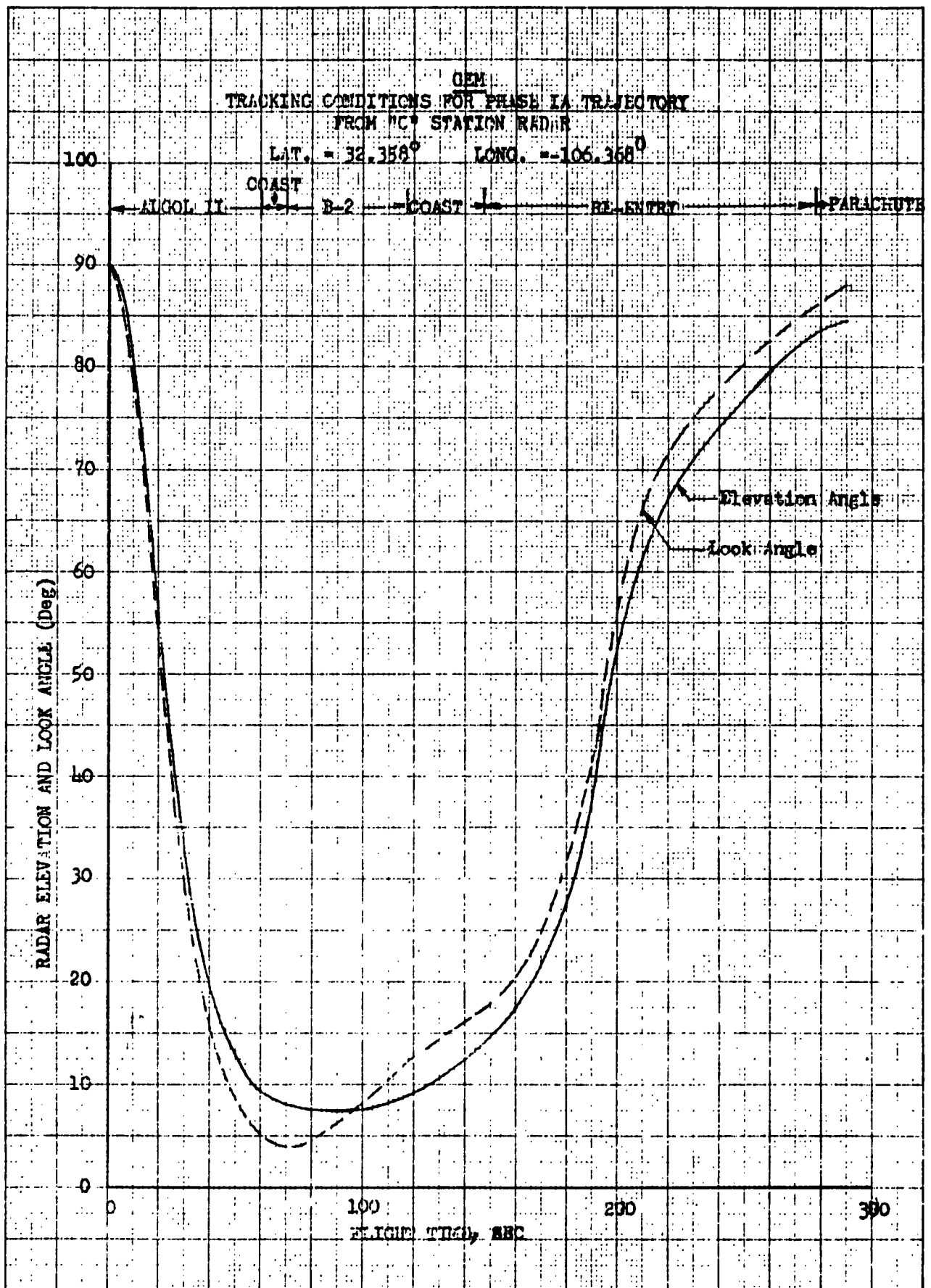
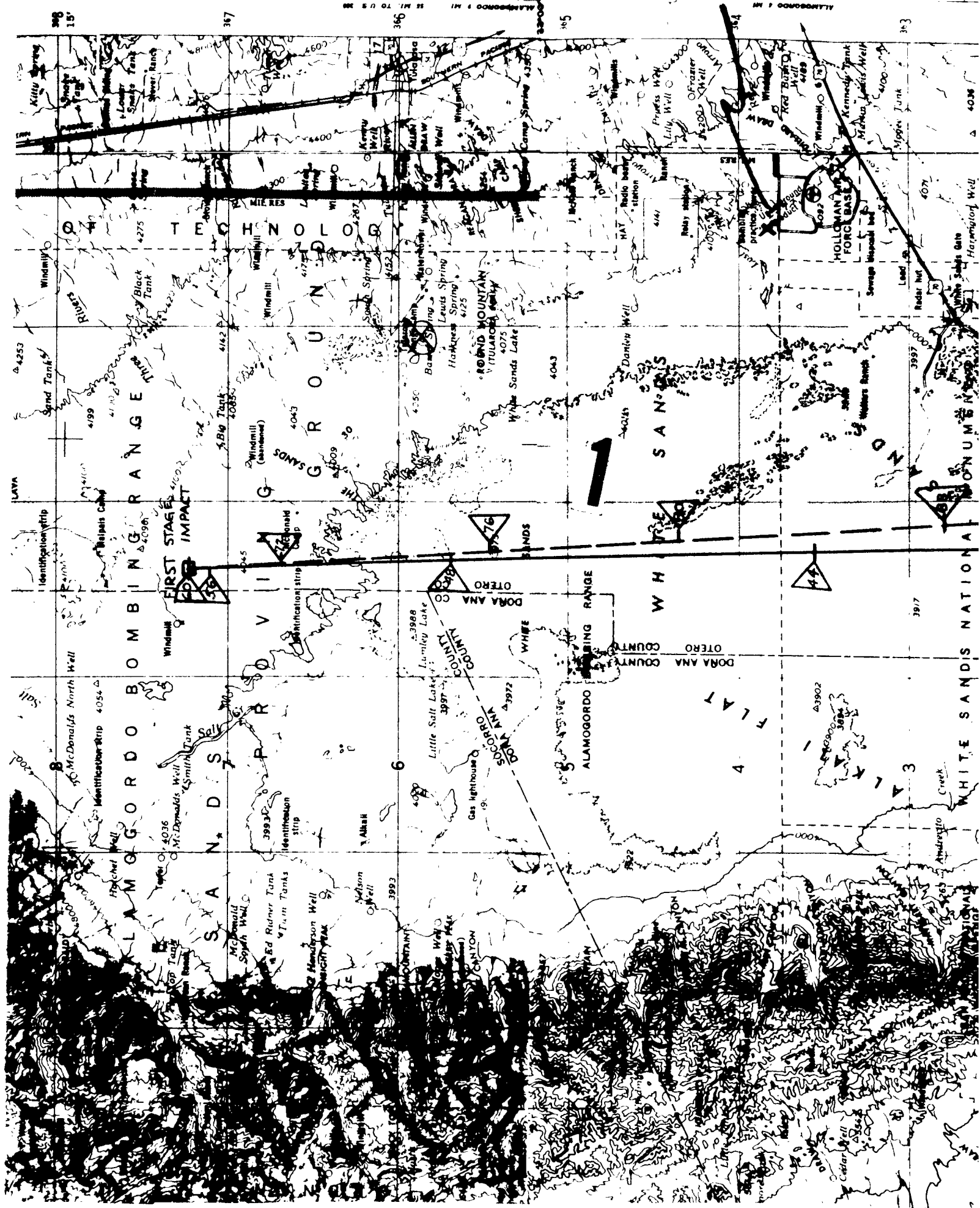
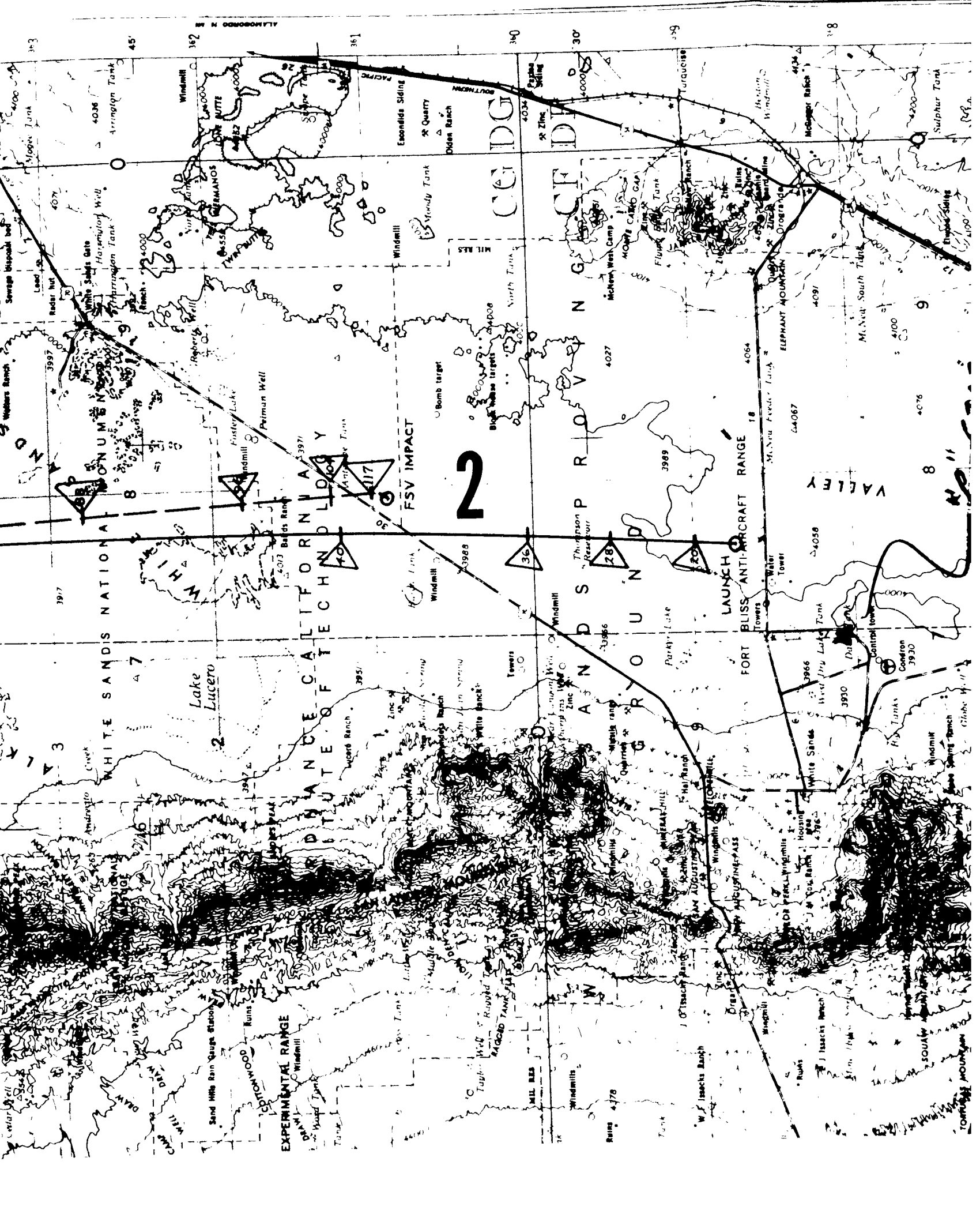


FIGURE 5





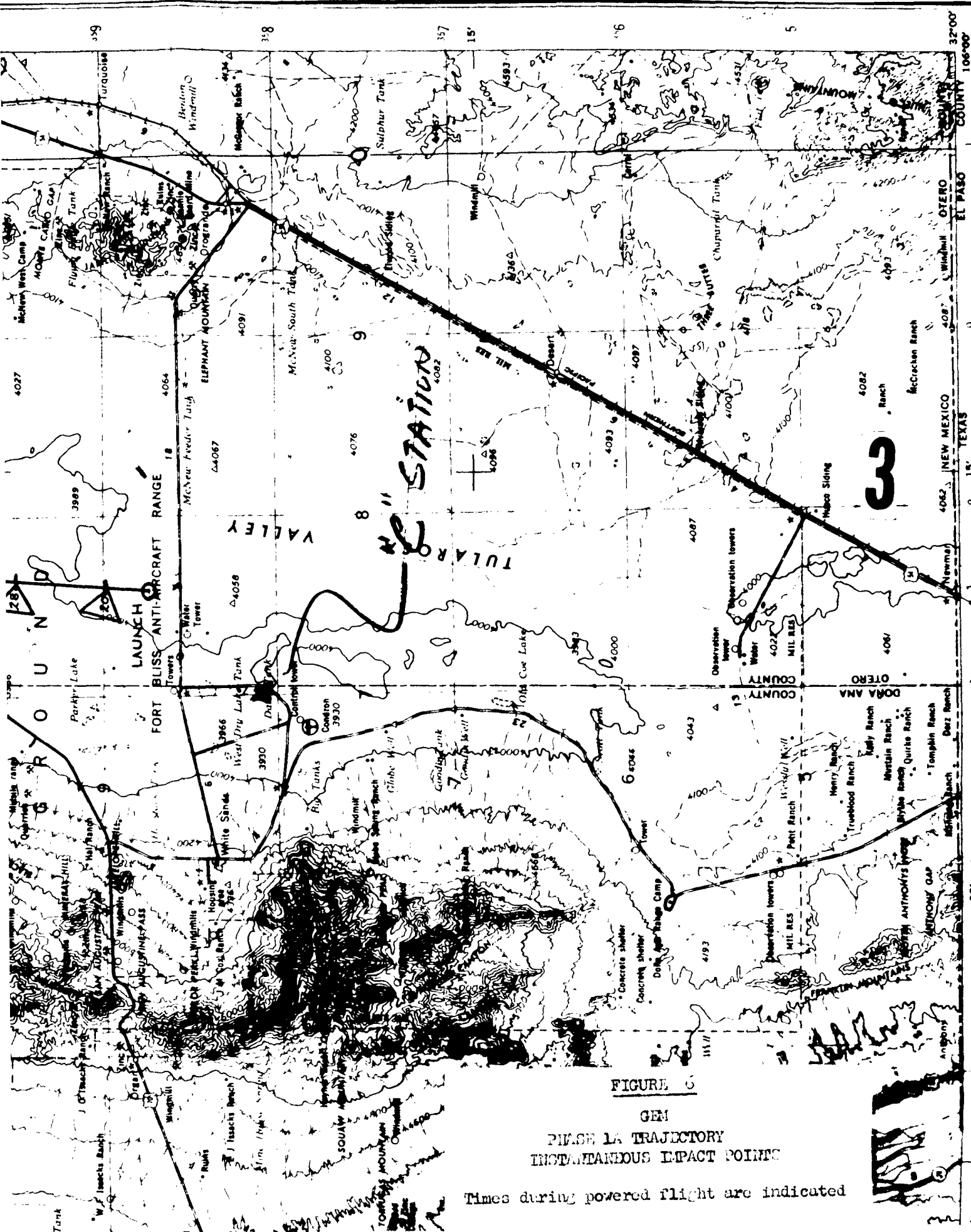


FIGURE 6

GEM
PHASE 1A TRAJECTORY
INSTANTANEOUS IMPACT POINTS

Times during powered flight are indicated

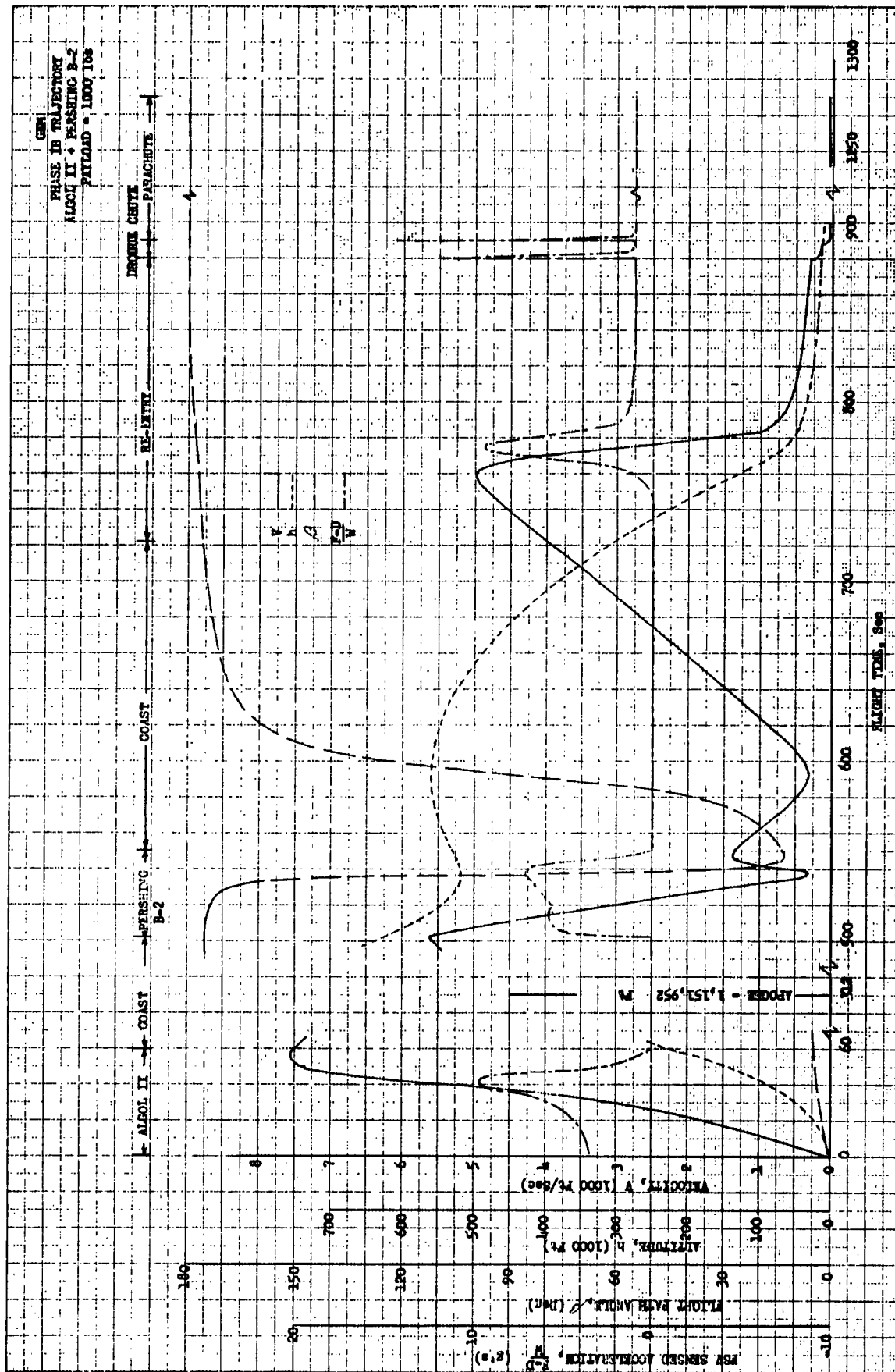


FIGURE 7

APPENDIX 5

GEM AERODYNAMIC COMPUTATIONS

The aerodynamic coefficients C_A , CN_A and the center of pressure $\frac{x_{CP}}{L}$ have been computed for the final configuration of the GEM ascent vehicle and will be used in the performance and trajectory studies (see Figures 1, 2 and 3).

In order to maintain the aerodynamic stability of the GEM entry vehicle at transonic speeds, the flap configuration was modified to the present deflection angle of 20° . The aerodynamic coefficients corresponding to this revised flap configuration have been computed for mach numbers from 0 to 6. (See Figures 4, 5 and 6.)

Pressure distributions on the ascent nose cone and the entire entry vehicle have been computed for mach numbers from 2 to 10 for corrective heating studies.

Load distributions on the ascent nose cone (at the point of maximum dynamic pressure during ascent) and on the entry vehicle at several points during the descending trajectory (maximum stagnation point heating and maximum dynamic pressure) were computed for the design of the primary structural components. (See Figures 7, 8 and 9).

Roll torques due to off-set center of gravity were also computed. (See Figure 10).

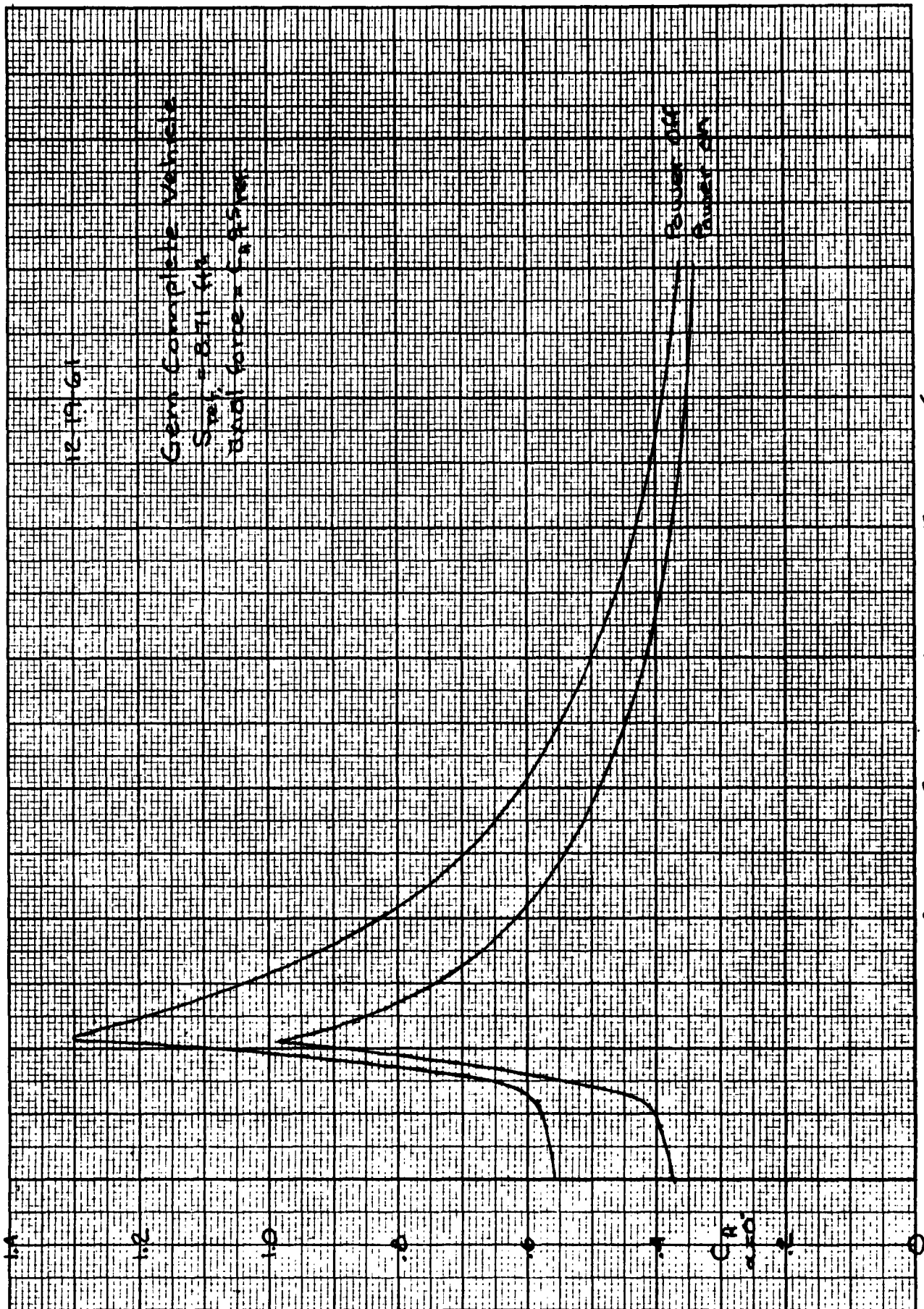


FIGURE 1

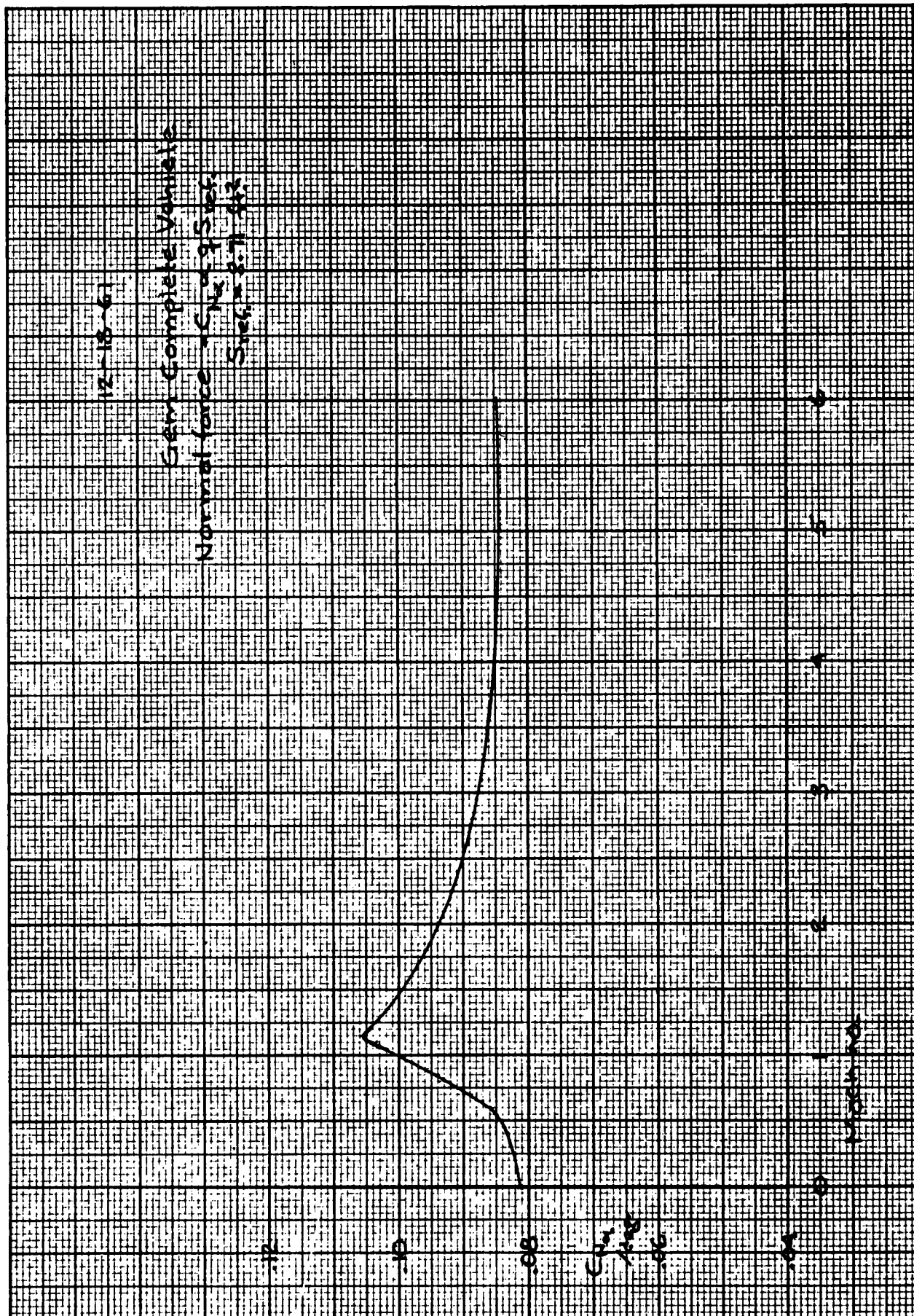


FIGURE 2

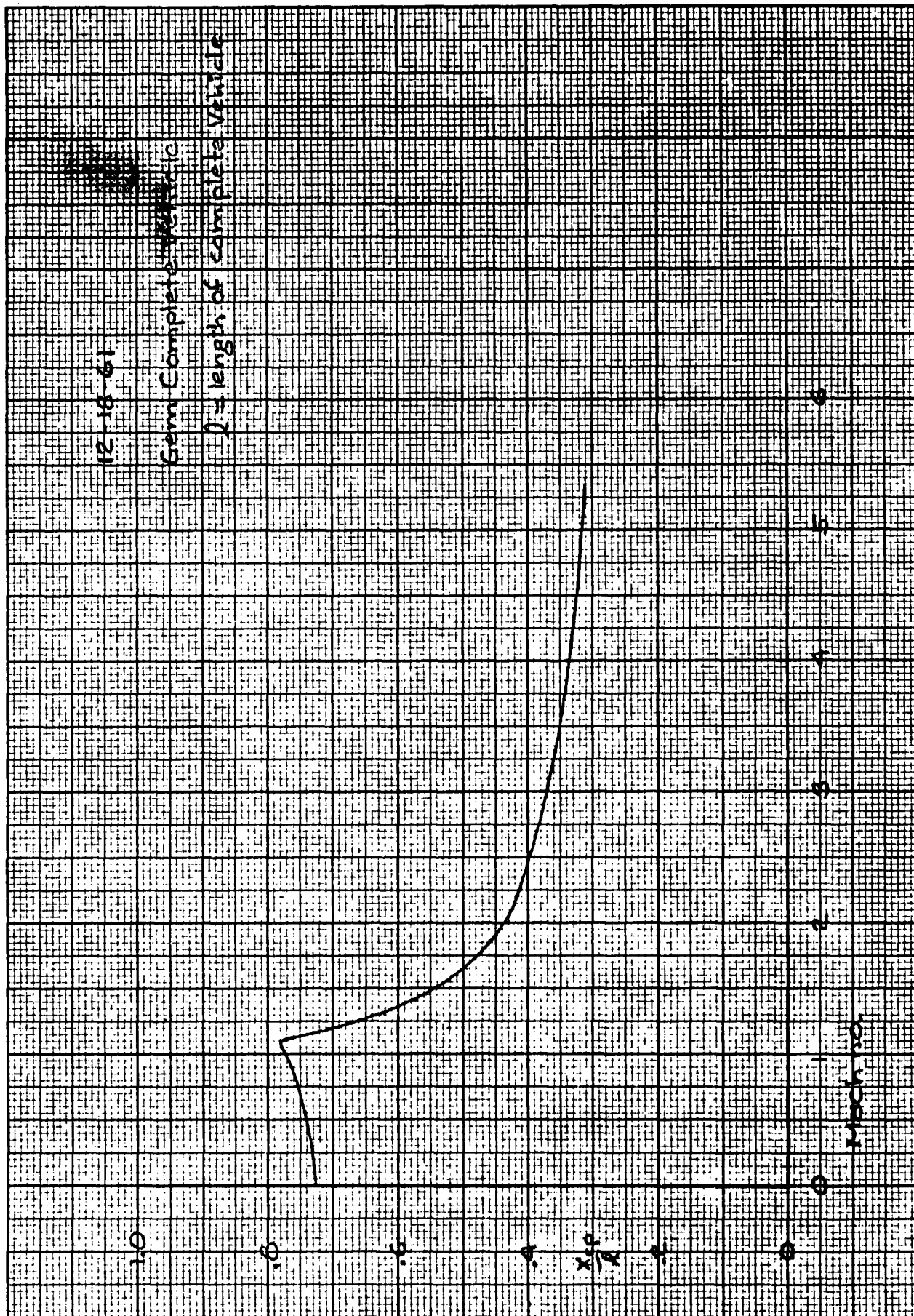


FIGURE 3

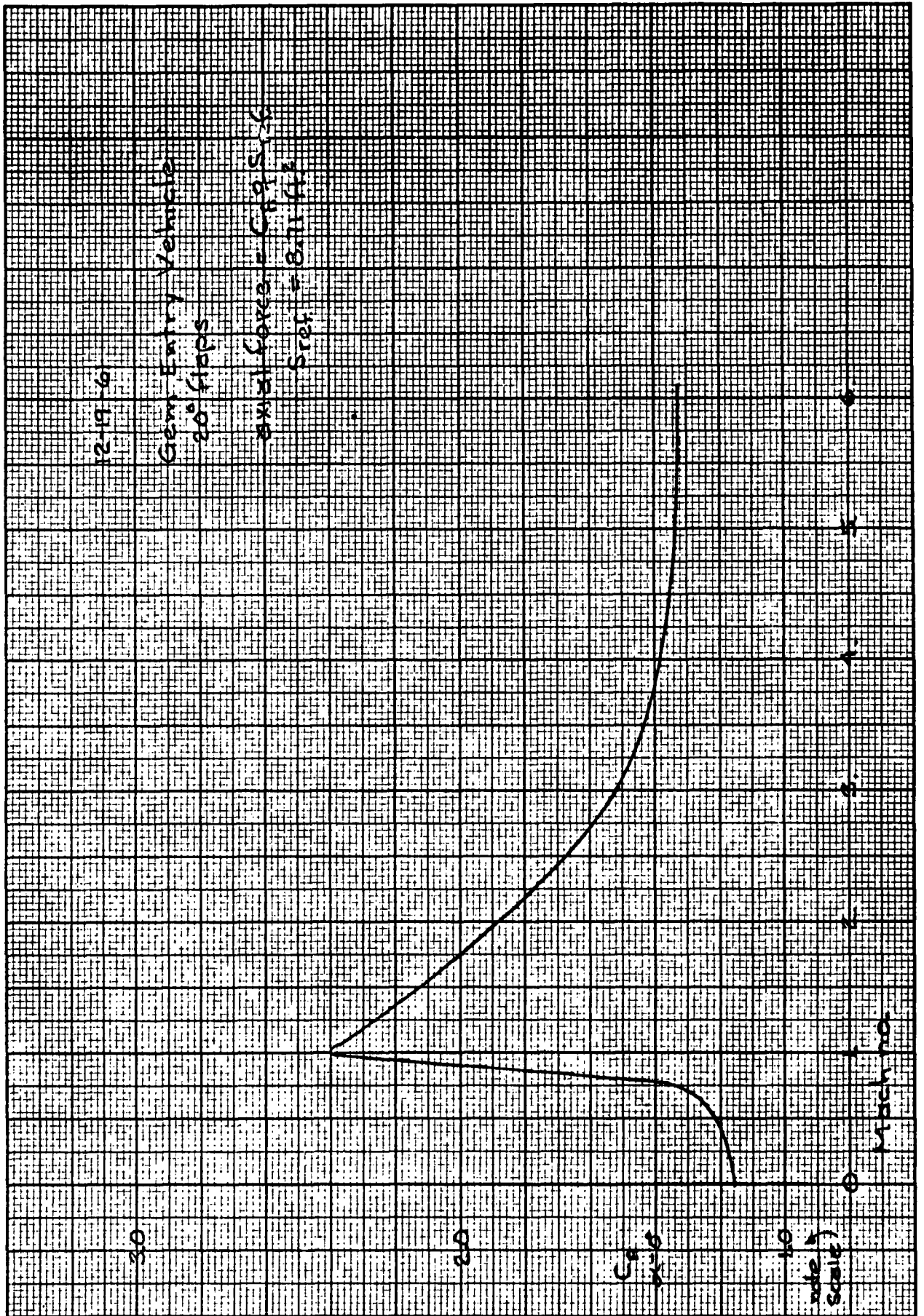


FIGURE 4

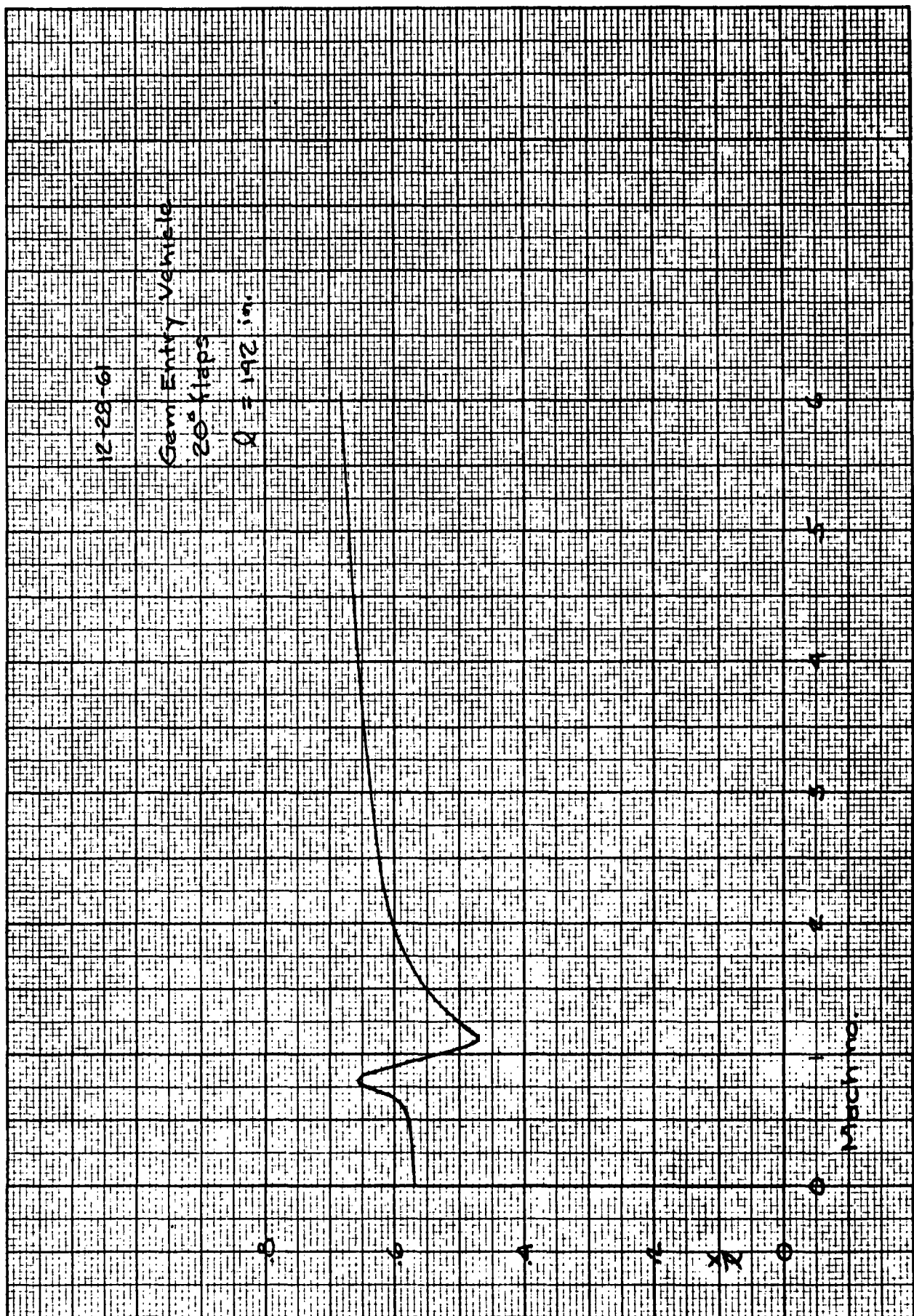


FIGURE 6

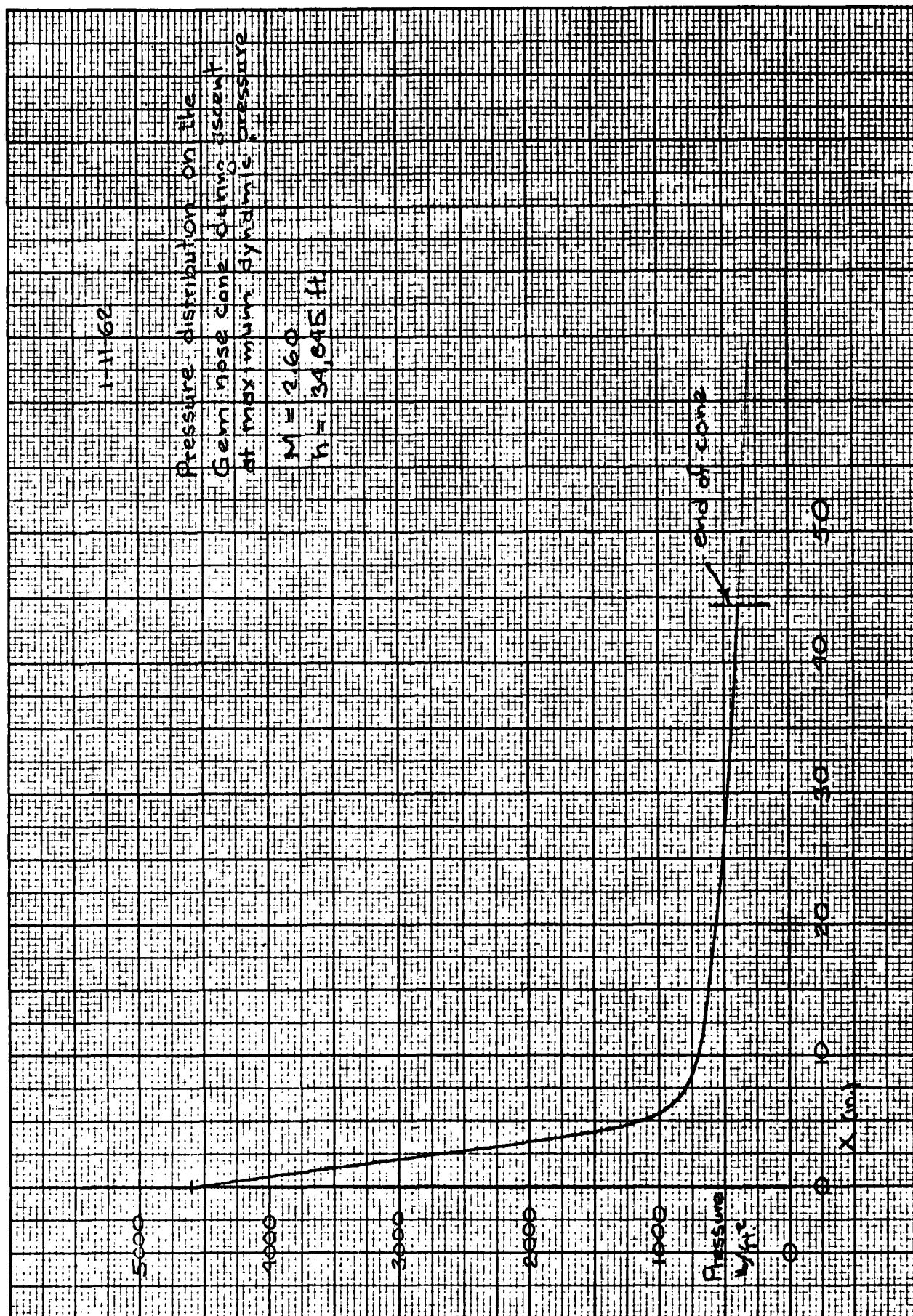


FIGURE 7

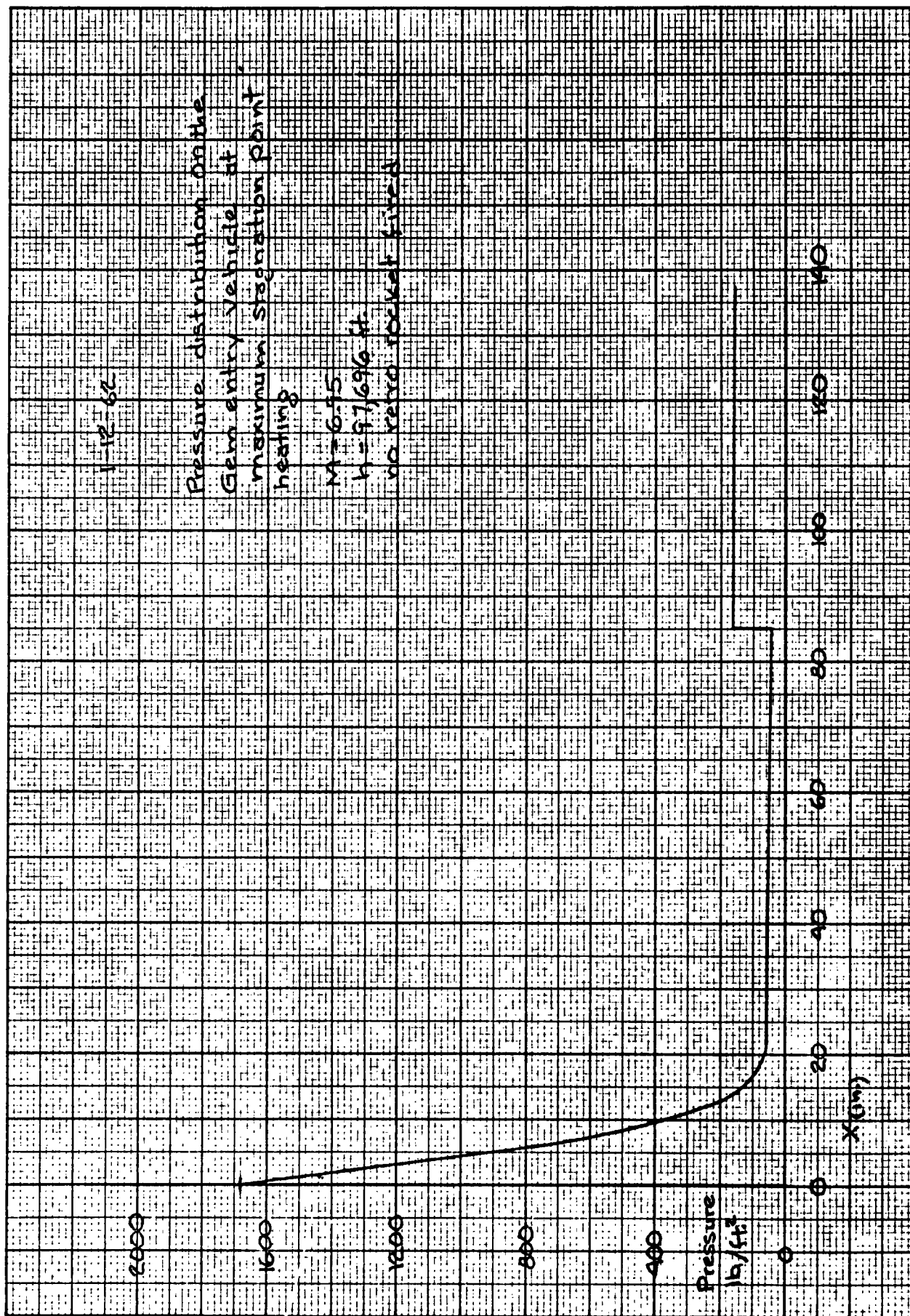


FIGURE 8

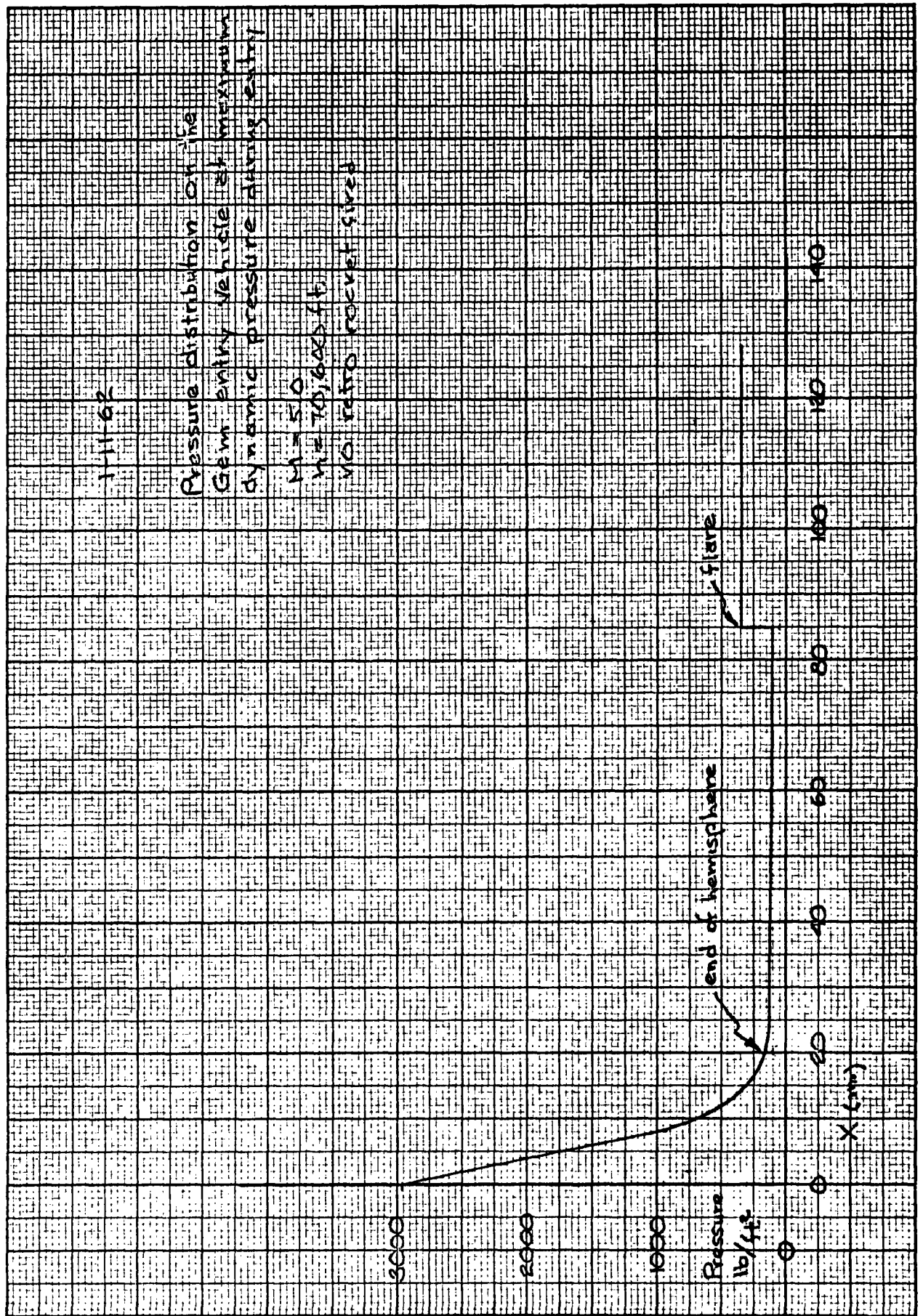


FIGURE 9

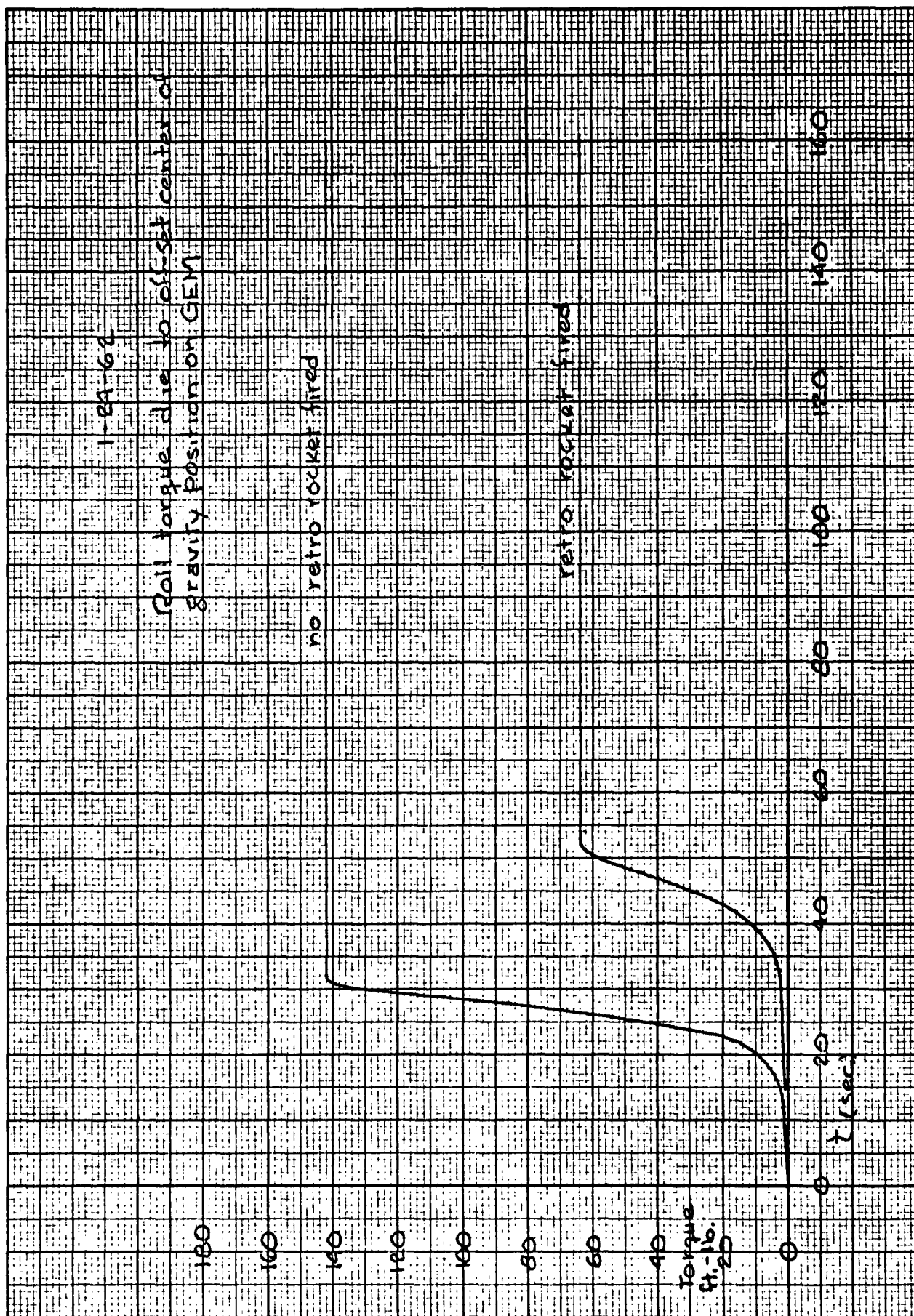


FIGURE 10

Appendix 6
THERMODYNAMICS

APPENDIX 6

GEM THERMODYNAMICS DATA

1. Ascent Stagnation Point (Thermal Analyzer Program)

The ascent stagnation point configuration is given below in Figure 1

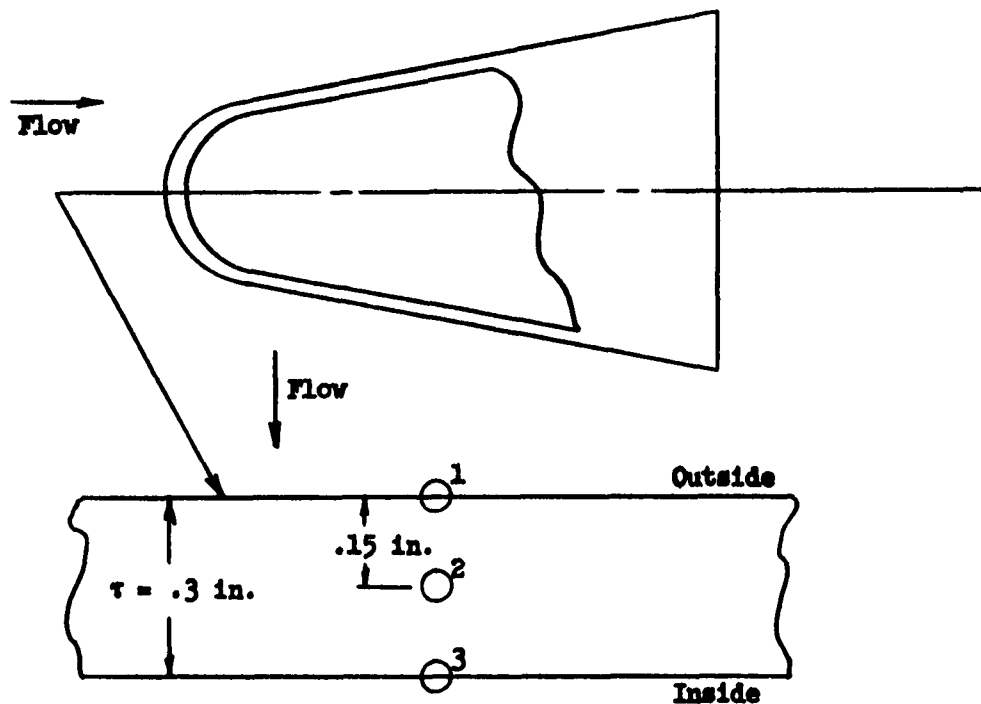


FIGURE 1

The material is fiberglass which has the following thermal properties.

density = 120 lb/ft³

specific heat = 0.25 BTU/ft-°F

thermal conductivity = 0.2 BTU/ft-hr-°F

emissivity = 0.8

Table I gives ascent trajectory and temperature data.

TABLE I (Ascent)						
TIME (sec)	ALTITUDE (ft)	VELOCITY (fps)	TEMP ₁ (°F)	TEMP ₂ (°F)	TEMP ₃ (°F)	DYNAMIC PRESSURE (psf)
0	4,000	0	60	60	60	0
5			71	60	60	
10	8,462	889	101	60	60	727
15			225	60	60	
20	21,880	1,830	403	62	60	1,991
25			744	67	60	
30	46,070	3,118	1,125	86	60	2,136
35			1,507	116	60	
40	86,740	5,263	1,813	175	61	859
45			1,635	248	65	
50	151,618	7,413	1,485	340	72	91.8
55			1,281	427	85	
60	226,805	7,530	1,037	474	105	6.20
65			920	517	132	
70	300,000	7,207				0

2. Re-entry Stagnation Point (Thermal Analyzer Program)

The re-entry stagnation point configuration is given below in Figure 2.

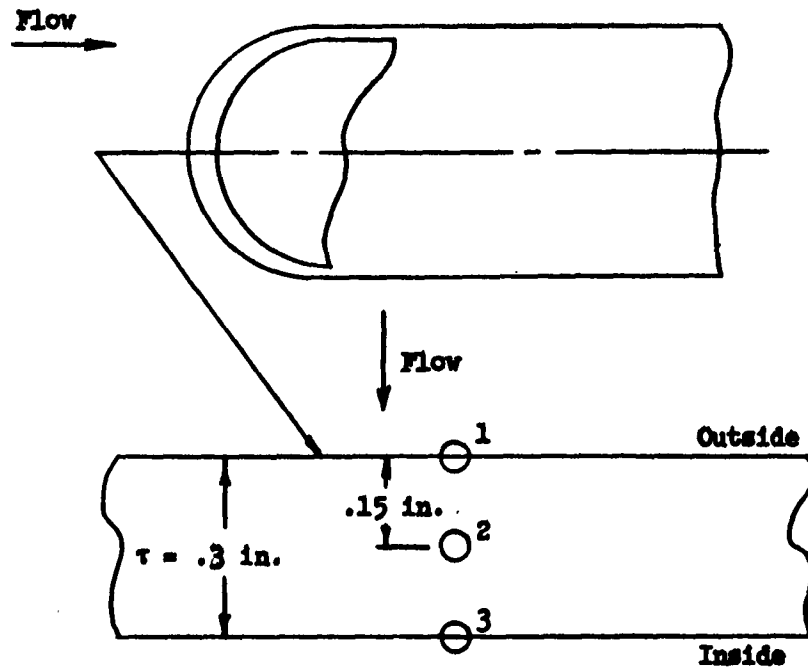


FIGURE 2

The material is fiberglass with the thermal properties as given in the ascent section.

Table II gives re-entry trajectory and temperature data.

The time spent in space (300,000 ft to 300,000 ft) is 485 sec. The cooling of the re-entry nose cap due to radiation during this time accounted for in the temperature calculation.

TABLE II
(Re-entry)

TIME (sec)	ALTITUDE (ft)	VELOCITY (fps)	TEMP ₁ (°F)	TEMP ₂ (°F)	TEMP ₃ (°F)	DYNAMIC PRESSURE (psf)
0	300,000	7,207	39	43	45	.1
5	263,600	7,362	112	43	45	1.0
10	226,300	7,513	251	43	45	6.3
15	188,500	7,644	517	45	45	26.6
20	150,000	7,697	999	55	45	105
25	112,100	7,383	1,786	77	45	496
30	78,600	5,687	1,866	122	45	1,506
31.5	70,600	4,856				1,600
35	57,000	2,999	997	206	46	1,171
40	46,600	1,335	716	330	51	391
45	41,800	781	655	391	61	165
50	38,200	655	576	379	80	139
60	32,300	536	489	373	137	116
70	27,300	470	433	359	186	108
80	22,800	427	394	347	223	105
90	18,300	391	366	337	249	103
100	14,900	369	345	329	268	102
110	11,300	347	329	323	281	101
120	7,900	328	318	319	290	100
130	4,750	312	309	315	296	100
140	1,750	297	302	312	300	99
146	0	290	299	310	302	99

3. Ascent Payload Shell ("Thin Skin" Program)

The ascent payload shell configuration is given below in Figure 3

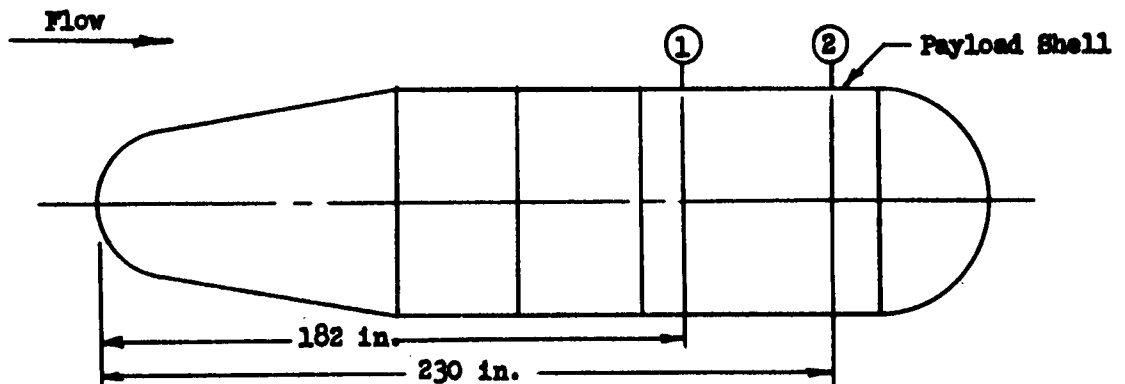


FIGURE 3

The material at stations (1) and (2) is 2014 T6 aluminum which has the following thermal properties.

Density = 175 lb/ft³

specific heat = .23 BTU/lb-°F

thermal conductivity = 89.6 BTU/ft-hr-°F

Four runs were made with the following combination of parameters

Run	Station	Emissivity	Thickness	Initial Temperature
1	2	0.05	0.090 in.	60°F
2	2	0.20	0.090 in.	60°F
3	1	0.05	0.090 in.	60°F
4	2	0.05	0.180 in.	60°F

The results of these runs are given in Table III.

TABLE III
(Ascent)

TIME (sec)	ALTITUDE (ft)	VELOCITY (fps)	TEMP _{Run 1} (°R)	TEMP _{Run 2} (°R)	TEMP _{Run 3} (°R)	TEMP _{Run 4} (°R)	DYNAMIC PRESSURE (psf)
0	4,000	0	520	520	520	520	0
4	5,785	356	519	519	519	520	126
8	7,570	711	519	519	519	520	479
12	11,146	1,077	524	524	524	522	982
16	16,513	1,454	536	535	536	528	1,504
20	21,880	1,830	556	556	558	540	1,990
24	31,556	2,345	587	587	589	558	2,312
28	41,232	2,860	627	626	631	581	2,265
32	54,204	3,547	674	673	679	609	1,873
36	70,472	4,405	724	723	731	638	1,328
40	86,740	5,263	769	768	777	663	859
44	112,691	6,123	800	799	810	682	331
48	138,642	6,983	819	817	829	692	138
52	166,655	7,436	830	828	840	698	52.9
56	196,730	7,483	833	831	845	700	19.2
60	226,805	7,530	834	831	847	701	6.2
64	256,083	7,401	835	831	848	701	1.6
68	285,361	7,272	835	831	848	701	.3
70	300,000	7,207	835	831	848	701	.1

4. Re-entry Payload Shell ("Thin Skin" Program)

The re-entry payload shell configuration is given below in Figure 4.

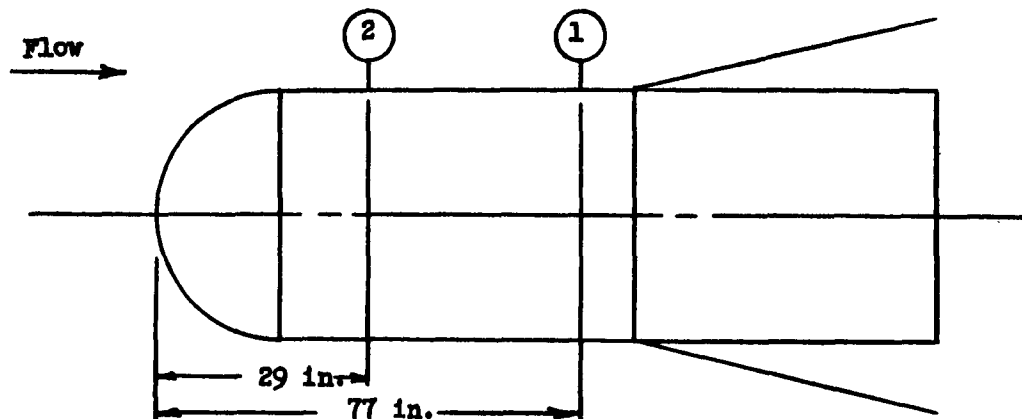


FIGURE 4

Note that stations ① and ② are the same stations discussed in the ascent payload shell section.

Again four runs were made with the following combinations of parameters.

Run	Station	Emissivity	Thickness	Initial Temperature
1	②	0.05	0.090 in.	500°F
2	①	0.05	0.090 in.	500°F
3	②	0.05	0.090 in.	200°F
4	①	0.05	0.090 in.	200°F

The results of these runs are given in Table IV.

TABLE IV
(Re-entry)

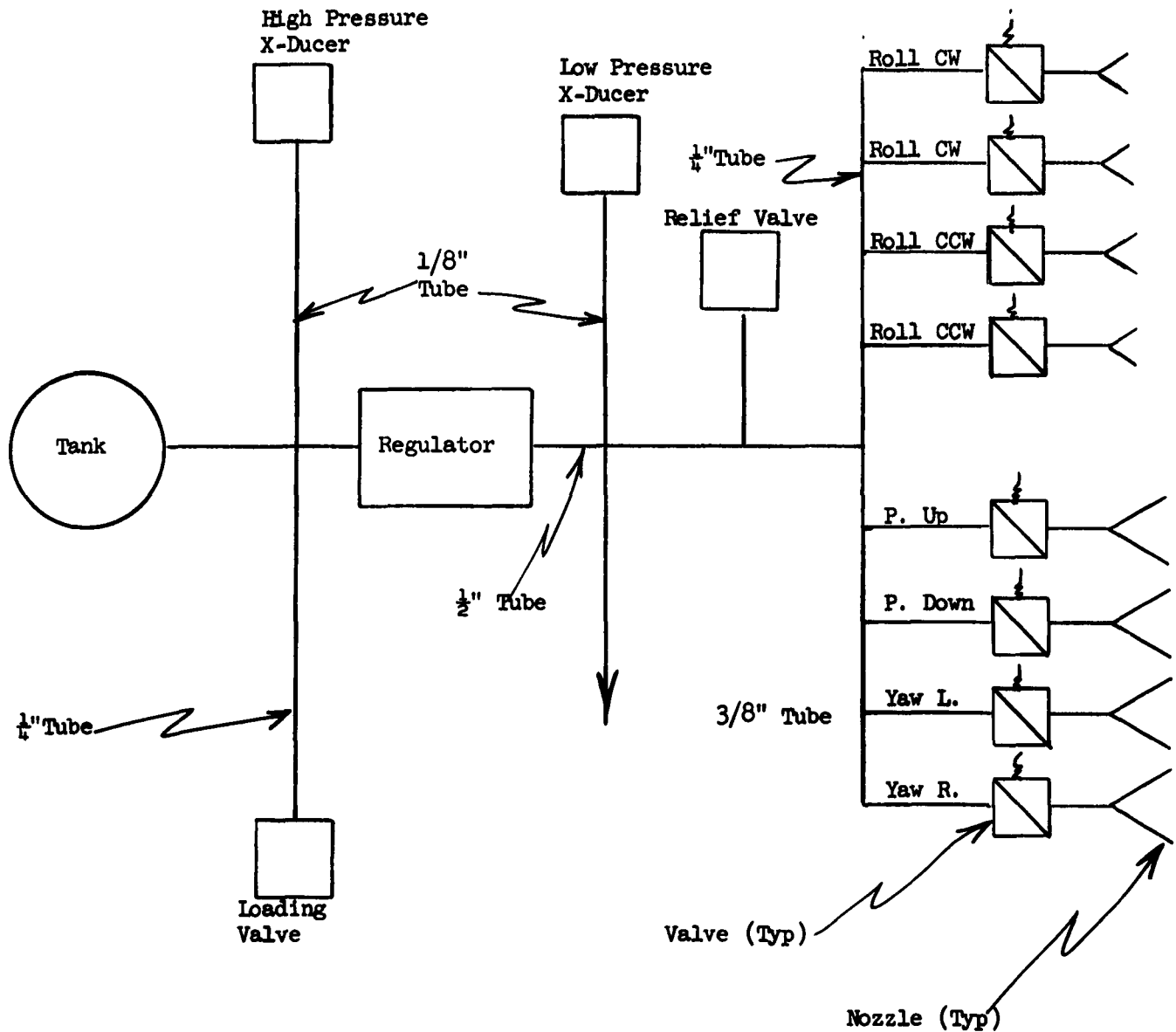
TIME	ALTITUDE	VELOCITY	TEMP _{Run 1}	TEMP _{Run 2}	TEMP _{Run 3}	TEMP _{Run 4}	DYNAMIC PRESSURE
(sec)	(ft)	(fps)	(°R)	(°R)	(°R)	(°R)	(psf)
0	300,000	7,207	960	960	660	660	.1
4	270,861	7,331	960	960	660	660	.7
8	241,260	7,453	961	960	661	661	3.2
12	211,219	7,565	962	961	663	662	11.6
16	180,792	7,655	965	963	666	665	34.4
20	150,064	7,697	970	967	673	670	105
24	119,670	7,446	989	985	697	698	357
28	91,317	6,526	1,043	1,036	768	758	1,048
32	68,288	4,573	1,106	1,090	854	834	1,588
36	54,235	2,561	1,118	1,101	886	862	975
40	46,728	1,235	1,091	1,079	871	851	325
44	43,325	1,004	1,060	1,052	848	832	252
48	39,922	773	1,030	1,027	825	813	176
52	37,086	636	1,002	1,003	803	795	137
56	34,819	593	974	979	782	777	131
60	32,551	550	947	955	761	759	123
64	30,283	507	920	932	741	742	113
68	28,409	487	893	909	722	726	112
72	26,591	469	867	886	704	710	111
76	24,773	452	842	864	686	694	110
80	22,955	434	817	842	668	679	108
84	21,136	417	793	820	653	665	106
88	19,439	402	770	799	638	651	104
92	17,944	391	748	779	624	638	104
96	16,448	380	727	760	611	626	103
100	14,953	369	708	741	599	615	102
104	13,653	362	688	723	588	604	102
108	12,352	355	671	706	578	595	103
112	11,052	348	655	690	569	586	103
116	9,752	341	640	675	562	578	103
120	8,452	335	627	661	555	571	103
124	7,151	328	614	648	549	565	103
128	5,851	321	603	636	544	559	103
132	4,551	314	593	625	540	555	102
136	3,251	307	585	615	537	551	102
146	0	290	568	594	533	544	100

Appendix 7
AFFIDAVIT COMPLAINT,
PROSECUTION LAYOUT

TENTATIVE ATTITUDE CONTROL PROPULSION LAYOUT

1. The following are preliminary layouts of the attitude control system. The exact combination to be utilized is still subject to investigation.

A. Cold Gas System



LAYOUT SCHEMATIC

A. Cold Gas System (Continued)

(1) Specification

All nozzles: .210 dia. throat, .728 dia. exit

$$\text{Expansion Ratio} = \frac{12}{1}$$

Average ISP = 63 Sec.

* Regulated Pressure: 300 \pm 15 PSI
Lockup 360 PSI Max.

Relief Valve: Crack 425 PSI Min.
Reseat 375 PSI Max.

* Included herein is nitrogen pressure for Hot Gas System.

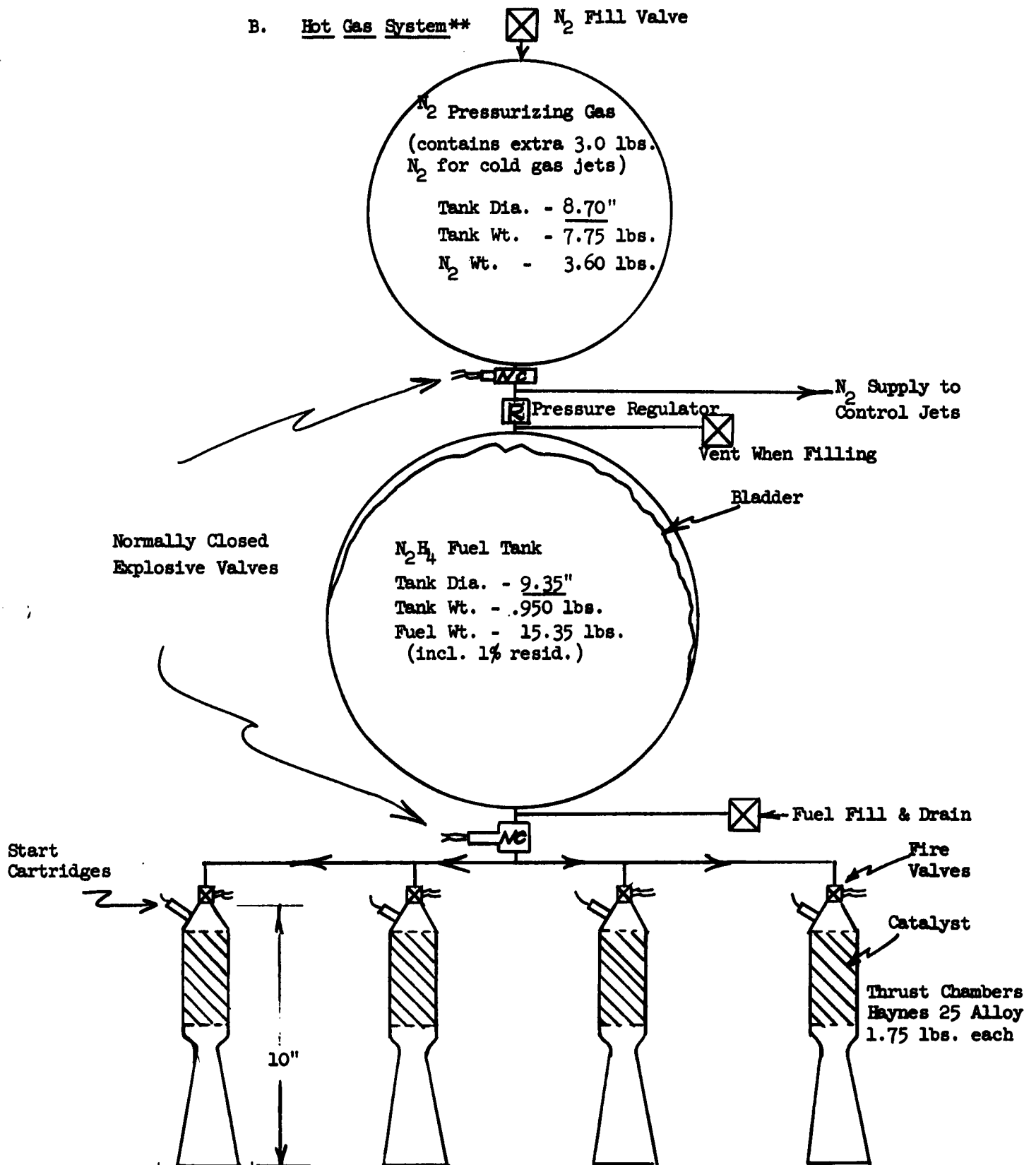
(2) System Weight

<u>Component</u>	<u>Weight (lbs)</u>	
	<u>Program A</u> 400# Sec.	<u>Program B</u> 2000# Sec.
1. Gas	8.90	40.80
2. Tank	11.57	53.10
3. H.P. X-Ducer	.25	.25
4. Loading Valve	.50	.50
5. Regulator	1.30	1.30
6. Low P. X-Ducer	.25	.25
7. Roll Valve (4 Total)	1.80	1.80
8. Roll Manifold (4 Total)	.80	.80
9. Pitch & Yaw Valves	4.40	4.40
10. Pitch & Yaw Manifolds	1.50	1.50
11. Nozzles (8 Total)	.27	.27
12. Plumbing & Fittings	1.86	3.19
13. Relief Valve	.25	.25
Total	33.65	108.41

(3) System Volume

	<u>Program A</u>	<u>Program B</u>
Fixed Hardware	100 cu. in.	100 cu. in.
Tank Volume (3000 PSI)	1060 cu. in.	4850 cu. in.
Tank Size (3000 PSI)	12.70 ID 12.94 OD	21.0 ID 21.40 OD
Tank Volume (4000 PSI)	790 cu. in.	3640 cu. in.
Tank Dia. (4000 PSI)	12.30 ID 12.61 OD	19.0 ID 19.48 OD

B. Hot Gas System**



LAYOUT SCHEMATIC

B. Hot Gas System (Continued)

(1) Specification

Four (4) Thrust Chambers, 25 lbs. thrust each

Total Impulse of 3500 lb/sec.

Pressure regulated system - N_2 gas with 3.0 lbs. gas for control jets.

Bladder in fuel tank

(2) Design Criteria

N_2H_4 monopropellant - I_{sp} = 230 sec.

Chamber pressure = 130 psia

Tank pressure = 250 psia

N_2 pressure = 4000 psia, regulated to 250 psia

Fuel tank - aluminum

N_2 tank - steel

Thrust Chambers - Haynes 25 alloy, radiation cooled

(3) Component Weight and Size Summary (Same for both Programs)

	<u>Weight</u>	<u>Size</u>	<u>Volume</u>
N_2H_4 tank	.950 lbs	9.35" Dia.	425 cu. in.
* N_2 gas tank	7.75 lbs	8.70" Dia.	396 cu. in.
Fuel Tank bladder	.20 lbs	-	-
Pressure regulator	-	-	-
Thrust Chambers (4) (1.75 lbs each)	7.00 lbs	10" long (each)	
Fire valves (4)	2.4 lbs	-	
Explosive valves (2)	.350 lbs	-	
Start Cartridges (4)	1.20 lbs	-	
Fill & Drain valves (3)	.75 lbs	-	
Dry weight	20.62	+ structure, lines, wiring	
Fuel (incl. 1%)	15.35 lbs		
N_2 gas	3.60 lbs	(incl. 3.0 lbs. for control jets)	
Total weight	39.57 lbs		

* Note: Only provided for information - nitrogen pressure is provided in cold gas estimate.

** Note: The above Hot Gas System layout is based on the use of hydrazine (N_2H_4) as the propellant. Hydrogen peroxide would require a slightly larger tank.



APPROVED
FOR THE BOARD OF DIRECTORS
DATE

APPENDIX 8

FPS-16 RADAR ACCURACY STUDY

1.0 Introduction

An accuracy study was performed on the FPS-16 radars at two sites at the White Sands Missile Range. The purpose of this study was to determine the applicability of the FPS-16's to adequately track GEM for backup radio guidance purposes.

The two FPS-16 site locations selected were Tula Range Camp situated about 240,000 ft. North and 50,000 ft. East of the launch point, and C Station located about 21,000 ft. South and 15,000 ft. West of the launch point.

Two trajectory points were chosen from the Phase I GEM trajectory. One point was taken near first stage burnout during maximum ascent velocity and the other point taken at low (about 10-20 degrees) elevation angles as seen by the site in question. It is expected that errors associated with intermediate trajectory points will not exceed those obtained for these points.

Velocity accuracies were derived in terms of an earth fixed Cartesian coordinate system located at the site under study. The axes were orientated with the X axis pointing true East, Y true North and Z along the local horizontal.

2.0 FPS-16 Accuracies

The 1σ FPS-16 accuracies assumed were:

$$\Delta R = 15 \text{ ft.}$$

$$\Delta A = .15 \text{ mr.}$$

$$\Delta E = .15 \text{ mr.}$$

$$\Delta \dot{R} = 3 \text{ ft./sec.}$$

$$\Delta \dot{A} = 30 \mu \text{ rad/sec.}$$

$$\Delta \dot{E} = 30 \mu \text{ rad/sec.}$$

It is assumed that the velocities were determined from the position measurements by differentiation using 3 to 5 seconds smoothing.

3.0 Trajectory Parameters

3.1 Tula Range Camp

3.1.1 Case A. High velocity point

$t(\text{time}) = 56 \text{ sec. (after liftoff)}$

$R (\text{range}) = 31.4 \times 10^4 \text{ ft.}$

$A (\text{azimuth}) = 192 \text{ deg. (measured from North)}$

$E (\text{elevation}) = 38 \text{ deg. (measured up from local horizontal)}$

$\dot{R} (\text{range rate}) = 4620 \text{ ft./sec.}$

$\dot{A} (\text{ang. rate}) = 0$

$\dot{E} (\text{ang. rate}) = 19 \text{ mr/sec.}$

3.1.2 Case B. Low elevation angle point

$t = 26 \text{ sec.}$

$R = 25 \times 10^4 \text{ ft.}$

$A = 192 \text{ deg.}$

$E = 7 \text{ deg.}$

$\dot{R} = 300 \text{ ft./sec.}$

$\dot{A} = 0$

$\dot{E} = 10 \text{ mr/sec.}$

3.2 C Station

3.2.1 Case A. High velocity point

$t = 56 \text{ sec.}$

$R = 19.2 \times 10^4 \text{ ft.}$

$A = 35 \text{ deg.}$

$E = 82.2 \text{ deg.}$

$\dot{R} = 7500 \text{ ft./sec.}$

$\dot{A} = 0$

$\dot{E} = 5 \times 10^{-3} \text{ mr/sec.}$

3.2.2 Case B. Low elevation angle point

$t = 16 \text{ sec.}$

$R = 2.8 \times 10^4 \text{ ft.}$

$A = 35 \text{ deg.}$

$E = 22.5 \text{ deg.}$

$\dot{R} = 512 \text{ ft./sec.}$

$\dot{A} = 0$

$\dot{E} = 47 \text{ mr/sec.}$

4.0 Analysis

The following equations were derived and used to transform the FPS-16 errors into a Cartesian coordinate system.

$$\dot{\Delta X} = \frac{\partial X}{\partial R} \dot{\Delta R} + \frac{\partial X}{\partial A} \dot{\Delta A} + \frac{\partial X}{\partial E} \dot{\Delta E} + \frac{\partial X}{\partial R} \dot{\Delta R} + \frac{\partial X}{\partial A} \dot{\Delta A} + \frac{\partial X}{\partial E} \dot{\Delta E}$$

$$\dot{\Delta Y} = \frac{\partial Y}{\partial R} \dot{\Delta R} + \frac{\partial Y}{\partial A} \dot{\Delta A} + \frac{\partial Y}{\partial E} \dot{\Delta E} + \frac{\partial Y}{\partial R} \dot{\Delta R} + \frac{\partial Y}{\partial A} \dot{\Delta A} + \frac{\partial Y}{\partial E} \dot{\Delta E}$$

$$\dot{\Delta Z} = \frac{\partial Z}{\partial R} \dot{\Delta R} + \frac{\partial Z}{\partial A} \dot{\Delta A} + \frac{\partial Z}{\partial E} \dot{\Delta E} + \frac{\partial Z}{\partial R} \dot{\Delta R} + \frac{\partial Z}{\partial A} \dot{\Delta A} + \frac{\partial Z}{\partial E} \dot{\Delta E}$$

5.0 Results

The results of the accuracy study are given in the following four tables which show the 1σ error contribution to the Cartesian velocities of the FPS-16 errors. The root sum square Cartesian velocity errors are also included.

5.1 Tula Range Camp. Case A

	$\dot{\Delta}$ ft/sec.	$\dot{\Delta}$ ft/sec.	$\dot{\Delta Z}$ ft/sec.
$\dot{\Delta R}$.04	.18	.22
$\dot{\Delta A}$.01	-	-
$\dot{\Delta E}$.22	1.13	.01
$\dot{\Delta R}$.495	2.35	1.84
$\dot{\Delta A}$	7.5	1.56	.00
$\dot{\Delta E}$	1.23	5.79	7.41
RSS	7.60	6.64	7.63

5.2 Tula Range Camp. Case B

	ΔX ft/sec.	ΔY ft/sec.	ΔZ ft/sec.
ΔR	-	.02	.15
ΔA	.05	-	-
ΔE	.08	.38	-
$\Delta \dot{R}$.63	3.00	.36
$\Delta \dot{A}$	7.5	1.57	-
$\Delta \dot{E}$.19	.9	7.5
RSS	7.50	3.52	7.51

5.3 C Station. Case A

	ΔX ft/sec.	ΔY ft/sec.	ΔZ ft/sec.
ΔR	.04	.06	.01
ΔA	-	-	-
ΔE	.65	.94	-
$\Delta \dot{R}$.22	.32	3.00
$\Delta \dot{A}$.62	.43	-
$\Delta \dot{E}$	3.26	4.72	.76
RSS	3.39	4.84	3.09

5.4 C Station. Case B

	ΔX ft/sec.	ΔY ft/sec.	ΔZ ft/sec.
ΔR	.14	.21	.66
ΔA	-	-	-
ΔE	.12	.17	-
$\Delta \dot{R}$	1.59	2.3	1.07
$\Delta \dot{A}$.64	.44	-
$\Delta \dot{E}$.17	.25	.79
RSS	1.73	2.37	1.48

6.0 Conclusions

Flame attenuation effects were not considered. These effects may eliminate C-Station as a possible tracking site but the Tula Range Camp radar accuracy is certainly adequate for use as a backup guidance system.

Based on other results of this study it is expected that the velocity accuracies determined with respect to the other FPS-16 sites at White Sands would approximate the values determined for the Tula Range Camp and C Station sites, and thus would also suffice for backup guidance purposes.

APPENDIX 9

TEST ITEM REQUIREMENTS

1. It is the purpose of this appendix to specify those requirements of the test item to be accommodated by the GEM Test System. These requirements detail the physical constraints that must be met by the testing system to accomplish a realistic evaluation and to insure that the test item is operating within its design environment. Further, the Test Item - Final Stage Vehicle (FSV) interface constraints and the AGE requirements will be established. The test trajectory parameters are specified elsewhere; this appendix is limited to the requirements on the vehicle and launch complex when subjecting the test item to the test trajectory.
2. As discussed in the section on test philosophy, in Monthly Progress Report No. 1 (Reference 6), guidance hardware testing will consist of two types of tests, component testing and system testing. The former will be accomplished by use of a specially designed test platform upon which the inertial components will be mounted. This platform will have capability of azimuth reference determination and of multiple component accommodation in selective orientations and attitudes. Guidance system testing will entail the operation of the specific guidance system under test within the GEM test compartment. The guidance system test capability will include stellar-inertial and re-entry guidance testing.
3. The requirements to be set forth are of sufficient broadness to provide test capability for all systems and components under consideration. The requirements have been developed from experience and from the current and forecast demands of guidance techniques.

4. Requirements on FSV

a. Test Item Space

The space to be provided for mounting of the test item will be as follows:

Cylindrical - 36 inches in diameter

- 65 inches minimum, 75 inches maximum in height

The cylindrical longitudinal axis will be parallel to the GEM longitudinal (or roll) axis.

b. Test Item Weight

The weight of the test item will not exceed 500 pounds. This does not include instrumentation, primary A/B power supply, nor the test item mounting fixture.

c. Test Item Mounting

Each system to be tested will have its individual mounting requirements and the test item compartment will be constructed so as to accommodate special mounting fixtures. Such mounting fixtures will be designed to provide satisfactory mounting of each system to undergo test. This interface will be accomplished at the time of test program initiation.

One exception to the above will be the preliminary design of the mounting fixture that will accommodate the component test platform. As the design criteria of such platform will be provided herein, so will the criteria for the mounting interface. It is desired that the mounting technique utilized for the test platform be adaptable to the mounting of individual systems.

d. Environmental Requirements

(1) Vibration - The test item will not be subjected to vibration in excess of the following along each axis:

- (a) 1.25 g's rms sinusoidal at one or more frequencies in the range 5 to 150 cps.
- (b) 2.5 g's rms sinusoidal at one or more frequencies in the range 150 to 2000 cps.
- (c) The above to be combined with a random component (Gaussian) of $.016 \text{ g}^2/\text{cps}$ below 150 cps and $.047 \text{ g}^2/\text{cps}$ from 150 cps to 2000 cps which rolls off at 12 db/octave above 1000 cps.

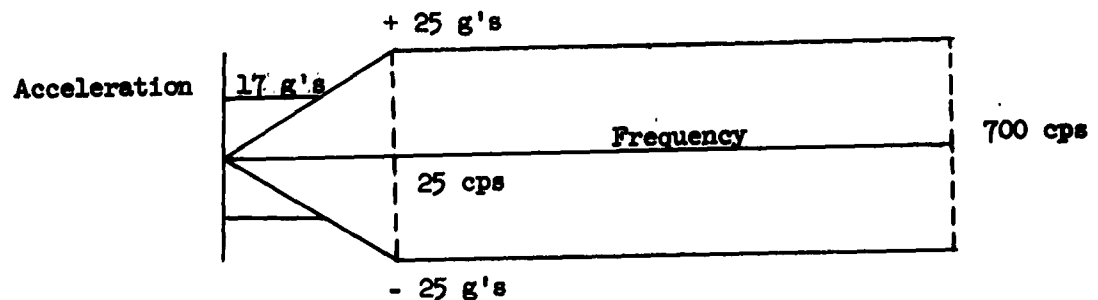
The above criteria is for the test item itself. However, it is desired that the structural design of the FSV be governed by the following criteria:

Equivalent static loading - 17 g's

Maximum resonance (Q) - 7

(2) Shock - Jerk inputs of 125 g/sec for 0.1 sec

The above shock requirements are for normal system/component A/B operation only. For abort missions, or for normal parachute blossom and landing impacts, the following shock spectrum will be the test item criteria:



Shock Spectrum

The 17 g level is derived from static loading design of the guidance system. This level is undoubtedly several magnitudes higher than 17 g's for destruction purposes.

(3) Acoustic Fields - Acoustic pressure of 150 db relative to 0.002 dynes/cm².

(4) Temperature Requirements

(a) Ground Operations

The surrounding air in the test item compartment will be controlled to a specific range within the broad range of 40° to 80° F. The specific range will be dictated by the temperature specifications of the individual components and/or system undergoing test. This temperature control will be provided by an AGE air conditioning unit capable of variable temperature regulation.

(b) In-Flight Temperature

The air temperature external to the test item shall not exceed 400° F. The heat produced by the internal heat source within the test item shall be dissipated by installation of a heat sink system. Such a system shall be coupled to the internal configuration used in the ground temperature controlling mode. Each type of test item will require an individual design to accommodate such cooling. The cooling capacity of such a sink will be 30 BTU/min for 8 minutes. Such a system will be required for those trajectories with an operational test longer than 3 minutes. The system will be simple and reliable, being activated during flight via a mechanical timer. Further study of the requirements for such a system will be initiated.

e. Optical Access

Two ports will provide optical access to system alignment mirrors or prisms. Further, these same two ports will provide stellar

tracking capability when such systems are undergoing test. When used during ground alignment, the ports may be optical flats sealed to the structure. During flight, when testing stellar tracking systems, the optical ports must be uncovered remotely by command to provide clear access for the stellar observation devices. Upon completion of the stellar observation, the ports must be resealed in flight. It would appear that the most practical scheme would be to design one set of optical ports for all types of test and open or close them upon command and as required by the mission. The ports will be centered on two mutually perpendicular radial axes. Provisions must be incorporated that will allow rotation of the port axes to suit requirements of specific test items.

f. Physical Access

The FSV will be constructed to provide access to the test item and instrumentation for maintenance, adjustment, replacement and repair. Such access must be available when the missile is in the launch position and when mounted on the transporter.

g. Umbilical Requirements

Provisions must be accomplished for electrical, liquid, and gas umbilical connections to the test item. As system testing would use the individual umbilical hardware designed for the particular system, the FSV must be designed to mount any of a number of umbilical connectors. An adaptable umbilical mounting panel would give such flexibility. This panel should be designed so as to accommodate a 7-inch diameter umbilical connector.

h. Power Requirements

The test item will be provided with electrical power from a supply located in the FSV. Such supply should be somewhat flexible as the

requirements may vary with each test. The requirement given below is based on a desired capability of concurrent testing of two systems. Telemetry power requirements are not included below but will be provided elsewhere. Power requirements are as follows (this is the most extreme case of testing two systems on the longest trajectory):

1400 watts nominal

2400 watts (peak) at 26-31 volts DC

Duration: 14 minutes

1. Dynamic Requirements

The test item will not be subjected to any roll dynamics in excess of the following:

Roll position - $\pm 5^\circ$

Roll rate - 15 cps

5. Requirements for universal test platform will be detailed elsewhere; however, criteria for such a platform will comply with these requirements.

APPENDIX 10

STELLAR INERTIAL TEST FIXTURE DESIGN REQUIREMENTS

1. PURPOSE

The purpose of the GEM Universal Stellar-Inertial Test Fixture (USITF), its associated electronics computers and ground support equipment is to provide a means for evaluating typical inertial and stellar guidance components such as gyroscopes, accelerometers, velocity meters, and star trackers on the GEM prior to their integration into a guidance system. The GEM/USITF will be a flexible inertial measurement unit serving as a test bed for GEM flights involving component testing.

A. The GEM/USITF will consist of, but not be limited to:

a. Airborne Equipment

- (1) The inertial measurement unit
- (2) The airborne Digital Computer (Buffer)
- (3) Interface to power supply (28V DC) signal conditioner and pulse code modulated telemeter multiplexer.

b. Ground Equipment

- (1) IMU checkout, erection and launch set
- (2) Azimuth alignment set
- (3) IMU test monitor console
- (4) IMU data recorder
- (5) Ground digital computer
- (6) Ground support equipment

B. The GEM/USITF will operate in, but not be limited to the following modes:

- a. Inertial
- b. Gyro drift test
- c. Accelerometer or velocity meter calibrate
- d. Stellar acquire
- e. Ready

2. GENERAL REQUIREMENTS

A. The velocity errors contributed by components other than the gyros, accelerometers and stellar sensors shall not exceed .07 ft/sec RMS for typical GEM trajectories. (This is roughly equivalent to $\pm 2 \text{ } \overbrace{\text{sec}}^{\text{arc}}$ total erection error for presently planned trajectories).

2. GENERAL REQUIREMENTS (Continued)

- a. Life - requirement to be specified
- b. Reaction time - requirement to be specified
- c. Interchangeability - Since the GEM/USITF platform will be used as a test fixture it will be essential to provide means for accepting gyro, accelerometer and star sensor fixtures of unknown design. The holding fixtures will be specified in outline only so that they may be modified depending on the component being tested.

3. STANDARD COMPONENTS

- A. The following represents a listing of standard components and subsystems but does not represent a complete design specification. The gyro, accelerometer and star tracker orientations are justified on the basis of analysis that will be included in the final report.
 - a. An easily removable platform and two gimbals integrated so as to allow access for alignment work and stellar sensor acquisition.
 - b. Three gimbal position pick-offs for sensing inner, middle and outer gimbal positions.
 - c. Three gimbal torque motors for a stabilization subsystem.
 - d. Elevation pendulum for erection of the system.
 - e. Reference pendulum for erection of the system.
 - f. Azimuth mirror for erection.
 - g. Standard (Azimuth and reference) star sensor with azimuth axis coincident with GEM thrust vector Z. This will be the only means of measuring drifts about Z.
 - h. Gyro fixtures to accommodate 3 orthogonal gyroscopes. The coordinate systems will be X, Y, Z (north, west and up) or α, β, γ in which β is west, α is north rotated up 45° , γ is \perp to α and β is normal to the α, γ plane.
 - i. Accelerometer - Velocity meter fixtures to accommodate 3 orthogonal accelerometers in the X Y Z (north, west, up) system.
 - j. Star tracker fixture to accommodate one unspecified star tracker so that azimuth axis of tracker will not be coincident with GEM thrust vector.

3. STANDARD COMPONENTS (Continued)

- k. Optical alignment provisions for measuring incremental mis-alignments between theoretical X, Y, Z accelerometer axis and actual X', Y', Z' axis, and between theoretical gyro α β γ and actual α' β' γ' axis.
- l. Fine balancing slugs for gimbals and platforms. Since the GEM/USITF must accept unspecified components, provision must be made for achieving fine balance of platform and gimbals once test components have been installed.
- m. Stabilization subsystem capable of operating on 3 unspecified signals from 3 SDF gyros or 2 TDF gyros.
- n. Erection Electronics - the erection electronics represent a subsystem controlled from the test console capable of erecting the platform to 2 $\overline{\text{sec}}$ or less using signals from an azimuth alignment set, pendulums, and gyroscopes.
- o. Airborne heat sink will be provided to absorb 30 BTU's/hr. for 12 minutes.
- p. Airborne computer will contain:
 - (1) Conditioning and sampling input device
 - (2) Three accelerometer accumulators capable of non-destruct readout twice per second
 - (3) Three gimbal pick off accumulators capable of non-destruct readout twice per second
 - (4) Four tracker gimbal pick off accumulators capable of non-destruct readout twice per second.

Essentially a buffer device, this computer should provide for the insertion of additional circuit modules in card form as required.
- q. Ground Computer - The ground computer will consist of a programmable digital computer with sufficient arithmetic, control and memory capacity to:
 - (1) Calibrate three accelerometers from data acquired in a minimum of six positions for scale factor and bias. Equations will be specified.
 - (2) Perform a gyro drift test in ground mode.
 - (3) Perform a stellar acquire test in ground mode.

3. STANDARD COMPONENTS (Continued)

B. Additional component and subsystem requirements must be made concerning:

- a. Ground equipment
- b. Airborne equipment
- c. Calibration requirements
- d. Accelerometer calibration equations
- e. Gyro calibration equations

APPENDIX 11

GYRO ORIENTATION STUDIES

Summary

The ability to identify gyro error coefficients on a GEM flight is dependent on both gyro and accelerometer orientations. Since the relative orientation of the gyros and accelerometers is usually fixed for a particular IMU, it is of interest to determine whether any orientation(s) of the IMU can be found which will be satisfactory and, if so, to consider the advantages of possible alternatives. This subject is considered herein for a particular platform whose components are oriented as in Figure 1. While no wholly satisfactory orientations exist, it is shown that an IMU rotation which places the X-accelerometer along the thrust vector will yield useful information.

Analysis

1. Drift Equations

The ability to detect drifts arising from gyro error coefficients depends on the generation of error angles about axes in the plane normal to the sensed acceleration, \bar{A} . For the GEM case, where the direction of \bar{A} is constant, gyro-caused velocity errors are proportional to $\bar{A} \times \bar{\phi}^*$, and hence this quantity serves as a figure of merit in considering alternate component orientations. If we restrict attention to drifts which are proportional to A and A^2 , the drift equations for the platform under consideration are:

*For gyro drift arising from any particular error coefficient, N , the resultant acceleration error is $\delta \bar{A} = \bar{A} \times \int \bar{\phi}_N dt$. During either stage, the direction of A is constant--it follows that the direction of $\bar{\phi}_N$ is also constant and therefore that

$$\delta \bar{A} = |\bar{A}| \int \frac{\bar{A}}{|\bar{A}|} \times \bar{\phi}_N dt$$

Thus the magnitude of the acceleration error is proportional to $|\bar{A} \times \bar{\phi}_N|$.

Gyro I

$$\begin{aligned}\bar{\phi} = & \bar{1}(CA_1 - DA_2 + BA_1A_3 - EA_2A_3) \\ & + \bar{2}(CA_2 + DA_1 - BA_2A_3 + EA_1A_3)\end{aligned}$$

Gyro II

$$\bar{\phi} = \bar{3}(\tilde{C}A_3 + \tilde{D}A_2 - \tilde{B}A_1A_3 + \tilde{E}A_1A_2)$$

where $\bar{1}$ and $\bar{2}$ are unit vectors along the sensitive axes of Gyro I and $\bar{3}$ is directed along the sensitive axis of Gyro II (whose other input axis is unused).

Forming the cross product, $\bar{A} \times \bar{\phi}$, we can construct the following table:

TABLE I

Gyro I

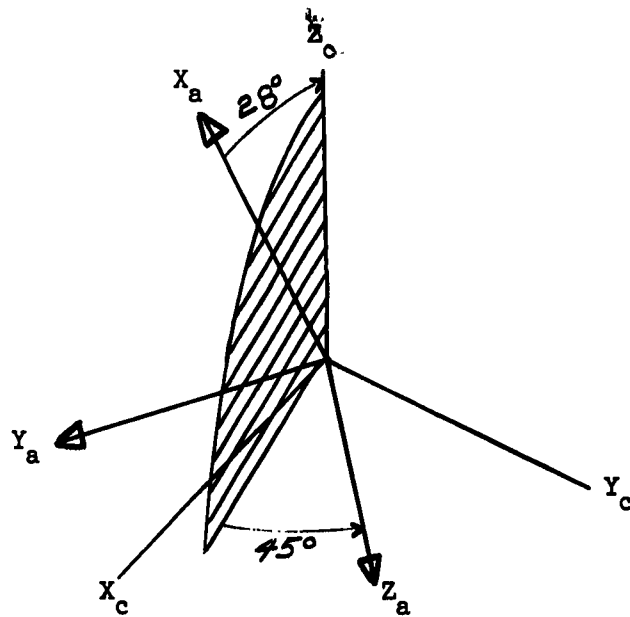
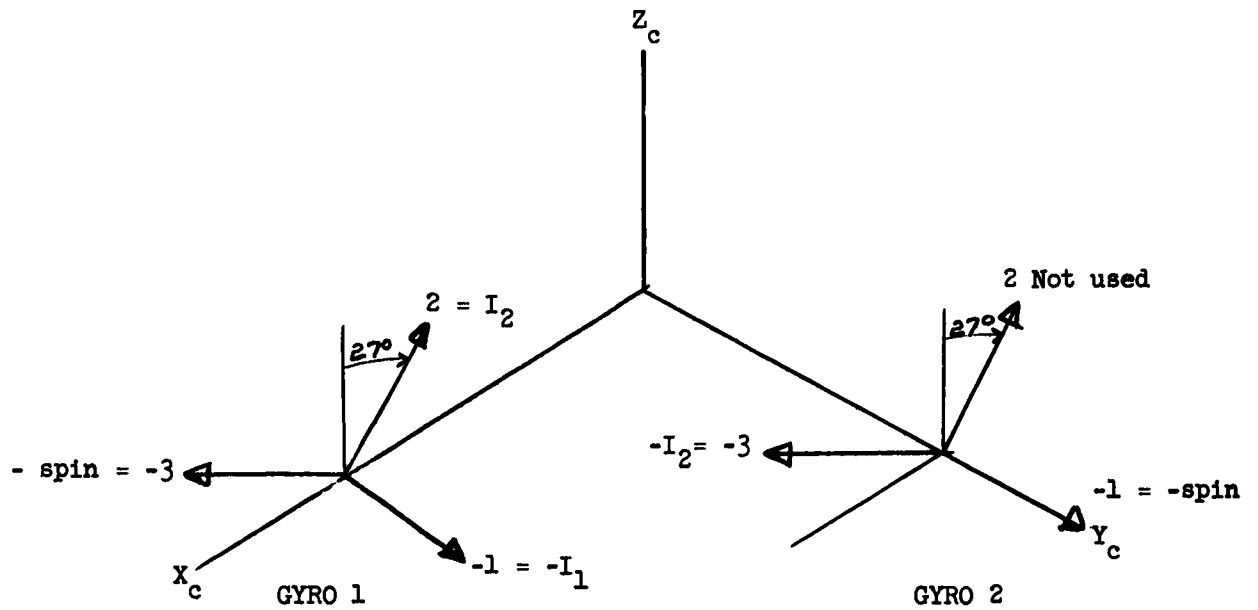
N	$ \bar{A} \times \bar{\phi} /N$	Direction of Drift
C	$ A_3 \sqrt{A^2 - A_3^2}$	along component of \bar{A} normal to $\bar{3}$
D	$A \sqrt{A^2 - A_3^2}$	perpendicular to component of \bar{A} normal to $\bar{3}$
B	$A_3^2 \sqrt{A^2 - A_3^2}$	same as C
E	$ A_3 A \sqrt{A^2 - A_3^2}$	same as D

Gyro II

\tilde{C}	$ A_3 \sqrt{A^2 - A_3^2}$	about $\bar{3}$
\tilde{D}	$ A_2 \sqrt{A^2 - A_3^2}$	about $\bar{3}$
\tilde{B}	$ A_1A_3 \sqrt{A^2 - A_3^2}$	about $\bar{3}$
\tilde{E}	$ A_1A_2 \sqrt{A^2 - A_3^2}$	about $\bar{3}$

FIGURE 1

GYRO, ACCELEROMETER AND COMPUTATIONAL COORDINATE SYSTEMS



At this point, it is desirable to make several observations based on the preceding:

a. Drifts proportional to A^2 are always accompanied by drifts proportional to A . Separation is possible by virtue of differences in the shape of the error profile although results are somewhat obscured by two integrations. It may be possible to obtain some improvement here by using supplementary data derived from star tracker measurements.*

b. Velocity errors arising from the C and B coefficients may be suppressed by directing the thrust entirely along axis 1 or 2--this permits an "uncontaminated" measurement of the D and E terms. Errors arising from D and E may not, however, be eliminated without simultaneously suppressing those produced by C and B.

c. While it is true that drifts produced by the C and B terms occurs about an axis which is perpendicular to that arising from the D and E coefficients, this fact is not quite as useful as it might appear. The difficulty stems from cross-coupling with velocity errors produced by Gyro II which in turn arises from the fact that the gyro and accelerometer axes do not coincide. Once again, supplementary information obtained from stellar measurements may be advantageous.

2. Accelerometer Orientations

For gyro testing, it is almost mandatory that one accelerometer coincide with the thrust direction for in this configuration the remaining accelerometers will be subject only to bias errors and hence are optimally suited to sense gyro-caused errors. This orientation is also optimum for observing the scale factor, quadratic and cubic uncertainties

* Data obtained from a second flight where the IMU orientation is reversed might also be used.

of the accelerometer directed along the thrust vector but is, of course, of no value in detecting its cross axis effects.

3. IMU Orientations

The standard platform orientation is shown in Figure 1. Reflection on the above suggests that only three orientations are worthy of serious consideration--namely, those for which the thrust vector coincides with the X, Y, or Z-accelerometer axes. (Changes which alter the relative gyro and accelerometer orientation have been ruled out since they require extensive hardware modifications internal to the IMU.) To facilitate a quantitative comparison, the magnitude of $A \times \vec{\theta}$ is listed in Table III. From the table, it is apparent that, despite certain drawbacks, a rotation which places the X-accelerometer along the thrust direction has many advantages and is, in any event, the best available choice. Some of the properties of this orientation are

- a. Velocity errors arising from all coefficients other than \tilde{B} and \tilde{E} (which should be statistically identical to B and E) are near their maximum values.
- b. Only the D and E terms contribute to errors in the X_c direction. Errors in the Y_c direction arise from C, B, \tilde{C} and \tilde{D} . Thus, if the A dependent and A^2 dependent terms are separated (as described above), the X channel provides a measurement of the D and E terms, and the B term may be extracted from the Y channel. The remaining coefficients (C, \tilde{C} and \tilde{D}) cannot be further separated on the basis of velocity data but, since the properties of D and \tilde{D} (and C and \tilde{C}) are identical, several flights will yield an estimate of the statistics of C. Again, it may be that stellar measurements will provide useful supplementary information--this subject will be considered further in future studies.

TABLE II

$$|A \times \bar{\phi}|/N \text{ for } |a| = 1$$

Error Coefficient N	Platform Rotated so that Thrust is along			Gyro-Oriented to Maximize Error
	X Accel.	Y Accel.	Z Accel.	
<u>Gyro I</u>				
C	.47	.37	.37	.5
D	.574	.914	.914	1.0
B	.385	.150	.150	.386
E	.47	.37	.37	.5
<u>Gyro II</u>				
\tilde{C}	.470	.37	.37	.5
\tilde{D}	.329	.529	.529	1.0
\tilde{B}	0	.262	.262	.386
\tilde{E}	0	.374	.374	.5

Appendix 12
References

APPENDIX 12

REFERENCES

- (1) R. A. Moore, D. F. Meronek, "A Digital Computer Program for a Generalized Inertial Guidance System Error Analysis," 30 March 1959 STL/TR-59-0000-00647
- (2) R. Bain, "Tracking System Free Flight Calibration Program," 27 November 1961 STL/IOC 9311.3-174
- (3) J. F. A. Ormsby, "Design of Numerical Filters with Applications to Missile Data Processing," September 1960 STL/TR-60-0000-09123
- (4) R. A. Moore, J. R. Westlake, "Inertial Guidance System Sled Tests: Accelerometer Evaluation," 16 March 1961. ARS 1630-16
- (5) Final Report on Advanced Guidance Studies, Volume IV, 13 May 1961, AFBMD-TR-61-591V
- (6) L. N. Jenks, Monthly Progress Report No 1., "Specification Design Study for Flight Testing Inertial Guidance Systems - GEM (Guidance Evaluation Missile)," 15 December 1961, 8640-6001-CU000
- (7) A. N. Drucker, "GEM Missile Configuration, Trajectory, and Instrumentation System Performance Criteria," Some Preliminary Study Results. 5 January 1962, STL/8640-6001-CC-001
- (8) "Tropospheric Scintillations," 24 October 1958. STL/GM/TM-0165-00308
- (9) "Final Report on Advanced Guidance Studies," Volume I System Studies and Flight Test Results. 31 May 1961. STL/7216-0003-RS-VOL
- (10) "Calculations of Ground-Space Propagation Effects," Counter and Riedal, Lockheed Missile System Division LMSD 2461, 22 May 1958.
- (11) A. J. Mallinckrodt, "UDOP Accuracy Study," 17 October 1960, STL/TR-60-0000-00329, dated 17 October 1960.
- (12) T. E. Sims and R. F. Jones, NASA Tech. Memo. X 529, Langley Research Center, "Rocket Exhaust Effects on Radio Frequency Propagation from a Scout Vehicle and Signal Recovery During the Injection of Decomposed Hydrogen Peroxide," February 1961.
- (13) G. A. Chadwick, "Static Force Data for Terminal Guidance Vehicles Two and Three", Avco Report RAD SR-61-147

REFERENCES (Continued)

- (14) R. B. Sherwood, "Data for Scout Boosters", 9313.1-148 dated 5 December, 1961.
- (15) R. J. Goad, "Pershing B-2 Control Data for GEM Study", 9352.1-6 dated 11 January 1962.
- (16) R. A. Bain, "Low Frequency Noise in Range Instrumentation Systems",
STL/TM-60-0000-19102 (downgraded to Unclassified), dated November, 1960.